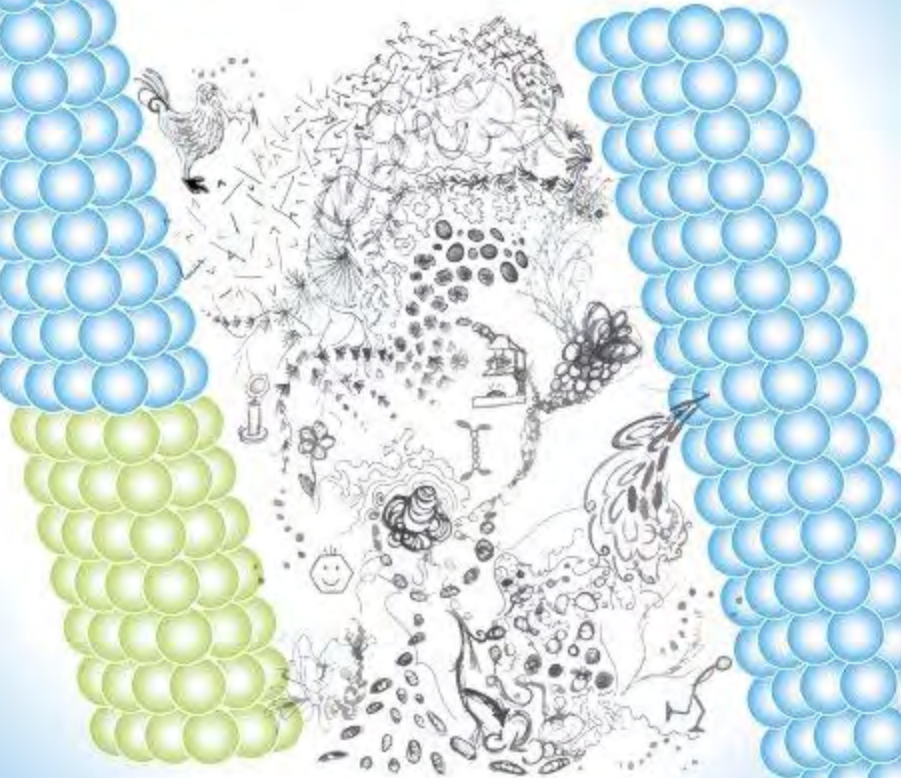




Control mechanisms of microtubule overlap regions Aniek Jongerius 2017

Control mechanisms of microtubule overlap regions



Aniek Jongerius

Propositions

1. Growth-limited sliding is an efficient way to maintain microtubule overlaps. (This thesis)
2. Directional switching by motor proteins can be used to control the length of microtubule overlaps. (This thesis)
3. To understand the cellular function of a protein by means of a reconstitution assay, it is important to also include interacting proteins.
4. Many scientific subjects, like hyperbolic planes or microtubules, can be crocheted to increase understanding of these structures.
5. Implicit learning is important for successful in vitro reconstitution experiments, as well as for predicting the shape of the inner white part of kiwifruit.
6. Doodling increases your attentiveness to what is being said in a meeting.
7. Geoengineering could be used to increase the chances of a next 'Elfstedentocht'.

Propositions belonging to the thesis, entitled
Control mechanisms of microtubule overlap regions

A.W. Jongerius
Wageningen, 5 July 2017

Control mechanisms of microtubule overlap regions

Aniek Jongerius

Thesis committee

Promotor

Prof. Dr Marcel E. Janson
Professor of Cell Biology
Wageningen University & Research

Other members

Dr Eva E. Deinum, Wageningen University & Research
Dr Liedewij Laan, Delft University of Technology
Prof. Dr Monique M. van Oers, Wageningen University & Research
Prof. Dr Wim Walter, Hamburg University, Germany

This research was conducted under the auspices of
the Graduate School Experimental Plant Sciences

Control mechanisms of microtubule overlap regions

Aniek Jongerius

Thesis

submitted in fulfilment of the requirements for the degree of doctor
at Wageningen University

by the authority of the Rector Magnificus,

Prof. Dr A.P.J. Mol,

in the presence of the

Thesis Committee appointed by the Academic Board

to be defended in public

on Wednesday 5 July 2017

at 11 a.m. in the Aula.

A.W. Jongerius

Control mechanisms of microtubule overlap regions, 134 pages

PhD thesis, Wageningen University, Wageningen, the Netherlands (2017)

With references, with summary in English

ISBN 978-94-6332-199-0

DOI 10.18174/417957

Table of contents



Chapter 1

General introduction

7



Chapter 2

An in vitro minimal midzone model

19



Chapter 3

Cl_s1 recruitment to microtubule overlaps by ase1

41



Chapter 4

Growth-limited sliding within antiparallel microtubule overlaps

57



Chapter 5

Motor proteins influence ase1 localization on microtubules

79



Chapter 6

General discussion

97

Bibliography

113

Summary

123

Acknowledgements

127

About the author

131

Education statement

132

Colophon

134

Chapter 1

General introduction

Abstract

Microtubule organization in cells is an important process. The bipolar organization of the spindle is an example of this tightly regulated organization. Microtubules emanate from the poles at both sides and form antiparallel overlaps in the centre of the spindle. These overlaps are essential to maintain the spindle and are the site where spindle elongation is induced in anaphase. We are interested in the regulation mechanisms of these overlaps. The organization of microtubules is regulated by various microtubule associated proteins. The microtubules in the overlaps are bundled by bundling proteins. Motor proteins can slide microtubules apart and regulators of microtubule dynamics can influence growth and shrinkage of microtubules. All these different functions at the overlap, sliding, growth/shrinkage and bundling, have to cooperate to maintain overlap length. We propose that a feedback mechanism is present where growth of the microtubules is limiting the sliding in the overlap. This would prevent sliding when the overlap decreases and helps to maintain the overlap. We will set up in vitro experiments to test how overlaps can be maintained. We will use bundling proteins (*ase1*), motor proteins (*klp9*) and dynamics regulators (*cls1*) from *S. pombe*.

General introduction

Microtubule overlaps and bipolar microtubule networks

Microtubule organization in cells is an important process. Microtubules give cells structural strength and are involved in transport throughout the cell. The fact that they have two distinct ends, the plus and the minus end, means that they can create polarity within the cell. Often, microtubules originate from specific microtubule organizing centres. In animal cells, this is the centrosome and in yeast the spindle pole body. When microtubules grow from these centres, all plus ends are pointing outwards and the minus ends are held together at the spindle pole body or centrosome. This microtubule organization in the form of a star is called an aster (Figure 1A). This is the basic building block for bipolar microtubule networks.

Bipolar microtubule networks are used to complete complex tasks as chromosome separation and cytokinesis. In many cases centrosomes or spindle pole bodies are at the two opposite sides of the bipolar structure (Figure 1B). The two asters emanating from these spindle poles meet in the middle and form an overlapping region. The microtubule orientation is tightly regulated with minus ends near the poles and plus ends in the overlapping region. Plants and some meiotic cells do not have centrosomes and build spindles without clear spindle poles (Szollosi *et al.*, 1972; Compton, 1998; Yamada and Goshima, 2017). Thus, clustering of microtubule minus ends is not essential for the functioning of the spindle. Nucleation of microtubules around the chromosomes and reorganization of microtubules into a bipolar spindle are mechanisms used in nonpolar spindles (Heald *et al.*, 1997).

The antiparallel overlaps in the centre of the spindle are referred to as the spindle midzone (Figure 1). The midzone is important for spindle integrity, without bundling protein spindles fall apart or show aberrant spindle morphology because overlaps do not form (Mollinari *et al.*, 2002; Loiodice *et al.*, 2005). Especially in anaphase the overlaps are well regulated, they are centred in the spindle and form short overlaps of constant length. In anaphase the overlaps are the site where the forces for spindle elongation are produced. Antiparallel overlapping microtubules can slide over each other and push spindle poles apart. To increase the length between the poles, the midzone microtubules also have to grow longer (Figure 1 D). Alternatively, when minus ends are depolymerized in metaphase at the spindle poles, antiparallel sliding induces spindle flux (Gaetz and Kapoor, 2004; Shirasu-Hiza *et al.*, 2004, Figure 1D).

Many proteins are specifically localized to the midzone. The length of the overlaps is constant and has to be maintained while the microtubules grow and slide (Loiodice *et al.*, 2005). Among the recruited proteins are kinesins and regulators of microtubule dynamics that can regulate the overlaps length. Other proteins that localize to the midzone have a signalling function, e.g. Aurora B that creates a phosphorylation gradient (Fuller *et al.*, 2008). Signalling gradients can provide spatial information in the spindle. Thus, antiparallel overlaps are important for the formation and functioning of bipolar microtubule arrays. However, the mechanisms by which the overlaps are regulated are not yet unravelled completely.

Self-organization of microtubule networks

Microtubules are organized into complex structures by self-organization. By the activation of different microtubule associated proteins (MAPs) at the right location and time, microtubules are reorganized. Some of these mechanisms, like sliding, are well understood, but it is often unclear how they work together. One important feature of microtubules that is required for microtubule organization is dynamic instability. Microtubules are not static in length, they can grow or shrink. Microtubules are nucleated and grow mostly at their plus end. The switch from growth to shrinkage is called a catastrophe. After a catastrophe, a microtubule can shrink back completely, annihilating the microtubule, or a switch back from shrinkage to growth can occur, which is called a rescue. There is constant turnover of microtubules in microtubule networks like the spindle, although on the whole the network does not change overall morphology. This turnover makes structures flexible to reorganize when different proteins start to act on the microtubules. Various proteins regulate the dynamics and thereby influence microtubule organization.

Other important organizers of microtubules are motor proteins. Motor proteins usually walk to either the minus or the plus end of a microtubule. Most motor proteins are homodimers, containing two heads that alternately bind to the microtubule lattice. Motors can attach to a cargo and transport that over the microtubule. Tetrameric motors but also some dimeric motors with secondary microtubule binding domains can bind to two bundled microtubules simultaneously. In parallel microtubule arrays this leads to clustering of microtubule ends, which can lead to aster formation (Surrey *et al.*, 2001, Figure 1C). These structures are reminiscent of the two spindle halves. On the other hand in antiparallel overlaps, microtubules will slide apart due to these motor proteins (Kapitein *et al.*, 2005; Fink *et al.*, 2009; Thiede *et al.*, 2013). This is an important mechanism in spindle elongation, which separates the spindle poles (Figure 1D). Tetrameric motors move the microtubules relative to each other, hence the term relative sliding. This is a process that takes place in the spindle midzone.

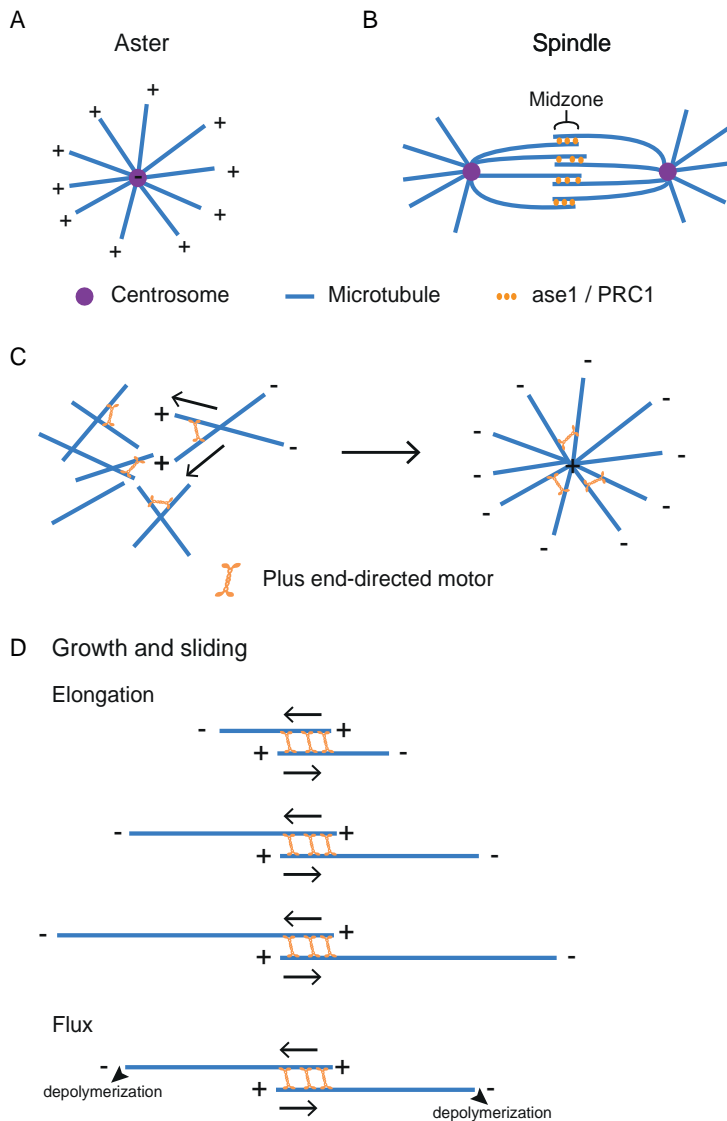


Figure 1 Several examples of microtubule organization. (A) Microtubules growing from a centrosome form an aster with all plus ends pointing outwards. (B) A bipolar spindle with centrosomes at the poles. The microtubules that emanate from the poles form antiparallel overlaps in the centre of the spindle and are bundled by a protein from the PRC1/ase1/ MAP65 family. These overlaps are termed the midzone. (C) Tetrameric motors can organize microtubules into an aster. When parallel microtubules are connected by a plus end-directed motor, this motor will cluster the microtubule plus ends. (D) Simultaneous growth and sliding within antiparallel microtubule pairs can lead to spindle elongation when minus ends are stable (top) or spindle flux when minus ends are depolymerizing (bottom).

Also important in microtubule organization are bundling proteins. Proteins from the PRC1/ase1/MAP65 family are essential bundlers in the spindle midzone (Mollinari *et al.*, 2002; Loiodice *et al.*, 2005). These proteins are homodimers that can bind to two different microtubules and are diffusive on single microtubules and in overlaps (Kapitein *et al.*, 2008). A specific feature of the PRC1/ase1/MAP65 proteins is that they preferentially bundle antiparallel microtubules (Kapitein *et al.*, 2008; Subramanian *et al.*, 2010). This preference is especially useful for the organization of bipolar networks and is the reason for their specific localization to the antiparallel overlaps of the midzone. Bundling proteins from the PRC1/ase1/MAP65 family also serve as a landmark in the midzone and are known to recruit many other MAPs to the overlaps (Duellberg *et al.*, 2013).

The major regulators of microtubule organization as mentioned above are microtubule associated proteins. Different types of motors have been proposed to slide bundled microtubules apart. Kinesin-5 is responsible for spindle elongation in many cases (Sawin and Mitchison, 1995; Collins *et al.*, 2014), but also kinesin-8, kinesin-12, kinesin-14 and dynein are known to induce relative sliding (Fink *et al.*, 2009; Tanenbaum *et al.*, 2009, 2013; Gerson-Gurwitz *et al.*, 2011; Roostalu *et al.*, 2011; Su *et al.*, 2013). Some of these motors are plus end-directed and some are minus end-directed. Kinesins can also have a different function. Kinesin-4 and kinesin-8 regulate microtubule dynamics, kinesin-4 by inhibiting growth and kinesin-8 by depolymerizing microtubules (Bieling *et al.*, 2010; Wang *et al.*, 2010). Other non-motor proteins, like CLASP can also regulate microtubule growth, CLASP for instance induces rescues on shrinking microtubules. Together with the bundling proteins PRC1/ase1/MAP65, these proteins have an important role in the formation, functioning and maintenance of the spindle.

Mechanism of length control and maintenance

We are interested in mechanisms that could stabilize overlaps and control the length of antiparallel overlaps. While there are so many proteins acting simultaneously in vivo, it is hard to identify mechanisms. Studying purified MAPs in combination with purified microtubules in a buffer is the preferred method to clarify mechanisms. Experiments with purified proteins are known as in vitro experiments. Importantly, in vitro experiments allow us to vary concentrations and conditions, which allows us to characterize a mechanism in detail. Especially in vitro experiments with combinations of MAPs are interesting, since many microtubule associated proteins work together in vivo.

Several mechanisms have been proposed, for stabilization and length control of antiparallel overlaps. One possible mechanism involves both plus end and minus end-directed motor proteins. These antagonistic motor proteins were thought to balance their forces in order to form a stable antiparallel overlap (Sharp *et al.*, 2000; Gatlin and Bloom, 2010; Goshima and Scholey, 2010). This notion was supported by experiments *in vivo* that showed that the deletion of a minus end-directed motor could rescue the spindle collapse caused by the deletion of a plus end-directed motor (Saunders and Hoyt, 1992; O'Connell *et al.*, 1993; Mountain *et al.*, 1999; Sharp *et al.*, 1999). However, *in vitro* relative sliding assays with antagonistic motors did not lead to a force balance in the overlaps (Tao *et al.*, 2006; Hentrich and Surrey, 2010). Instead, these experiments lead to bidirectional behaviour of the microtubule overlap. At every point in time one of the motors wins. The stochastically changing amount of motors of both types in the overlap is thought to induce frequent switches in directionality (Hentrich and Surrey, 2010). Furthermore, overlaps do not only have to be maintained, at the same time microtubules have to slide apart for spindle elongation. A balance in forces will not generate constant sliding. Moreover, the forces produced for spindle elongation should be regulated dependent on overlap length. How antagonistic motors can on one hand allow constant sliding and on the other hand control overlap length is not clear. So while antagonistic motor proteins are balanced *in vivo*, a combination of these motors alone does not seem to regulate overlap length.

Other mechanism that are proposed to regulate overlap length involve not only motors but also microtubule cross linkers like PRC1/ase1/MAP65. A few *in vitro* studies that combine PRC1/ase1/MAP65 with another MAP were done. We will describe them here. Braun *et al.*, 2011 combined ase1, a bundling protein from *S. pombe*, with ncd, a minus end-directed motor from *Drosophila melanogaster*. Ncd is a dimeric motor with a second microtubule binding site at the tail that can slide two microtubules apart (Fink *et al.*, 2009). With only ncd present, microtubules remain sliding until the microtubules are separated. However, the presence of ase1 prevents microtubules from sliding apart and retains the antiparallel overlap. This is caused by the combination of two effects. First, Braun *et al.* observed that ncd sliding is slowed by ase1 in a dose-dependent manner. Second, ase1 that is present in a bundle is confined to that bundle, while motors are lost in proportion with the decrease in overlap length. The microtubule ends form a diffusive barrier for ase1, thereby retaining ase1 in shrinking overlaps. When microtubules reach the end of the surface microtubule, the overlap length is reduced. This causes an increase of ase1 per overlap length and a decrease in motors. As a result, ase1 starts to reduce ncd velocity. So by sliding off the microtubule, a braking mechanism is triggered. However, friction caused by high

densities of *ase1* can slow sliding, but is not able to prevent microtubules from sliding apart. Though, another mechanism that expands the overlaps is induced when microtubules slide apart. The crowded environment with a high density of *ase1* in the short overlap is unfavourable and the diffusing *ase1* in the overlap creates an expanding force. Therefore, *ase1* in a decreasing overlap is able to expand the overlap again by entropic forces (Lansky *et al.*, 2015). This retrograde force is needed to maintain overlaps.

So far, these mechanisms did not include microtubule dynamics. But regulating growth may also be a mechanism for length control since overlap is governed by growth and sliding. To investigate this, assays have been developed with dynamic microtubules and regulators of dynamic instability. Bieling *et al.*, 2010 investigated antiparallel microtubule overlaps with PRC1 and kinesin-4 Xklp1 both from *Xenopus*. They show that the two proteins have a direct interaction with each other and that PRC1 is needed to recruit kinesin-4 to antiparallel overlaps. Bieling *et al.* construct antiparallel overlaps bundled by PRC1 in vitro using dynamic microtubules. Kinesin-4 is recruited to the overlap by PRC1 and is thought to move towards the microtubule plus ends. This leads to a kinesin-4 accumulation at the growing microtubule plus end, where it inhibits microtubule growth. In this mechanism, the length of the overlaps dictates the amount of kinesin-4 that binds there. This results in larger accumulations of kinesin-4 in longer overlaps, leading to more growth inhibition, and smaller accumulations in shorter overlaps, leading to less growth inhibition. This leads to a stable state, in which the overlap length does not change (Bieling *et al.*, 2010). This shows that the combination of a bundler/recruiter and a processive motor/growth inhibitor can form a minimal system to obtain overlap length control.

We now looked at the regulation of growth to control overlap length, but overlaps could easily fall apart if one of the microtubules switches to shortening due to a catastrophe. Dynamic microtubules do not only grow, they also occasionally switch to shrinking. This shrinkage of the microtubule possibly leads to the loss of overlaps. Therefore, a regulator of microtubule dynamics that induces rescues would be interesting to investigate. One such microtubule regulator that could function to maintain overlaps is CLASP. This protein is confined to the midzone and induces rescues where it is abundant (Bratman and Chang, 2007; Al-bassam *et al.*, 2010). This could prevent microtubules to shrink into the midzone and could help to maintain overlap length. So multiple regulators may be present to regulate multiple aspects of dynamic instability.

All these different functions at the overlap, sliding, growth/shrinkage and bundling, have to cooperate to maintain overlap length. While too much sliding leads to loss of overlaps, too much growth leads to overextended overlaps. We propose that sliding and growth are coupled. Coupling may involve an adaptive braking mechanism as seen with *ncd*. *Ase1* bundling proteins that are confined to shrinking overlaps could induce friction to slow gliding and induce opposing entropic forces. If growth lags behind sliding and overlaps shorten, at this time adaptive braking could kick in. Furthermore direct interactions between motor proteins and *ase1* could influence the behaviour of motors in the overlap as is seen with kinesin-4 and PRC1 (Fu *et al.*, 2009; Bieling *et al.*, 2010).

Physical mechanisms play an important role in the proposed mechanism. *Ase1* diffusive properties and overlap length are involved. Another physical mechanism that can play a role on microtubules is crowding. In general, many different MAPs compete for a limited amount of microtubule binding sites in the overlap, so they mutually affect each other presence. Possibly this crowding can affect the behaviour of proteins in the overlap. Motor proteins and diffusive proteins are shown to influence each other in vitro as well as in simulations (Subramanian *et al.*, 2013; Johann *et al.*, 2014). On one hand motors may change MAP localization by transporting MAPs through a direct interaction. On the other hand it was proposed that the diffusion of MAPs may be biased in one direction, as motors form mobile barriers for their diffusion. These kind of mechanisms could be used to create differences in protein profiles according to microtubule length.

All these mechanisms give insight into how the function of multiple proteins, like sliding and bundling, can be coordinated to create complex microtubule organizations. We want to create a minimal model for the antiparallel overlaps in the fission yeast spindle to get a better understanding of mechanisms that could maintain antiparallel overlaps. Similar to Braun *et al.* we want to combine relative sliding with *ase1* bundling proteins. However, we will use *klp9*, the plus end-directed motor protein that interacts with *ase1* and which drives spindle elongation in anaphase B of fission yeast. Additionally, we want to know how microtubule dynamics affect the overlap when microtubules start sliding apart. Growth-limited sliding may work as long as microtubules grow. However, overlaps might be lost when microtubules start to shrink. Therefore we want to introduce a protein that affects microtubule dynamics, like Bieling *et al.*. In our case *cls1*, fission yeast CLASP, that induces rescues and has a direct interaction with *ase1*. Furthermore, we are interested in the influence of motor proteins and diffusive proteins. The spindle midzone is crowded with different

proteins, and it is not known how this affects localization and function. We investigated this on single microtubules for simplicity and we do a similar experiment as Subramanian *et al.* with a non-interacting motor and *ase1*.

Thesis outline

In **chapter 2** we develop methods for in vitro experiments that mimic the midzone. In these experiments, bundling and sliding are combined. We designed in vitro experiments specifically to combine ase1 with another MAP and with dynamic microtubules. Eventually multiple MAPs can be combined with ase1 in dynamic overlaps to gain more insight in antiparallel overlap regulation.

In **chapter 3** we show that cls1, an inducer of rescues, can be recruited to microtubules by ase1. Furthermore, we show that the direct interaction between cls1 and ase1 is essential for recruitment. We did not succeed in confining the rescue activity of cls1 to the overlaps. Further regulation might be necessary to achieve specific rescues at overlaps.

In **chapter 4** we characterize the yeast motor klp9 and conclude that it is a bidirectional kinesin-5. Ase1 is affecting sliding with klp9 and introduces directional switching. The normally plus end-directed klp9 successively switches rapidly between plus and minus end-directed motion. Switching is triggered when microtubules slide apart. This is a new mechanism for overlap maintenance. We are the first to combine sliding with dynamic microtubules in vitro. Using dynamic microtubules, we could reconstitute spindle elongation with microtubules that grow and slide at the same time. In absence of growth microtubules do not slide apart, showing that processes are coupled. Combined with in vivo experiments in yeast that show decreased spindle elongation when microtubules growth is slowed down, we conclude that sliding by klp9 in overlaps containing ase1 can be growth-limited.

In **chapter 5** we investigate the mutual influence of a motor protein and a passive diffuser on single microtubules. We find that ase1 is hardly disturbing motor protein runs, even at high densities. Ase1 on the other hand shows end accumulations in presence of the motor, although not in all our experiments. This shows that localization of passive MAPs can be influenced by motor proteins.

In **chapter 6** we discuss the implications of our findings for spindles and suggest some interesting directions for further research.

Chapter 2

An in vitro minimal midzone model

Aniek Jongerius and Marcel E. Janson

Abstract

We designed in vitro experiments to make antiparallel overlaps in vitro. In these experiments we use purified proteins from *S. pombe*. Ase1 bundling proteins are used to make antiparallel overlaps. Additionally we introduce relative sliding using the motor protein klp9. This motor is known to have a direct interaction with ase1 and is responsible for spindle elongation in *S. pombe*. In our experiments we combine relative sliding with dynamic microtubules for the first time. This allows us to test how these activities are coordinated. In other experiments we combine ase1 and cls1 with dynamic microtubules to see if the rescue activity of cls1 can be confined to the overlaps.

Introduction

Many proteins act on the microtubules in the spindle midzone. The midzone consists of microtubules that originate from both spindle poles. Where these interpolar microtubules meet, they are bundled with their plus ends. Bundling proteins from the PRC1/ase1/MAP65 family mediate this antiparallel bundling (Loiodice *et al.*, 2005; Duellberg *et al.*, 2013). The bundles are not static structures: the microtubules are dynamic and motors induce sliding between microtubules (Sagolla *et al.*, 2003; Fu *et al.*, 2009). The combination of different protein activities leads to a midzone with a constant overlap length that is capable to induce spindle elongation in anaphase (Loiodice *et al.*, 2005). The midzone is also necessary for the structural integrity of the spindle: when the midzone disappears, spindles collapse (Sagolla *et al.*, 2003; Loiodice *et al.*, 2005). As explained in chapter 1, we want to understand how proteins work together to form and maintain the antiparallel overlaps in the midzone. To get a better understanding of the midzone, we decided to build a minimal model that mimics the midzone. This minimal model was created in vitro, where combinations of proteins and concentrations of components can be controlled and varied. Since the spindle of fission yeast is relatively simple and mitosis is well studied, we decided to work with proteins from *S. pombe* (Mallavarapu *et al.*, 1999; Sagolla *et al.*, 2003; Loiodice *et al.*, 2005; Janson *et al.*, 2007; Fu *et al.*, 2009).

To mimic the spindle midzone, antiparallel bundles of microtubules had to be created. Bundling proteins of the PRC1/ase1/MAP65 family are abundant in the antiparallel overlaps of the midzone in vivo (Duellberg *et al.*, 2013). Proteins of this family bundle microtubules preferentially in an antiparallel configuration (Gaillard *et al.*, 2008; Kapitein *et al.*, 2008; Subramanian *et al.*, 2010). We used the fission yeast homolog ase1 in our assays. Ase1 is a homodimer that can bind to two microtubules, thereby forming a bundle (Janson *et al.*, 2007). Since ase1 preferentially binds two microtubules in an antiparallel fashion, the use of ase1 ensured that the majority of bundles formed in our in vitro model were antiparallel bundles of microtubules.

Another feature that had to be captured in a minimal model is relative sliding between the antiparallel microtubules. In cells, this sliding causes spindle elongation (Fu *et al.*, 2009). While microtubules slide apart, the antiparallel overlaps decrease in length. It is not known how the overlap is maintained while microtubules are sliding apart. In vitro research suggested that the bundling protein ase1 can act as a brake when microtubules are sliding apart (Braun *et al.*, 2011). However, this was done with a non-processive minus end-directed motor protein. We decided to introduce sliding

with the kinesin-5 from *S. pombe*, klp9. Klp9 is responsible for spindle elongation in anaphase B and has a direct interaction with ase1 (Fu *et al.*, 2009). This motor was not yet characterized in vitro.

Microtubules in the spindle midzone are dynamic. Therefore, our next aim was the introduction of dynamic instability into our assays. Growth of bundled microtubules can elongate microtubule overlaps. The introduction of dynamic instability of microtubules in antiparallel bundles enabled us to investigate the balance between this lengthening of overlaps and the shortening of overlaps caused by relative sliding. Furthermore, the activity of proteins that influence dynamic instability, such as fission yeast cls1, the homolog of CLASP, could be tested once microtubules were made dynamic in our assays.

Thus, the minimal midzone model that we decided to create had to consist of antiparallel bundles of dynamic microtubules, undergoing dynamic instability and relative sliding. We designed in vitro experiments to achieve this, specifically to combine ase1 with another MAP and with dynamic microtubules. Eventually multiple MAPs can be combined with ase1 in dynamic overlaps to gain more insight in antiparallel overlap regulation. Here we provide the rationale behind the consecutive steps in our protocols for in vitro assays.

Preparation

Here we describe the protocols we use in the preparation for an in vitro experiment and the choices we made to design protocols.

Tubulin purification

The tubulin we used was purified from porcine brains following the protocol of Castoldi & Popov, 2003. Neuron cells have several protrusions to transmit and receive signals. Transport into and from these protrusions relies on microtubules, hence microtubules are abundant in neurons. Porcine tubulin is widely used in in vitro experiments (Tran *et al.*, 1997; Kapitein *et al.*, 2005; Gell *et al.*, 2010; Fourniol *et al.*, 2014; Baumann and Surrey, 2015). Since tubulin is highly conserved over many species, porcine tubulin can be used in assays with MAPs from other species (Sullivan, 1988). This was frequently shown with proteins from *S. pombe*, as we have used (Bieling *et al.*, 2007; Janson *et al.*, 2007; Kapitein *et al.*, 2008; Erent *et al.*, 2012). Nonetheless specific regulation of the MAP-microtubule interface may differ between species. This needs to be considered when interpreting our results.

For purification, the tubulin was cycled in several steps of polymerization and depolymerization (details in Materials and Methods, Figure 1A). After every step, the tubulin/microtubules were spun in an ultracentrifuge. When tubulin dimers were in solution, debris and stable protein aggregates were pelleted and discarded. After polymerization of the tubulin into microtubules, the microtubules themselves were pelleted and MAPs and tubulin that failed to polymerize stayed in solution and were discarded. This ensured that the tubulin finally aliquoted was free of MAPs and able to polymerize.

In assays with dynamic microtubules, we found that microtubules created with our purified porcine tubulin did not undergo many catastrophes. Therefore, in all dynamic assays we decided to use tubulin purchased at Cytoskeleton, Inc. This tubulin, which was purified on a phosphocellulose column, showed more catastrophes when grown under similar circumstances. All stabilized microtubules were polymerized from our own purified tubulin.

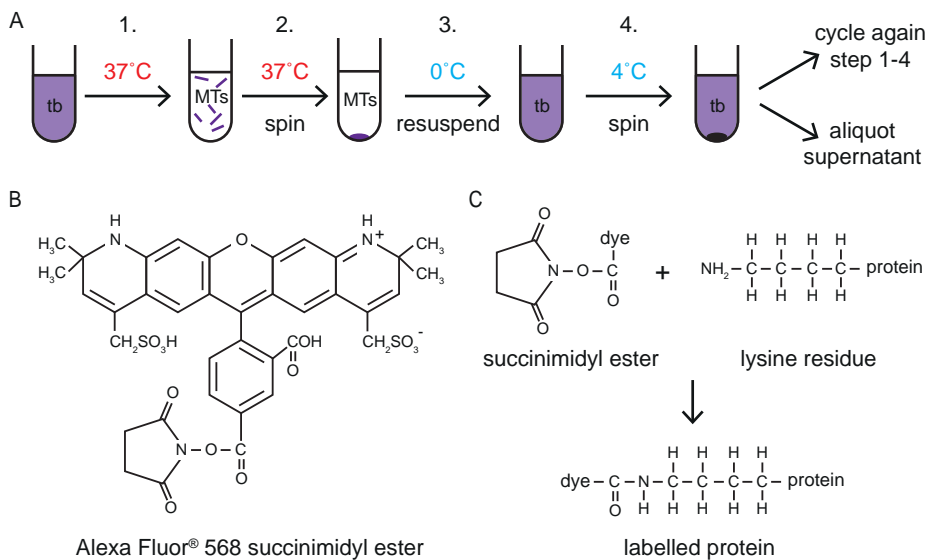


Figure 1 Microtubule cycling and labelling. (A) A schematic representation of the cycling of tubulin (purple). In step 1, microtubules (purple lines) are polymerized at 37°C . In step 2, the microtubules are spun down and form a pellet. The supernatant, containing MAPs, is decanted and in step 3, the microtubules are resuspended and depolymerized on ice. Step 4, is a cold spin, where aggregates are pelleted. The pellet is discarded and the successfully cycled tubulin can now be cycled again, repeating steps 1. – 4 or aliquoted and snap frozen for later use. (B) Chemical formula of Alexa Fluor 568 conjugated with a succinimidyl ester. (C) The reaction scheme of a succinimidyl ester with a lysine residue, leading to a labelled protein.

Tubulin labelling

Tubulin was labelled based on published protocols by (Hyman *et al.*, 1991; Peloquin *et al.*, 2005). The tubulin we used was our own purified tubulin. We labelled tubulin with Alexa Fluor 568 and 647 and with biotin. The labels were bought with conjugated succinimidyl esters (Figure 1B). These reactive groups react with lysine residues of the tubulin (Figure 1C). The labelling reaction was done on polymerized microtubules. This ensured that labels were not attached to tubulin sites that are important for polymerization. The resulting tubulin was cycled as described above to ensure active tubulin dimers. Before use, the labelled tubulin was mixed with unlabelled tubulin to form mixes with 1-10 % labelled tubulin.

The fluorescent dyes we used were Alexa Fluor 568 and 647. Alexa Fluor dyes have high yields and are resistant to photobleaching (Berlier *et al.*, 2003). Furthermore, the Alexa Fluor dyes are engineered to be more hydrophilic, limiting aggregation of tagged proteins. We imaged Alexa Fluor 568 and 647 using 561 nm and 638 nm lasers for excitation.

Microtubule polymerization

In our experiments stabilized microtubules were required to robustly form microtubule overlaps. Dynamic microtubules can grow from stabilized microtubules when tubulin and GTP are added. Since we wanted to introduce dynamic instability in the samples, we could not use taxol stabilized microtubules. When using taxol stabilized microtubules, taxol has to be present in all solutions. This would instantly stabilize the newly grown microtubules, preventing catastrophes (Caplow *et al.*, 1994). Therefore, we used GMPCPP to polymerize microtubules for all our assays. When microtubules are polymerized with GMPCPP, a non-hydrolysable GTP analogue, dynamic instability is completely suppressed (Hyman *et al.*, 1992). This results in stabilized microtubules that can function as a seed for growth of dynamic microtubules.

To make bundles of two microtubules in a controlled way, we needed different sets of microtubules. First, microtubules were attached to the cover slip surface. Second, microtubules from the solution were allowed to bind to these surface-attached microtubules. To have a maximal chance of bundle formation, the surface-attached microtubules needed to be long. The second layer of microtubule consisted of shorter microtubules, so that landing microtubules completely overlapped with the underlying microtubule. This had the advantage that sliding could be studied over a substantial length. The GMPCPP-stabilized microtubules used to form overlaps could also be used as seeds for dynamic microtubules. When the dynamic part of the microtubule started shrinking because a catastrophe occurred, it usually shrunk back completely

to the stabilized seed. So, while the overlap was maintained by the GMPCPP-stabilized seeds, we could study dynamically unstable microtubules that grew from them.

Long and short microtubules were grown at 37°C with different labels (Alexa Fluor 568 and Alexa Fluor 647), to simplify the observation of bundles (details in Materials and Methods). Additionally, the long microtubules had biotin attached to a percentage of the tubulin subunits, to enable attachment of the long microtubules to the surface via surface-adsorbed antibiotin antibodies. Short seeds were centrifuged in an airfuge, resuspended and made fresh every day (Figure 2A). When we polymerized microtubules at a low tubulin concentration, the resulting microtubules were longer. At a low concentration of tubulin less microtubules were formed since nucleations were rare (Fygenon *et al.*, 1994). We suspect that all tubulin went to these fewer seeds, hence microtubules grew longer. After standing for two days at room temperature, the microtubules were even more elongated, probably by giving microtubules the time to connect head-to-tail with other microtubules. This resulted in a dense solution of very long microtubules ranging from 15 to 50 μm that was used for up to a week (Figure 2B).

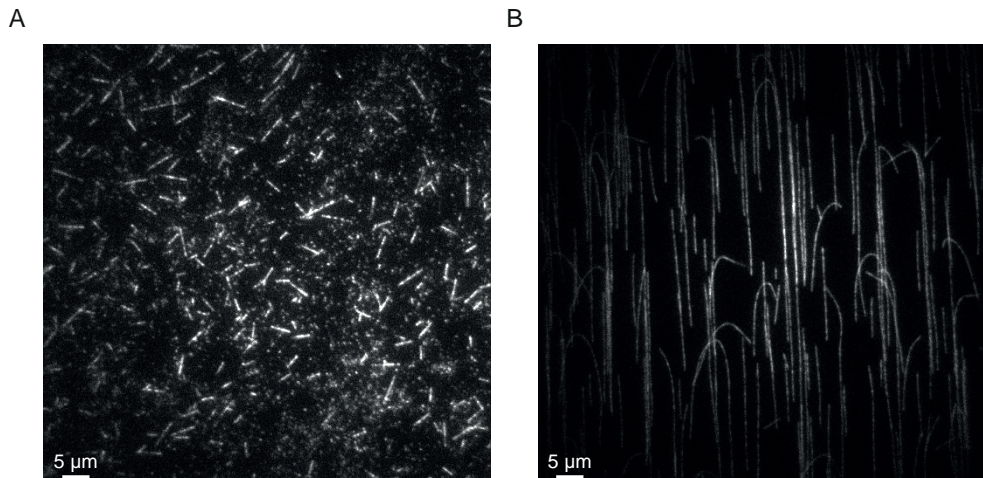


Figure 2 Stabilized microtubules as used in *in vitro* assays. (A) Short GMPCPP-stabilized seeds, labelled with Alexa Fluor 568. (B) Long, GMPCPP-stabilized microtubules, labelled with Alexa Fluor 647 and attached to the surface via antibiotin antibodies.

Protein purification

The proteins we used were purified from *E.coli*. This was already shown to work for ase1 (Kapitein *et al.*, 2008). The motor used here, klp9, is a kinesin-5 motor. Traditionally, kinesin-5 motor proteins, like eg5, are purified from insect cells (Kapitein *et al.*, 2005). Both kinesin-5 proteins from budding yeast, kip1 and cin8, were purified before in insect cells (Gordon and Roof, 1999; Gerson-Gurwitz *et al.*, 2011; Roostalu *et al.*, 2011) or from yeast cells overexpressing the protein (Gordon and Roof, 1999; Gerson-Gurwitz *et al.*, 2011; Fridman *et al.*, 2013). However, cut7, the other kinesin-5 from *S. pombe* was purified successfully from *E. coli* before (Edamatsu, 2014). We chose to purify klp9 from *E. coli* and that proved to give functional motors able to slide microtubules apart. Purification from bacteria might have worked because of the relatively small size of klp9 compared to kinesin-5 from other species. The proteins were expressed in *E. coli* and the cells were lysed using a French press. All proteins had a his-tag and were purified on nickel columns (details in Materials and Methods).

Glass cleaning and DDS coating

In our in vitro assays, we needed biotin antibodies to coat the glass surface of the cover slips homogeneously and in a reproducible manner. Therefore, cover slips were coated with dimethyldichlorosilane (DDS) (Fink *et al.*, 2009; Braun *et al.*, 2011). The silane group renders the surface hydrophobic and prone to antibody attachment. Clean cover slips were incubated in a solution of 5 mM DDS in trichloroethylene (TCE). After rinsing in ethanol, cover slips were ready for use. Cover slips maintained their hydrophobicity for several weeks.

Flow cells

Flow cells are widely used in in vitro experiments. It is a convenient way of exchanging the fluid in a glass chamber and the samples can be observed with (fluorescence) microscopy (Gell *et al.*, 2010; Laan and Dogterom, 2010; Al-Bassam, 2014; Fourniol *et al.*, 2014; Stanhope and Ross, 2015). Flow cells were constructed with microscope slides directly from the box and silanized cover slips (Menzel). On the microscope slide, lines of vacuum grease were spaced approximately 5 mm apart. The vacuum grease lines were made using a syringe with a 200 μ l pipet tip at the end. A cover slip (24x24mm) was put on top creating three flow cell chambers (Figure 3). In the first step of the assay, a volume of 10 μ l was pipetted directly next to each lane such that fluid was sucked into them and filled them partly. By pushing gently on the cover slip, the vacuum grease barriers were squeezed, decreasing the volume of the chamber. The volume of the chamber was adapted until the 10 μ l filled the whole channel.

In the next steps, buffers and protein solutions were flowed through the flow cell by pipetting fluid on one side and holding a tissue paper on the other side. This method drew the fluid through the flow cell because of the capillary force created by the tissue. The solution in the flow cell could be replaced multiple times, usually over ten times. However, care was taken that no air entered the chamber, since that blocks the chamber and inhibits further flow. Solutions were either left to incubate in the flow cell, often followed by a washing step with buffer, or solutions were replaced by other solutions in quick succession. Thus, our flow cells are suitable for complicated microtubule assays with many sequential building steps.

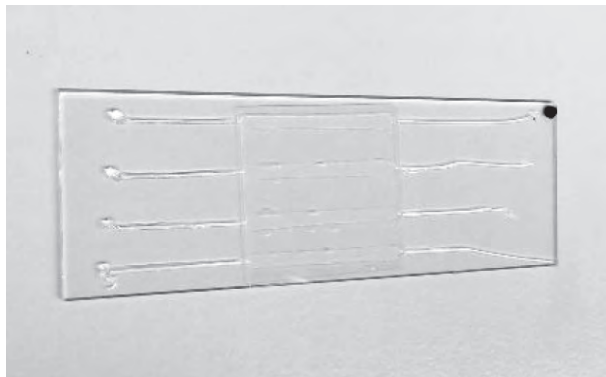


Figure 3 A flow cell with three lanes as used for in vitro experiments.

Imaging

In our vitro assays, microtubules and/or proteins were attached to the cover slip surface in flow cells. Objects that are constrained to the cover slip are easier to image than those diffusing around in the bulk solution. Furthermore, surface-attached structures are observed with high contrast using TIRF microscopy (total internal reflection microscopy). In TIRF microscopy, only the ± 100 nm of the sample that are closest to the cover slip are excited (Wazawa and Ueda, 2005). So, events that take place at the cover slip surface are visible, while fluorescently labelled proteins in the bulk are not visible. This suppresses background intensities, while events at the surface can be imaged at high quality.

Ase1 bundling assays

Different kinds of proteins localize in vivo to overlapping microtubules, like the midzone. The protein holding these overlapping microtubules together is ase1. Additionally ase1 recruits many other proteins to the midzone (Duellberg *et al.*, 2013). These proteins can be studied in vitro separately, but it is more relevant to test these proteins in bundles and in combination with ase1. Apart from the antiparallel microtubule geometry, also the interaction with ase1 might influence protein activity and behaviour.

The basis for more complicated experiments with multiple proteins is an ase1 bundling assay. We adapted the method of Braun *et al.*, 2011 to make in vitro overlaps. Microtubules were attached to the surface (surface microtubules) and shorter microtubules (seeds) were bundled with the surface microtubules by ase1 (Figure 4A). Bieling *et al.*, 2010 chose a different setup to make antiparallel overlaps. They attached stabilized seeds to the surface and added free tubulin and GTP. Growing microtubules could meet and with PRC1 in solution, the meeting microtubule ends became bundled (Figure 4B). This microtubule geometry is less suitable for experiments where microtubules slide apart. Since the microtubules are attached to the surface at one end, sliding would introduce microtubule buckling. Results would be difficult to interpret as buckling forces may resist sliding. Therefore we choose the system with one microtubule completely attached and one microtubule free to move (Figure 6B).

In our assay, long GMPCPP-stabilized microtubules were attached to the cover slip surface of a flow cell. The microtubules contained a small percentage of biotin-labelled tubulin. The flow cell was coated with anti-biotin antibodies and the microtubules stuck to these antibodies. This created the first layer of microtubules that formed the base of the ase1 bundles. Microtubules aligned when liquid was kept flowing into the flow cell causing them to attach to the surface mostly in one direction. The aligned pattern allowed for higher densities of microtubules per experiment since the surface microtubules were neatly arranged and did not intersect, simplifying analysis (Figure 2B).

After binding of surface microtubules, we did not want the other proteins to stick to the surface. To prevent protein adsorption a block copolymer was added. Pluronic (F127) consists of two hydrophilic tails and a hydrophobic central part. The hydrophobic part adsorbs onto the hydrophobic surface, leaving the hydrophilic tails sticking out into the solution. The hydrophilic tails are composed of polyethylenegly-

col (PEG) known for its lack of nonspecific binding to proteins (Jeon and Andrade, 1991). Multiple lanes could be prepared up until this point for use within a few hours. After flushing out the pluronic solution, the experiment had to be finished in one go, since surface blocking decreases when leaving flow cells for prolonged periods in buffer without pluronic. From this moment on, all solutions used contained 1 mg/ml casein. The idea is that this further prevented our proteins of interest to bind to the surface, as casein far outnumbers them and occupies most of the available sites.

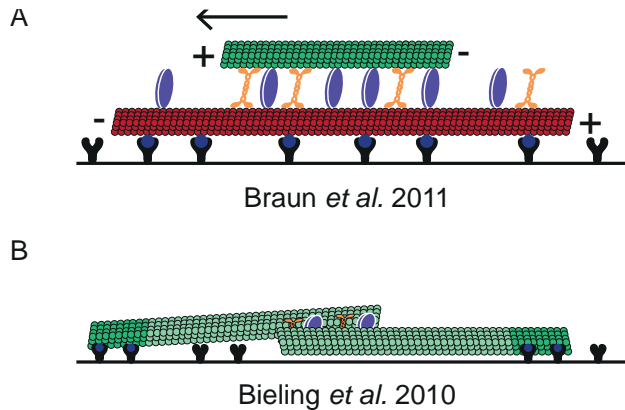


Figure 4 Schematic representations of in vitro experiments from literature, where PRC1/ase1/MAP65 is combined with a motor protein. (A) Depiction of the relative sliding assay as performed by Braun *et al.*, 2011. Stabilized microtubules that are attached to the surface (red) support sliding of a short stabilized microtubule on top of them (green). The motor protein used is *ncd*, a minus end-directed motor (orange). *Ase1* is also present in the bundles (blue). (B) Depiction of the bundling assay as performed by Bieling *et al.*, 2010. Short stabilized seeds (dark green) are attached to the surface. Dimly labelled tubulin in the solution supports microtubule growth (dim green, dynamic part of microtubules). PRC1 (blue) and Xklp1 (kinesin-4, orange) are in solution and PRC1 bundles microtubules that meet in the assay.

Subsequently, an *ase1* solution was flowed in. *Ase1* bound to the microtubules on the surface. Although the affinity of *ase1* is high for overlapping microtubules, *ase1* also binds single microtubules with lower affinity (Kapitein *et al.*, 2008; Lansky *et al.*, 2015). Immediately after flowing in *ase1*, a solution with short microtubule seeds was flushed in. The seeds were flushed out directly with buffer. Seeds bundled with the *ase1*-incubated surface microtubules. The short incubation time reduced the number of seeds that attached to the surface of the flow cell, rather than to surface microtubules. We observed that the majority of *ase1* localized to the bundles. This protocol thus resulted in robust bundle formation with *ase1* located at the bundles (Figure 5, A and B).

In principal, to control ase1 levels in solution, ase1 concentration can be controlled in the last step, by flushing in ase1 again after bundle formation (Braun *et al.*, 2011; Lansky *et al.*, 2015). However, when seeds are not flushed out, as in our relative sliding assays (see below), this strategy did not work. Adding ase1 and seeds at the same time bundled seeds and decreased the chance of one-to-one bundling of a seed to a surface microtubule. Therefore, we added ase1 only once after surface microtubules were attached and washed ase1 out with the seed solution. To test how the amount of ase1 that attached to the microtubules depended on the ase1 concentration in the solution, we investigated the GFP-ase1 fluorescence intensity in formed bundles at different initial ase1 concentrations. The amount of GFP-ase1 was clearly dependent on the initial concentration of ase1 (Figure 5, B and C). We observed that the level of

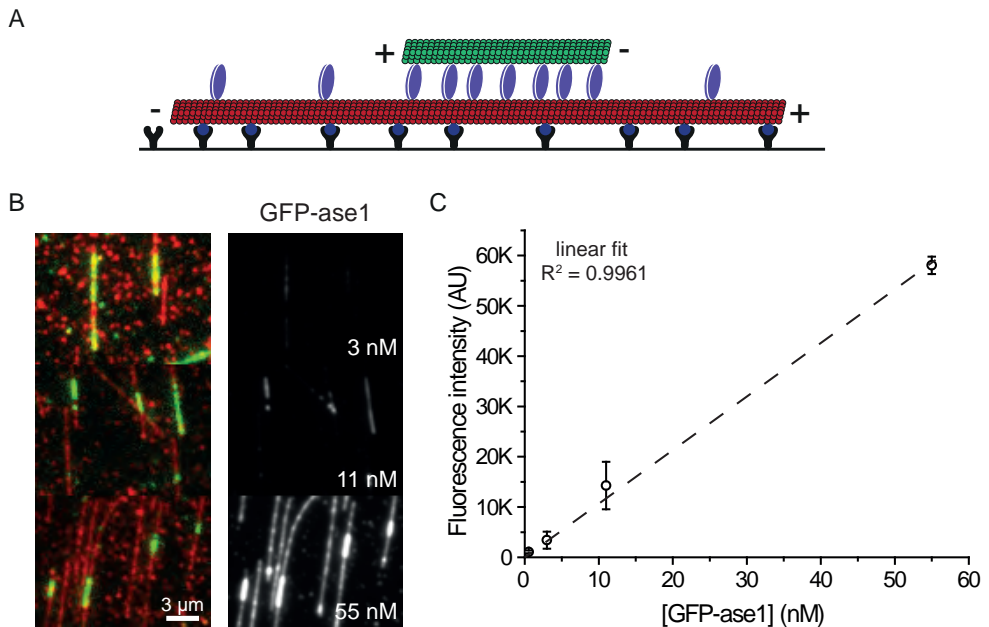


Figure 5 Ase1 bundling assay. (A) A schematic representation of an ase1 bundling assay. A long biotinylated microtubule (red with blue biotin, referred to as surface microtubule) is attached to the surface with antibodies against biotin (black Y). Ase1 (blue) bundles the surface microtubule with a short microtubule (green, referred to as seed). (B) Images of bundling assays at GFP-ase1 concentrations ranging from 3-55 nM. On the left side, an overlay of surface microtubules (red) and seeds (green) is shown. On the right side, the corresponding images of GFP-ase1. The GFP-ase1 images are all on the same grayscale. (C) The average fluorescence intensity of GFP-ase1 in bundles as a function of initial GFP-ase1 concentration. Error bars indicate SD. (0.5 nM, n = 8 ; 3 nM, n = 10 ; 11 nM, n = 10 ; 55 nM ase1, n = 9)

ase1 in bundles correlated linearly with the initial concentration for the range studied (0.5 - 55 nM). For all experiments, the concentration mentioned for ase1 bundling assays is the concentration of the ase1 solution that we initially flowed into the sample.

Building on this protocol for ase1 bundles, more complicated experiments were designed. Other proteins of interest, like cls1 in chapter 3 or klp9 in chapter 4, could be added. Additionally, dynamic instability was introduced, bringing the assay one step closer to an in vitro minimal model of midzone overlaps (detailed protocols in Materials and Methods).

Motor protein assays

There are many different motor proteins and a simple way to identify their properties are in vitro assays. In vitro assays have the benefit that only the motor of interest is studied and concentrations and microtubule configurations can be adapted. Motors induce active transport and this can be assessed in surface gliding assays, looking at microtubule movement, or single molecule imaging, looking at the movement of individual motor proteins. Tetrameric motors but also some dimeric motors with secondary microtubule binding domains can bind two microtubules at the same time, giving them the opportunity to rearrange microtubule networks by inducing sliding (Matthies *et al.*, 1996; Sharp *et al.*, 1999; Miyamoto *et al.*, 2004; Fu *et al.*, 2009). This is especially interesting for the mitotic spindle in anaphase. Relative sliding assays are a way to study this behaviour. Here we describe the in vitro assays we adapted and designed to study motor proteins. Additionally, we describe how existing assays can be adapted to allow for dynamic instability.

Gliding assay

Gliding assays are a simple way to assess the properties of motor proteins. The directionality of the motor can be established when using polarity marked microtubules. Usually, a gliding assay is also the first test to see if a batch of purified motor proteins is active. Motor proteins are attached to the surface and stabilized microtubules are added in solution. The microtubules can land on the surface, being bound by the motor domains of the motor proteins, and are propelled so they appear to glide over the surface (Figure 6A). The velocity of gliding depends on ATP concentration which sets the enzymatic rate.

In the simplest form of the gliding assay, motor proteins are adsorbed at the surface

randomly by the nonspecific adsorption of proteins to untreated glass. We did not observe movement with klp9 in this way. Some microtubules did land and were at least partially attached to the surface. However, the microtubules were not propelled along the surface. For cut7 (kinesin-5 from fission yeast) it is known that it also does not support gliding in this way, but when specifically attached to the surface gliding assays do work (Edamatsu, 2014). We mimicked this approach and attached our klp9-his with an antibody against the his tag. DDS coated cover slips were used to enhance antibody attachment. The his-tag is positioned at the C-terminus of klp9, ensuring that the motor domains stick up into solution. This made the chances of successfully binding and transporting a microtubule higher. Indeed, with anti-his antibodies the gliding assays did work. However, still a lot of microtubules were only partially attached to the surface. This suggested that klp9 binding to microtubules was weak.

Relative sliding

Tetrameric motor proteins can slide microtubules apart. This is a very important feature of microtubule overlaps in the spindle midzone because it drives spindle elongation. An *in vitro* assay to investigate this is the relative sliding assay. In this assay, microtubules were attached to the surface and seeds, motor proteins and ATP were flowed in in the final step. Seeds were able to land on top of the surface microtubules being bound to them by the motor proteins. Since seeds stayed in the sample, new seeds could land throughout the experiment. Our relative sliding assay is similar to relative sliding assays with eg5, Ncd and DK4mer as described before (Kapitein *et al.*, 2005; Fink *et al.*, 2009; Thiede *et al.*, 2013) (Figure 6B).

In the antiparallel overlaps of the midzone, ase1 is abundant. Relative sliding in presence of ase1 mimics midzone sliding more accurately. Especially for studying motors that have an interaction with ase1, this is an interesting approach. Ase1 was shown to influence motor movement especially when microtubules start to slide apart (Braun *et al.*, 2011). When combining a relative sliding assay with ase1, several approaches can be taken. Braun *et al.* first incubated the surface microtubules with either ase1 and Ncd or only Ncd after which bundles were formed and seeds were washed out. The gliding assays indicated that klp9 is not a strong microtubule binder, so although this approach works for Ncd motors, it was not likely to succeed with klp9. Therefore, we started from the relative sliding assay as described above with only motors and added an ase1 step. The relative sliding protocol with ase1 is similar to the ase1 bundling protocol, except motor proteins were added together with the seeds and the seeds were not washed out. So, ase1 was added first, followed by a mixture of seeds,

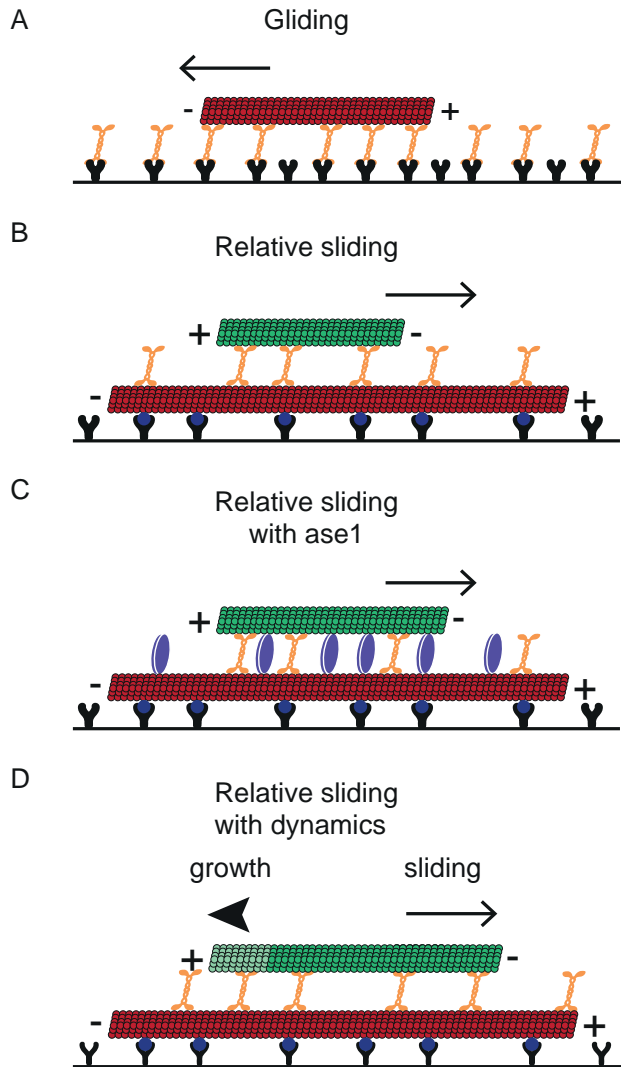


Figure 6 Schematic representations of different motor protein assays. (A) A schematic representation of the gliding assay with klp9 (orange tetramer) attached to a glass surface via anti-his-antibodies (black Y) and a polarity-marked, GMPCPP-stabilized microtubule (red) gliding on top. (B) A schematic representation of the relative sliding assay. A surface microtubule is attached as in B. Motor proteins (orange) transport a short microtubule (green, referred to as transport microtubule) over a longer surface-adhered microtubule. (C) A schematic representation as in figure 3A. Ase1 bundling proteins (blue) are simultaneously present. (D) A schematic representation of the relative sliding assay with dynamic microtubules. The stabilized seed is shown in bright green, the dynamic part of the transport microtubule is pale green. The arrowhead denotes growth, while the arrow denotes the direction of sliding.

motors and ATP (Figure 6C). The seeds stayed in the flow cell, so new seeds could land throughout the experiment. This strategy succeeded in the production of sliding seeds on top of surface microtubules. The lowest concentration at which we could produce relative sliding with only motor proteins was 150 nM klp9 (Chapter 4). The addition of 3 nM ase1 made relative sliding possible at concentrations as low as 15 nM klp9. When seeds reached the end of the surface microtubule and slid apart, the microtubules overlapped only with their plus ends. Especially this feature mimics antiparallel overlaps of the midzone very well.

Dynamic relative sliding

To mimic midzone overlaps even better, dynamic instability was introduced into the experiment. In the final mix, free tubulin and GTP were added as well as seeds, motors and ATP (Figure 6D). The free tubulin was dimly labelled with the same label as the seeds. To ensure constant growth velocities, the microscope objective was pre-heated to 30 °C and kept at a stable temperature during imaging.

When a growing seed slid on top of a surface microtubule, imaging was straightforward since the microtubules were confined close to the cover slip glass. However, when the seed reached the end of the surface microtubule and started to slide off, the position of this seed was only restricted where it was attached to the surface microtubule. With only stabilized seeds, this was not a problem, since the seeds were short and the free end did not move much out of the TIRF field. However, when the seed was growing, the seed was moving steadily further away from the attachment point, gaining more length and thus freedom to move out of the focus plain. This made it difficult to determine sliding velocities. Often the seed was not in focus at all or only for short periods. To prevent the pivoting of the seed, we added methylcellulose, a crowding agent that confines microtubules to the surface. Thus methylcellulose should decrease the fluctuations of the seeds (Bieling *et al.*, 2007; Gell *et al.*, 2010; Laan and Dogterom, 2010; Fourniol *et al.*, 2014). At 0.05% methylcellulose, seeds attached all over the cover slip and no bundles were formed. At a ten times lower methylcellulose concentration bundles formed, but partly attached microtubules still moved out of focus. So while methylcellulose can affect microtubule behaviour it was not usable in our sample. We did not find a solution to this problem yet. Nevertheless, we found some events that we could analyse in experiments without methylcellulose.

Materials and methods

Tubulin purification

The brains were taken directly from the freshly slaughtered pigs and put immediately on ice. After homogenizing the brains in a blender, the supernatant was used for several polymerization-depolymerization cycles (Figure 1A). In a high PIPES buffer, microtubules were polymerized at 37°C. The polymerization was followed by centrifugation in an ultracentrifuge at 37°C. During this spin, microtubules remained polymerized and were spun down to form a pellet. Tubulin unable to polymerize, MAPs and other proteins stayed in the supernatant and were discarded. Depolymerization of the microtubules in the pellet was done in a MES buffer on ice. The low temperature caused depolymerization and ultracentrifugation of the solution at 4°C separated the tubulin dimers in solution from any impurities and aggregated proteins. The supernatant containing tubulin underwent one more cycle of polymerization and depolymerization before being aliquoted and snap frozen in liquid nitrogen. Purified tubulin was stored at -80°C and aliquots were thawed on ice before use. Leftovers from thawed aliquots were discarded, because subsequent freeze-thaw cycles hamper the quality of the tubulin.

Tubulin labelling

For tubulin labelling a similar cycling protocol was used as described above (Hyman *et al.*, 1991; Peloquin *et al.*, 2005). The tubulin was polymerized at 37°C and a pellet of the polymerized microtubules was formed in an ultracentrifuge. The pellet was kept warm and was resuspended in warm buffer, leaving the microtubules polymerized. Then, the dye dissolved in anhydrous DMSO was added and the labelling reaction took place while the microtubules were shaken at 37°C. The reactive group attached to the dye was a succinimidyl ester that interacted with available lysine groups on the tubulin subunits (Figure 1, B and C).

Microtubule polymerization

Short 'seed' microtubules were grown for 30 min at 37°C from a 20 µM porcine tubulin solution (8% Alexa 647-labelled, 92% unlabelled tubulin) in 10 µl MRB80 (80 mM Pipes/KOH pH6.8, 4 mM MgCl₂, 1 mM EGTA), supplemented with 1mM GMPCPP (Jena Bioscience). After 30 min, 90 µl MRB80 was added and the microtubules were centrifuged in a Beckman airfuge at 100,000g for 10 min to separate seeds from smaller tubulin assemblies. The pellet was resuspended in 90 µl MRB80 with 1 mg/ml casein and 72 mM KCl.

Surface microtubules were grown for 3 hrs at 37 °C from a 5 µM porcine tubulin solution using unlabelled mix (2% biotinylated, 98% unlabelled tubulin) or fluorescently labelled mix (2% biotinylated, 6% Alexa 568-labelled, 92% unlabelled tubulin) in 50 µl MRB80, supplemented with 1mM GMPCPP. After 3 hrs incubation, assembled microtubules were left at room temperature for at least 2 days before being used. These microtubules were used for up to a week.

Protein purification

First, the plasmid containing the code for the desired protein was transformed into *E.coli*. After selection on an antibiotic, the bacteria were grown to log phase. Protein production was induced by adding IPTG and the culture was grown for 6 hours at 20 °C. The bacteria were harvested by spinning them down. The pellet was stored at -80 °C until protein purification.

After thawing the bacteria pellet, it was resuspended and mechanically lysed by using a French press. The lysate was centrifuged and the supernatant was incubated with nickel-NTA beads for 1 hour at 4 °C on a rotating wheel. During this time, his-tagged proteins attached to the Ni-NTA beads, while untagged proteins could be washed off easily. The beads were transferred to a column and washed with 30 nM imidazole. The proteins were eluted at 500nM imidazole. Imidazole causes the his-tagged proteins to be displaced from the column. The different collected fractions were analysed further by SDS-page gel and in vitro tests.

Glass cleaning and DDS coating

Cover slips were rinsed in acetone for half an hour and in a mixture of KOH in water (10%) and isopropanol (2:1) for one hour. After rinsing with water, the glass was dried in an oven. For silanization, clean cover slips were incubated with 5mM DDS in TCE for one hour. After three washing steps with ethanol, cover slips were dried with nitrogen gas and stored until use. The DDS coating made the cover slips hydrophobic and ensured better protein adsorption to the surface.

Dynamic bundling assay with ase1 and cls1 (Chapter 3)

- DDS glass flow cell
- Flow in:

1.	5min	10 μ l	goat antibiotin 100 μ g/ml in PBS
2.	flush	100 μ l	PBS
3.	15min	20 μ l	1% F127 in PBS
4.	flush	100 μ l	MRB80
5.	flush	10 μ l	Alexa568-biotin MTs 10x dilution
6.	flush	100 μ l	MRB80
7.	10min	20 μ l	casein 10mg/ml in MRB80
	flush	100 μ l	cas/KCl MRB80
8.	flush	10 μ l	ase1(-GFP) in cas/KCl MRB80
9.	flush	10 μ l	undiluted Alexa 647 seeds in cas/KCl buffer
10.	flush	100 μ l	cas/KCl buffer
11.	flush	10 μ l	cls1-GFP in cas/KCl buffer
12.	flush	10 μ l	extension mix in cas/KCl MRB80

 - 1 μ l cls1-GFP in cas/KCl buffer
 - 1.5 μ l Alexa 647 tb mix 150 μ M
 - 1 μ l GTP 10 mM
 - 0.5 μ l oxygen scavenging system
 - 0.5 μ l catalase 16 μ g/ml
 - 0.5 μ l glucose 35 mM
 - 0.5 μ l glucose oxidase 166 μ g/ml
 - 6 μ l cas/KCl MRB80
- Imaging at TIRF

NB The steps in bold have to be flushed in in quick succession. This is how experiments with cls1 were done. When repeated now, I would replace steps 1-7 with steps 1-5 from the relative sliding protocol on the next page.

cas/KCl MRB80 is MRB80 + 72 mM KCl + 1 mg/ml casein

Dynamic relative sliding with Ase1 and klp9 (Chapter 4)

- DDS glass flow cell

- Flow in:

1.	5min	10 μ l	goat anti-biotin 100 μ g/ml in PBS
2.	flush	90 μ l	PBS
3.	>1h	20 μ l	1% F127 in PBS
4.	flush	90 μ l	MRB80
5.	flush	4 μ l	Alexa647-biotin MTs undiluted
6.	flush	90 μ l	cas/KCl MRB80

check surface microtubules on microscop

7.	flush	10 μ l	(GFP-)ase1 in cas/KCl MRB80
8.	flush	10 μ l	motor/seed mix in cas/KCl MRB80

- 1 μ l klp9 in cas/KCl MRB80
- 1 μ l ATP 10 mM
- 1.5 μ l Alexa 568 tb mix 150 μ M
- 1 μ l GTP 10 mM
- 0.5 μ l oxygen scavenging system
 - 0.5 μ l catalase 16 μ g/ml
 - 0.5 μ l glucose 35 mM
 - 0.5 μ l glucose oxidase 166 μ g/ml
- 5 μ l A568 seeds

- Imaging at TIRF

NB The steps in bold have to be flushed in in quick succession.

cas/KCl MRB80 is MRB80 + 72 mM KCl + 1 mg/ml casein

Chapter 3

Cls1 recruitment to microtubule overlaps by ase1

Aniek Jongerius and Marcel E. Janson

Abstract

Cls1 is a member of the CLASP family that induces rescues on microtubules. It is known that cls1 is recruited to the microtubule midzone by ase1 in fission yeast. Cls1 has a function in maintaining the midzone, possibly by inducing rescues selectively in the midzone. With in vitro experiments, we show that ase1 is sufficient to recruit cls1 to overlaps. Not only in bundles, but also on single microtubules ase1 recruited cls1. Furthermore, experiments with a truncated version of ase1 (ase1 Δ C) show that a direct interaction is necessary for recruitment of cls1 by ase1. We did not observe specific rescues in overlaps because the cls1 localization was not specific enough. However, we did show that ase1 as well as cls1 are following dynamic overlaps. Further experiments with more specific cls1 localization are necessary to be able to confirm specific rescues of bundled microtubules.

Introduction

Eukaryotic cells build a variety of complex microtubule networks throughout the cell cycle to ensure proper functioning. To organize these structures, it is key to localize microtubule regulators to specific places within networks. One way of localizing regulators properly is by binding to specific Microtubule Associated Proteins (MAPs) that recognize specific microtubule features. EB1 and ase1 localize to growing microtubule ends and antiparallel overlaps respectively, thereby creating landmarks for other microtubule regulators (Duellberg *et al.*, 2013). Both EB1 and ase1 recruit a diverse set of proteins. Ase1 and its plant and mammalian homologues (MAP65 and PRC1 respectively) are known to recruit motor proteins like kinesin-5 and regulators of microtubule dynamics like kinesin-4 and CLASP (Kurasawa *et al.*, 2004; Bratman and Chang, 2007; Fu *et al.*, 2009; Liu *et al.*, 2009).

Experiments in fission yeast have been instrumental for deciphering mechanisms of microtubule organization. In fission yeast, the CLASP homologue *cls1* is an essential protein that induces microtubule rescues and thereby prevents the removal of individual microtubules from microtubule networks. *Cls1* is recruited to the zone of interdigitating microtubules, termed the midzone, at the onset of anaphase B by ase1 (Figure 1) (Bratman and Chang, 2007). In yeast, antiparallel microtubule overlaps are necessary for a stable spindle: without overlaps spindles collapse (Loïdice *et al.*, 2005). At the same time, microtubules in the antiparallel overlaps have to be dynamic. They are growing to enable spindle elongation and also occasionally start shrinking. However, the microtubules usually do not shrink into the midzone until late anaphase, maintaining a stable midzone during spindle elongation (Sagolla *et al.*, 2003). Bratman and Chang showed that if *cls1* is deactivated during anaphase microtubules disassemble starting from the midzone, resulting in spindle collapse. Thus, *cls1* is present in the midzone and stabilizes the antiparallel overlaps by inducing rescues when microtubules reach the midzone while shrinking.

In interphase, *cls1* is also present in the antiparallel overlaps of cytoplasmic microtubule bundles. Single microtubules within these bundles grow towards the cell tip and occasionally undergo catastrophes (Figure1). In wildtype cells, these single microtubules shrink all the way to the overlapping zone (Sagolla *et al.*, 2003). Overlap zones persist upon treatment with MBC, a microtubule depolymerizing drug. *Cls1* at overlaps may thus prevent microtubule shortening locally. Thus, *cls1* stabilizes the overlaps where it is localized, while single microtubules in the same cell are not rescued. When *cls1* was overexpressed 200-300 fold, *cls1* also localized to single microtubules.

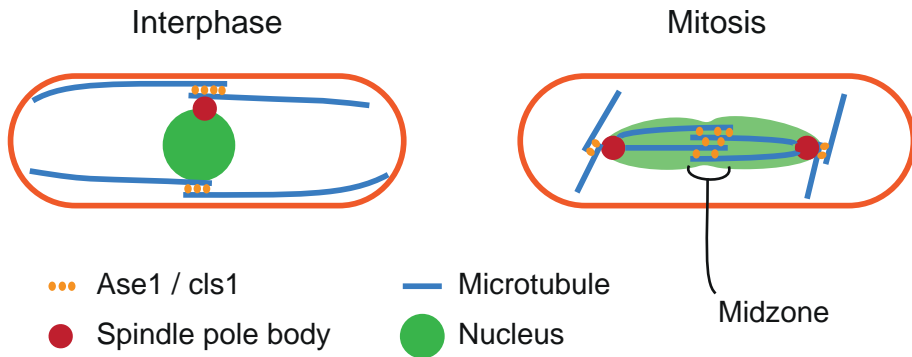


Figure 1 A schematic representation of *S. pombe* microtubules in interphase and mitosis. In interphase multiple bundles are present, overlapping near the nucleus and extending single microtubules to the far ends of the cell. In mitosis, the spindle is formed by two antiparallel arrays of microtubules nucleating from the spindle pole bodies. The midzone is the region where antiparallel inter-polar microtubules are bundled. Ase1 and cls1 are located in the antiparallel overlaps in both interphase and mitosis.

In this case, catastrophes were usually followed by rescues on single microtubules (Bratman and Chang, 2007). So, cls1 can generate rescues on individual microtubules as well as microtubules in bundles depending on the specificity of its recruitment. Previously, the functioning of cls1 was examined using in vitro assays. Although cls1 acts in vivo mainly on microtubules in bundles, the only in vitro experiments were done with cls1 on single microtubules. Cls1 reportedly binds in clusters to single microtubules and patches of cls1 are stationary for at least 8 minutes (Al-bassam *et al.*, 2010). Cls1 induces rescues when microtubules shrink back and reach a spot enriched in cls1. Necessary for cls1 functioning in vivo are the two TOG-like domains at the N-terminus. These domains can bind a free tubulin subunit in the cls1 homodimer (Al-bassam *et al.*, 2010). By recruiting tubulin to microtubules it is thought that cls1 can locally generate rescues. It was shown that cls1, free tubulin and GTP are sufficient to introduce rescues.

Cls1 has a direct interaction with ase1. Bratman and Chang therefore postulated that cls1 is recruited to overlapping microtubules by ase1 to locally enhance the microtubule rescue rate. In this study, we investigated whether the ase1/cls1 combination forms a minimal module that can form microtubule overlaps in which the rescue activity is high, while leaving rescue rate low at single microtubules. Furthermore, we investigated whether the direct interaction between ase1 and cls1 is necessary for recruitment to overlaps.

Results

Ase1 and cls1 localize to microtubule overlaps

In vivo, the interaction between *ase1* and *cls1* is necessary to recruit *cls1* to microtubule overlaps (Bratman and Chang, 2007). This suggests that a minimal system with *ase1* can bundle microtubules and recruit *cls1* to them. We tried to reconstitute these features by creating *ase1* bundles and consecutively adding *cls1*. The base of the bundles was formed by long GMPCPP-stabilized microtubules that were attached to the cover slip surface of a flow cell (surface microtubules). Then a mixture of mCherry-*ase1* (mCh-*ase1*) was flowed in, followed by short GMPCPP-stabilized microtubules (seeds). At positions where seeds (labelled with Alexa 647) landed on top of the surface microtubules (unlabelled), mCh-*ase1* was abundant (Figure 2A) (Janson *et al.*, 2007). In contrast, single microtubules were only dimly labelled with mCh-*ase1*. After flushing with buffer, a *cls1*-GFP solution was introduced. To investigate whether *cls1*-GFP is recruited specifically to microtubule overlaps, the *cls1*-GFP signal was compared between bundles and single microtubules. For this, line scans along surface microtubules with a seed on top were made in all channels and the location of the seed was determined (Figure 2, A and B). We compared the average fluorescence intensity of *cls1*-GFP in bundles (I_{bundle}) with that of *cls1*-GFP on an adjacent stretch of single microtubule ($I_{\text{single MT}}$). The ratio of $I_{\text{bundle}} : I_{\text{single MT}}$ is a measure for specific bundle localization. The ratio was on average 3.7 ± 0.5 (\pm SE; $n=15$) (Figure 2C). For bundles that do not specifically recruit *cls1*, a twofold increase in *cls1*-GFP binding was expected since the two bundled microtubules double the amount of binding sites compared to the single microtubule geometry. The observed preferential binding of *cls1* to overlaps could be independent from *ase1* if *cls1*'s affinity for microtubules is locally enhanced by binding to two microtubules simultaneously. On the other hand, *ase1* may be required to recruit *cls1* to overlaps. To differentiate between these possibilities we compared the intensity of mCh-*ase1* and *cls1*-GFP within overlaps. If *cls1* is recruited to bundles independently of *ase1*, the amount of *cls1* in an overlap should not depend on the amount of *ase1* in an overlap. The intensities of mCh-*ase1* and *cls1*-GFP were plotted against each other for pixels within bundled regions (Figure 2D). The Pearson correlation coefficient was 0.691, indicating a high correlation between the local amounts of mCh-*ase1* and *cls1*-GFP within bundles. This observation strongly suggested that *cls1* is recruited by an interaction with *ase1*.

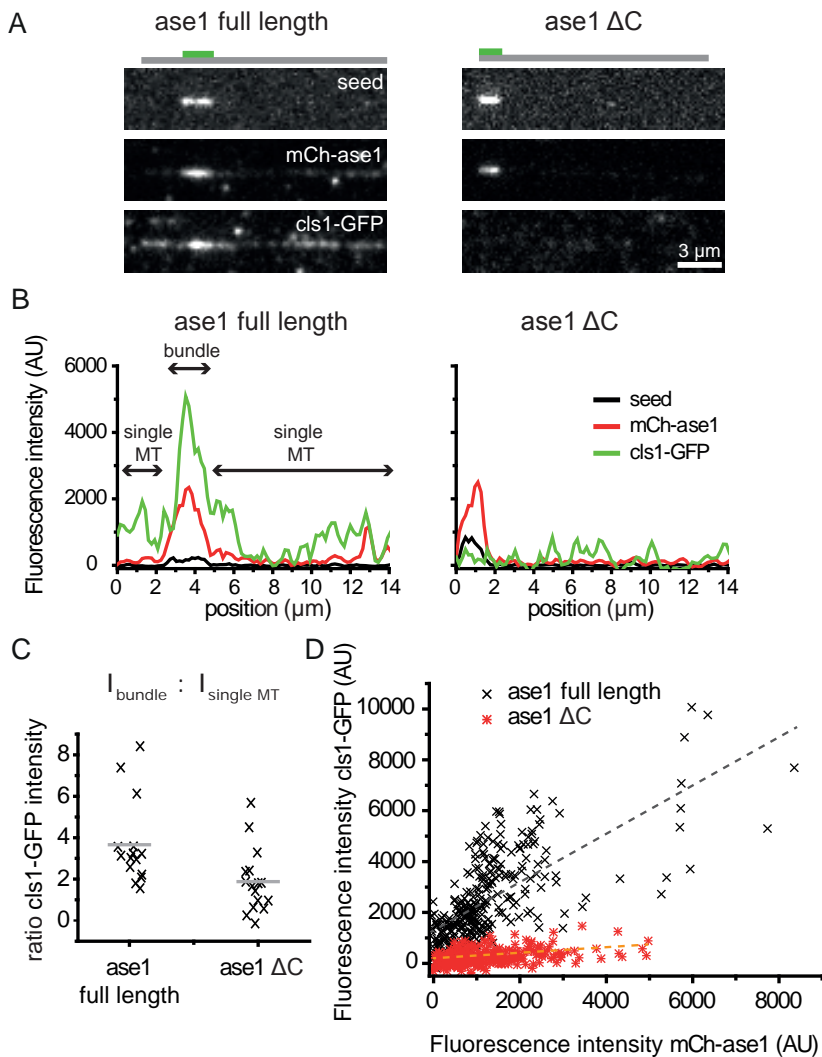


Figure 2 Correlation between mCh-ase1 and cls1-GFP in bundles. (A) Snap shots of a bundle with mCh-ase1(left) and mCh-ase1 Δ C (right). A schematic representation of the situation with surface microtubule (unlabelled, gray) and seed (Alexa 647, green) is shown above. (B) Line scans of the bundles shown in A in three channels: seed (black), mCh-ase1 (red) and cls1-GFP (green). (C) Plot of the ratio of $I_{\text{bundle}} : I_{\text{single MT}}$ for both mCh-ase1 (n=15) and mCh-ase1 Δ C (n=16). Crosses mark the ratio for individual bundles, while the horizontal line denotes the average ratio. (D) The fluorescence intensity of cls1-GFP plotted against the fluorescence intensity of mCh-ase1 in the same pixel of a line scan. Only pixels from the overlap regions were plotted for every line scan (mCh-ase1, red stars, n=15 line scans; mCh-ase1 Δ C, black crosses, n=16 line scans).

A direct interaction with ase1 is necessary for recruitment of cls1

To find further support for a recruiting mechanism based on a direct interaction between ase1 and cls1, we investigated if we can eliminate cls1 recruitment by deletion of the cls1 interacting C-terminus of ase1 (ase1 Δ C). A 67 amino acid stretch at the C-terminus of ase1 is responsible for the interaction with cls1 (Bratman and Chang, 2007). Ase1 mutants without this interaction domain localize normally to bundles. However, cls1 is not recruited by these ase1 proteins in vivo, suggesting that cls1's rescue activity is recruited through an interaction with ase1. Bundling with mCh-ase1 Δ C created overlaps where the truncated protein localized abundantly, similar to full length ase1 (Figure 2A). However, the cls1-GFP intensities observed in the images were lower than with full length ase1. We performed the same analysis as described above, making a line scan and averaging the fluorescence intensity over bundles and single microtubules (Figure 2, A and B). For ase1 Δ C, the cls1-GFP ratio $I_{\text{bundle}} : I_{\text{single MT}}$ was 1.9 ± 0.4 (\pm SE; n=16) (Figure 2C). This is significantly lower than the 3.7 found for full length ase1 ($p < 0.05$) and corresponds to the twofold increase expected for binding without specific recruitment to the bundles. Furthermore, a higher fluorescence intensity of the truncated version of ase1 barely resulted in an increase in cls1-GFP (Fig 2D). These results indicated that the presence of two overlapping microtubules is not sufficient for recruitment of cls1 to microtubule overlaps.

Ase1 recruits cls1 to single microtubules

To further investigate the mechanism of cls1 recruitment by ase1 we observed single molecules of cls1 on single microtubules in absence and presence of ase1. Adding ase1 to the assay had a clear effect on cls1 localization. In experiments with ase1, an ase1 solution was flushed in first, followed by the 0.5 nM cls1-GFP solution. With ase1, 3.7 times more cls1 bound to microtubules (Figure 3, A and B and D). Using ase1 Δ C, without the interacting region, the cls1 fluorescence intensity was similar to the situation without ase1. To examine changes in cls1 behaviour, we compared kymographs of cls1-GFP on single microtubules (Figure 3C). Cls1-GFP was mobile in our assays. Kymographs showed traces of the diffusion of single cls1-GFP proteins. A minority of cls1-GFP was stationary and formed patches, but these tended to last shorter than the two minute observation time in all our assays. Without ase1 or with ase1 Δ C, there were many short-lived interactions between cls1-GFP and the microtubule (Figure 3C, open arrow heads). With full length ase1 in the assay, cls1-GFP interactions lasted longer (Figure 3C, closed arrow heads), which suggests that ase1 may recruit cls1 by prolonging its residence time on microtubules. Within bundles, possibly the same mechanism increases cls1-GFP localization. Both experiments on ase1 bundles and on single microtubules showed that the C-terminus of ase1 is indeed required for cls1 recruitment.

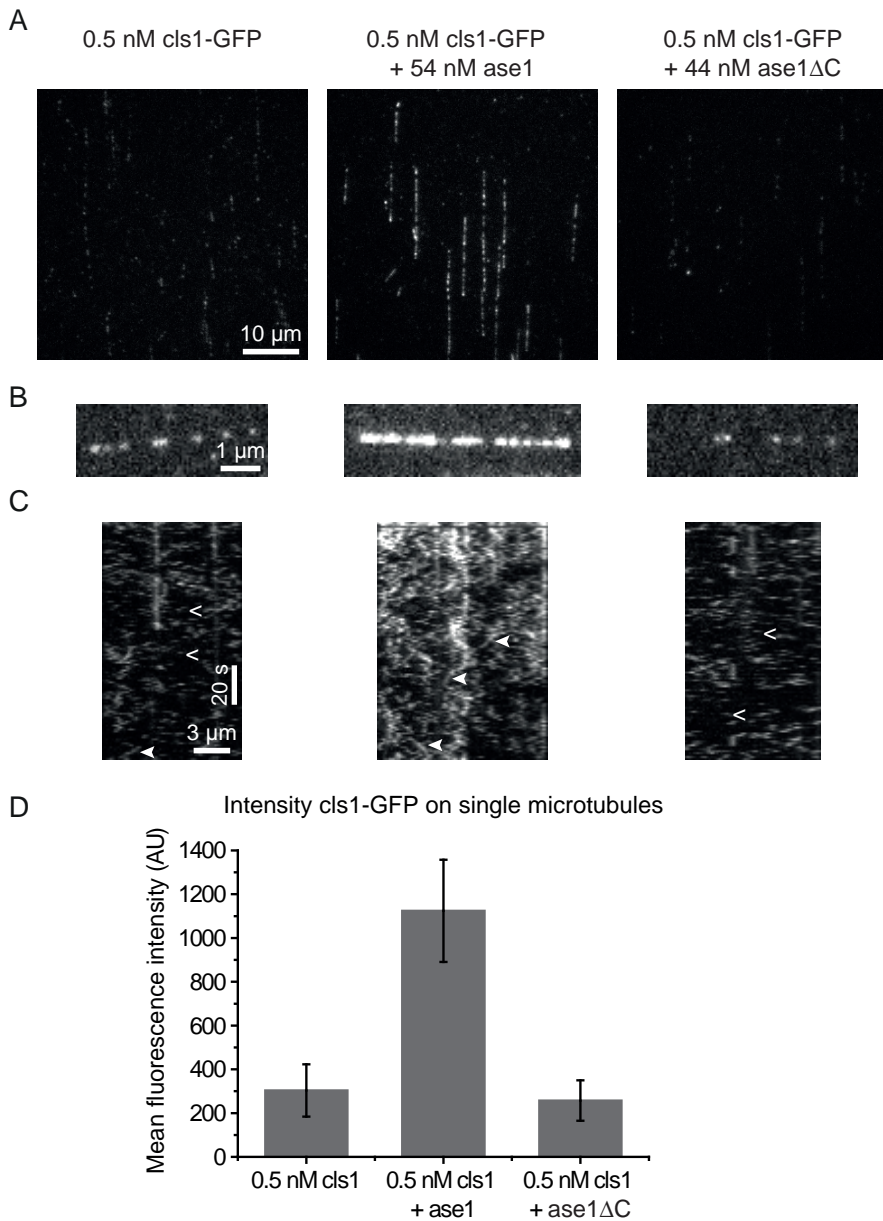


Figure 3 Cls1-GFP on single microtubules. (A) Cls1-GFP on single microtubules without ase1, with ase1 and with ase1ΔC. (B) A close up of cls1-GFP on a microtubule taken from the pictures in A. (C) Kymographs of cls1-GFP on the microtubules shown in B. Open arrow heads point out short-lived binding of cls1 to the microtubule, closed arrow heads point out events where cls1 binds longer to the microtubule. Within the panels (A), (B) and (C) the contrast is the same for all pictures. (D) Mean fluorescence intensity of cls1-GFP without ase1 (n=13, number of line scans), with ase1 (n=14) and with ase1ΔC (n=14) on single microtubules. Error bars indicate SD.

Cls1 induces rescues, but not specifically at overlaps in our assay

We next tested whether *ase1*-mediated recruitment of *cls1* to overlaps can locally increase the occurrence of rescues. Therefore we created a bundling assay with dynamic microtubules, by adding free tubulin and GTP to our samples in the final step of sample preparation (Figure 4). In this assay, surface microtubules and seeds on top of a surface microtubule both showed growing extensions. The latter events caused overlaps to grow in length. At a tubulin concentration of 15 μM the extensions also exhibited frequent catastrophes, decreasing overlap length again. At a low concentration of *cls1*-GFP (5 nM), we rarely found any rescues within overlaps or on single microtubules. The rescue rate for single microtubules was 0.04 min^{-1} (1 rescue over a total of 1610 s observed shrinkage time) and within overlaps 0.06 min^{-1} (1 rescue over 980 s shrinkage time). The rates are only indicative because of the very low number of occurrences. At a 10 times higher *cls1*-GFP concentration of 50 nM, the rescue rate in overlaps was 0.52 min^{-1} (8 rescues over 925 s shrinkage time). The rescue rate for single microtubules was 2.05 min^{-1} (49 rescues over 1435s shrinkage time). We thus found no evidence for an increased rescue activity within overlaps for the tested conditions. On the contrary, we found an apparent decreased rescue activity in overlaps. However, this difference may be caused by the poor visibility of microtubule growth within overlaps, in contrast to single microtubules, causing an underestimation of the actual number of rescues specifically in overlaps.

Ase1 and cls1 follow dynamic overlaps

In our assay with dynamic microtubules we noted a lack of specific accumulation of *cls1*-GFP in overlaps, which forms a likely explanation for our failure to observe specific rescue activity in overlaps (Figure 4, A and B). At a *cls1*-GFP concentration of 50 nM the intensity ratio $I_{\text{bundle}} : I_{\text{single MT}}$ measured over the time course of the assay was 1.4 (n=2), which is close to 2 as expected for overlap-independent recruitment (Figure 4B, middle and right). Surprisingly, at the start of the assay the intensity ratio was higher (3.0 ± 0.4 ; $\pm\text{SE}$; n=5; Figure 4A, right). This suggested that *cls1*-GFP is redistributed within the sample during the assay causing loss of specific *cls1*-GFP recruitment to overlaps. Results obtained at a lower concentration of *cls1*-GFP (5 nM) suggested a similar redistribution during the experiment. At the start of the experiment *cls1*-GFP was clearly visible in overlaps and the intensity ratio $I_{\text{bundle}} : I_{\text{single MT}}$ was 7.5 ± 1.1 ($\pm\text{SE}$; n=4; Figure 4A, left), whereas throughout the experiments *cls1*-GFP was almost not detectable (Figure 4B left).

The lack of specific accumulation of *cls1*-GFP in overlaps may be rooted in the amount of *ase1* in the overlaps. *Ase1* was not labelled in our initial dynamic bundling assay (Figure 4A), hence we repeated the assay with GFP-*ase1* in absence of *cls1* to

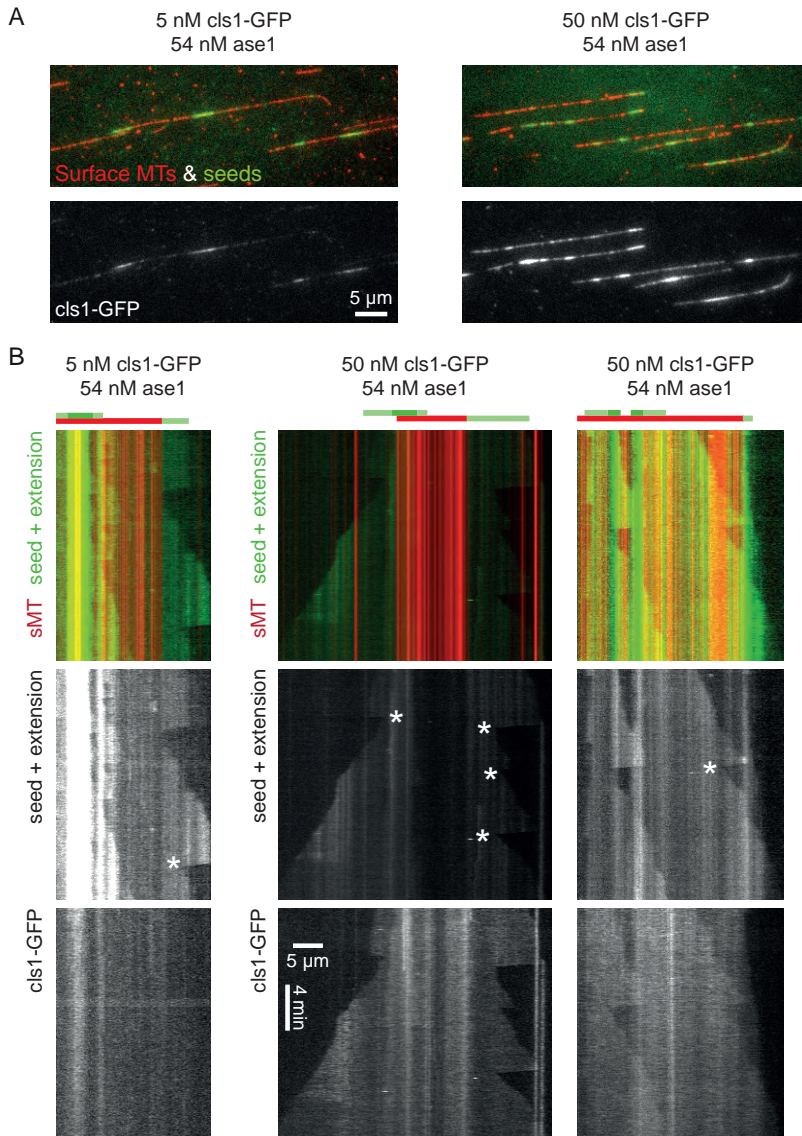


Figure 4 Cls1-GFP in dynamic bundles. (A) Ase1 bundles with cls1-GFP in a dynamic bundling sample at 5 nM and 50 nM cls1-GFP. Both samples were made with 54 nM ase1. (B) Kymographs of single microtubules and bundles in dynamic bundling assays. Concentrations are the same as in A. A schematic representation of the situation with surface microtubule (sMT, Alexa 561, red), seed (Alexa 647, green) and extension (dimly labelled with Alexa 647, pale green) is shown above the kymographs. The ‘kymograph’ from the surface microtubule is constructed from a picture taken before the movie was recorded. Rescues are marked with asterisks.

test for ase1 localization. At a GFP-ase1 concentration of 11 nM, the protein localized selectively to the overlaps and was nearly undetectable along single microtubules (Figure 5B). The GFP-ase1 localization dynamically adapted itself to the fluctuating length of overlaps. The intensity ratio $I_{\text{bundle}} : I_{\text{single MT}}$ was 7.24 over the course of the experiment (Figure 4B). For ase1-homologues PRC1 and MAP65 similar localization to dynamic overlaps have been reported (Bieling *et al.*, 2010; Fache *et al.*, 2010; Subramanian *et al.*, 2010). At a higher concentration of 55 nM GFP-ase1, the protein also clearly localized along single microtubules and the specificity ratio for overlaps was only 3.3 ± 0.6 (\pm SE; n=4) (figure 5C). This nonspecific localization of ase1 at this concentration explains why cls1-GFP was recruited to overlaps and single microtubules in similar amounts in the assays of Figure 4 (50 nM cls1 and 54 nM ase1). Although the contrast between bundle and single microtubule was poor, at 50 nM of cls1-GFP the outlines of the growing microtubules were visible in the cls1-GFP kymographs. Thus, cls1-GFP followed dynamic overlaps in our dynamic assays.

Discussion

We demonstrated that cls1 can be recruited to overlapping microtubules by ase1 and that a direct interaction involving the C-terminus of ase1 is needed for recruitment. This confirms *in vivo* work that suggested that an interaction between ase1 and cls1 is sufficient for recruitment of cls1 to overlapping microtubules. Using our *in vitro* assay, we demonstrated that cls1 can also be recruited to single microtubules by ase1. This suggested that the interaction of cls1 and ase1 is independent of the binding geometry of ase1 to microtubules, i.e. bound to a single microtubule or bound in between two microtubules. The extended microtubule residence time of cls1 in presence of ase1 moreover suggested that cls1 remained associated to ase1 after its recruitment to microtubules. The diffusive behaviour of cls1 in assays with ase1 resembled ase1 diffusion over a single microtubule (Kapitein *et al.*, 2008). This not necessarily implies co-diffusion of ase1 and cls1 but may also be generated by successive interactions of cls1 with neighbouring ase1 proteins. To verify if cls1 and ase1 maintain their interaction while diffusing, double-labelled experiments and colocalization analysis are necessary.

Previously it was established that purified cls1 has the ability to generate rescues on microtubules grown from purified tubulin. The rescue rate we found on single microtubules was similar to the rescue rate found by Al-bassam *et al.*, 2010 at a similar cls1 concentration. We might have expected a higher rescue rate in our experiments since in contrast to the earlier work, ase1 was present. Ase1, at the used concentration, also

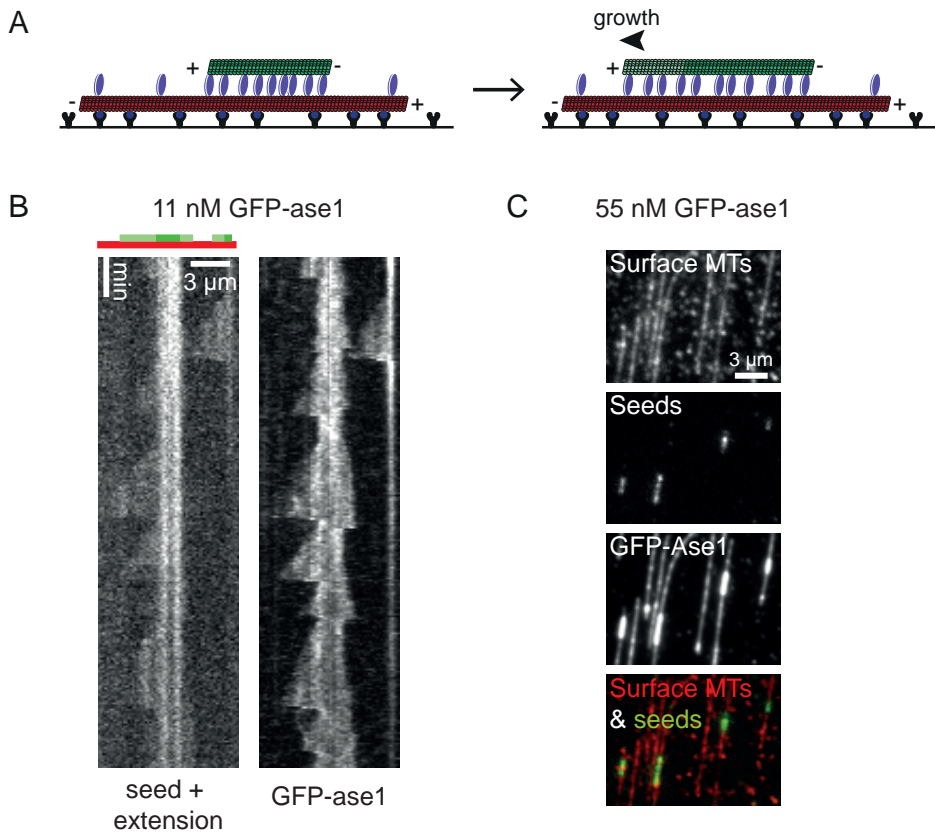


Figure 5 GFP-ase1 in dynamic bundles. (A) A schematic representation of ase1 bundling dynamic microtubules. A long biotinylated microtubule (red with blue biotin, referred to as surface microtubule) is attached to the surface with antibodies against biotin (black Y). Ase1 bundling proteins (blue) bundle the surface microtubule with a short stabilized microtubule (green, referred to as seed). The dynamic part of the seed is pale green. When the overlap grows, the newly formed overlap region quickly reaches the higher concentration of ase1 normally seen in overlaps. (B) Kymograph of a growing seed on top of a surface microtubule. A schematic representation of the situation of this kymograph with surface microtubule (sMT, Alexa 561, red), seed (Alexa 647, green) and extension (dimly labelled with Alexa 647, pale green) is shown above the kymographs. The GFP-ase1 concentration was 11nM. (C) An example of the GFP-ase1 distribution in overlaps at a concentration of 55 nM.

localizes along single microtubules and thus recruits additional cls1 to them (Figure 4). Al Bassam showed that cls1-dependent rescue rates increase with higher cls1 concentrations (Al-bassam *et al.*, 2010). It would therefore be interesting to prepare microtubules at a similar concentration of cls1 in presence of varying levels of ase1. Differences in rescue rates could indicate whether the pool of ase1-recruited cls1 is indeed active in generating rescues on microtubules.

So far we have been unable to find evidence for increased rescue rates at overlaps but this may be due to our inability to recruit cls1-GFP specifically to overlaps in the dynamic assay. It proved to be challenging to recruit cls1 preferentially to overlaps in the dynamic assay with dynamic microtubules. Rescue rates in overlaps were not higher than on single microtubules which showed that cls1 by itself does not have a higher activity on overlaps. In cells, a mechanism for preferential recruitment of cls1 to overlaps will be required to achieve localized rescue activity. To obtain more insight in factors that affect the recruitment of cls1 by ase1, experiments with dynamic microtubules need to be conducted in which the amounts of ase1 and cls1 can be monitored simultaneously using two different fluorophores. In order to recruit as little as possible cls1 to single microtubules, a level of ase1 has to be found in which recruitment to single microtubules is limited to a minimum. Figure 5 suggests that the required level will be around 11 nM. Then the amount of cls1 needs to be varied such that maximum specificity to overlaps is obtained. From our current results we conclude that the ase1/cls1 module can lead to specific recruitment onto microtubule overlap regions. However we still need to address whether the recruited proteins are active as rescue factors.

Materials and methods

Protein purification

Recombinant histidine-tagged full-length *S. pombe* ase1 (pPT179, Fu *et al.*, 2009), mCherry-ase1 (mCherry + ase1 from pPT179) and GFP-ase1 (GFP + ase1 from pPT179) were expressed in *E. coli* and cell extracts were made using a French press. The proteins were immobilized on Ni-NTA agarose beads and eluted in 20 mM phosphate buffer with 500 mM NaCl and 500 mM imidazole. Cls1-GFP was purified from insect cells by Jawdat al-Bassam as described previously (Al-bassam *et al.*, 2010). Porcine tubulin was purified as described previously (Castoldi and Popov, 2003) and labelled with Alexa Fluor® 568, Alexa Fluor® 647 and biotin (Fisher Scientific) (Hyman *et al.*, 1991; Peloquin *et al.*, 2005).

Bundling assays

See chapter 2 for protocol.

For the colocalization assay (Figure 1) unlabelled surface microtubules and 20nM mCherry-ase1 or 19nM mCherry-ase1 Δ C were used.

For bundling assays with dynamic microtubules (Figures 4 and 5), the final mixture also contained 15 μ M tubulin (3% Alexa 647-labelled, 97% unlabelled porcine tubulin (T240, cytoskeleton)) and 1 mM GTP (Jena Bioscience). For dynamic bundling assays with cls1-GFP, first a sample was prepared with 5 nM cls1-GFP as described above. To this sample, a final mix was added with free tubulin, GTP and 5 or 50 nM cls1-GFP.

For single microtubule assays (Figure 2), A568-labelled surface microtubules were adhered to the surface as described before. After flushing out unbound microtubules, the final solution of 0.5-5 nM cls1-GFP with oxygen scavenging system was flushed in. In experiments with ase1, a 54 nM ase1 solution was flowed in prior to the final cls1 solution (all in cas/KCl MRB80).

Imaging

Flow cells were imaged by using an inverted fluorescence microscope (Nikon eclipse Ti) with a Nikon 100x oil immersion 1.49 NA TIRF objective in combination with an QuantEM:512C (Photometrics) EMCCD camera controlled by Metamorph image acquisition software (Molecular Devices Corporation). For TIRF illumination, three DPSS lasers were used: 473 nm (Cobolt Blues), 561 nm (Cobolt Jive), 638 nm (Lasos RLD-XT 38). Dual- or Tri-colour images were acquired sequentially through a quad-band dichroic mirror (zt473/561/633/748rpc-TIRF, Chroma Technology) and the appropriate bandpass filters. For dynamic bundling assays, the time between frames was 5 s. Kymographs were made using imageJ image analysis software. Intensities were measured on lines with a width of 3 pixels and background values were subtracted. To measure intensities over the course of an experiment, kymographs were used. In the kymograph, areas were drawn distinguishing overlaps and single microtubules. Intensities were measured per area and averaged per category (overlap or single microtubule).



Chapter 4

Growth-limited sliding within antiparallel microtubule overlaps

Aniek Jongerius¹, Koen Hoogendoorn¹, Liang Ji², Phong T. Tran², Hannie S. van der Honing¹, and Marcel E. Janson¹

¹ Laboratory of Cell Biology – Wageningen University, the Netherlands

² Institut Curie, CNRS UMR144, Paris 75005, France

Abstract

Spindle elongation and spindle flux are driven by simultaneous growth and sliding of antiparallel microtubules within short regions of microtubule overlap. How growth and sliding are coordinated to control overlap length is unclear. Slow spindle elongation in fission yeast cells upon drug-induced inhibition of microtubule growth suggested that cells adapted motorized sliding to the rate of growth. To investigate how this “growth-limited sliding” may work we simultaneously reconstituted three microtubule activities: growth, sliding and bundling, using components from fission yeast. We first characterized klp9, a motor that based on our results classified as an exceptionally short, 633 amino-acid long, kinesin-5. In a relative sliding assay, klp9 moved microtubules apart in a primarily unidirectional manner. The direction of sliding however started to alternate in the presence of the microtubule bundling protein ase1 and when microtubules moved apart. We added tubulin to extend the formed overlaps through growth, in essence reconstituting spindle elongation. Sliding then became coupled to the dynamic state of microtubules enabling overlaps to maintain their length. We propose that cells use this form of feedback to stabilize their overlaps and potentially to regulate sliding, not by adapting motor action, but by changing rates of microtubule growth in overlaps.

Introduction

Eukaryotic cells form bipolar microtubule networks to coordinate cell division. First, the mitotic spindle segregates chromosomes and afterwards cytokinesis is coordinated by the central spindle or the plant phragmoplast. The plus ends of microtubules from both halves of these networks are connected by short regions of antiparallel overlap (Subramanian and Kapoor, 2012; de Keijzer *et al.*, 2014). Overlaps, amongst others, generate and maintain spindle bipolarity and resist forces during chromosome positioning (Mitchison *et al.*, 2004; Kajtez *et al.*, 2016). Their position is restricted to the centre of bipolar networks and regulation of overlap length appears to be an important aspect of spindle functioning. The central spindle is a good example. Here, overlaps provide a spatial cue for plasma membrane invagination during cytokinesis (Lekomtsev *et al.*, 2012) and mutants with abnormally extended overlaps are associated with cytokinetic defects (Kurasawa *et al.*, 2004). The length of an antiparallel overlap is changed when its microtubules grow or slide relative to each other. Both processes occur simultaneously to drive spindle elongation and spindle flux and coordination is thus required to maintain a constant overlap length (Mallavarapu *et al.*, 1999; Miyamoto *et al.*, 2004; Rogers *et al.*, 2005). However, it is currently not known how coordination between growth and sliding can be established. Too much sliding may cause loss of overlaps whilst too much growth will decrease the confinement of overlaps to the centre of bipolar networks.

We hypothesized that two different strategies can be followed to coordinate activities. In the “sliding-driven growth” strategy, sliding is leading and microtubule growth is continuously adapted to follow its rate. This strategy was proposed for animal spindles in which the number of recruited kinesin-4 growth inhibitors within overlaps may decrease with decreasing overlap length (Bieling *et al.*, 2010). A feedback would then be established between growth and overlap length that enables overlaps to grow after motors slide microtubules apart. A second strategy is “growth-limited sliding” in which the sliding velocity is down-regulated when overlap extension by microtubule growth lags behind. In cells, control over sliding velocity likely arises from the coordinated action of multiple types of motors present at overlaps during cell division. These may include variants that move to microtubule plus and minus ends (Hentrich and Surrey, 2010; Tanenbaum *et al.*, 2013). How motor activities can be mutually regulated to change sliding velocity in response to overlap length is not clear. It was shown, however, that the presence of passive microtubule cross linkers of the PRC1/ase1/MAP65 family in overlaps can prevent motors from sliding microtubules apart from each other (Braun *et al.*, 2011; Lansky *et al.*, 2015). Their restraining

effect on sliding increases when microtubules are driven apart because linkers have a high affinity for overlapping microtubules and are retained in overlaps even as they shorten. We hypothesized that a combination of a motor and a passive linker may facilitate “growth-limited sliding” and took a two-tier approach to investigate this possibility. First we perturbed microtubule growth during anaphase-B in fission yeast cells and observed the response in spindle elongation rates. Second, we purified a motor (klp9) and passive cross linker (ase1) that act in fission yeast spindle elongation and performed a relative sliding assay featuring dynamic microtubules.

Results

Spindle elongation velocity is perturbed by a microtubule growth inhibiting drug in a dose-dependent manner

Spindles in fission yeast (*S. pombe*) cells strongly elongate in anaphase-B to increase the distance between the two sets of segregated chromosomes. Elongation is driven by the simultaneous growth and sliding of microtubule plus-ends contained within a single, approximately 2 μm long zone of overlapping microtubules that is termed the midzone (Ding *et al.*, 1993; Mallavarapu *et al.*, 1999) (Figure 1A). We hypothesized that if growth and sliding would be independent processes, microtubules in the midzone would slide apart after growth is slowed down or stopped. To test this hypothesis we added the microtubule-growth inhibiting drug MBC (Carbendazim) to fission yeast cells. MBC was shown to disassemble spindle microtubules at a concentration of 50 $\mu\text{g}/\text{ml}$ (Akeru *et al.*, 2012) but we observed dividing cells with slowly elongating spindles at concentrations of 25 $\mu\text{g}/\text{ml}$ and lower (Figure 1, B and C). The disassembly of microtubules by MBC was likely prevented by the clasp-homologue cls1 that localizes to midzones (Bratman and Chang, 2007). The up to tenfold decrease in spindle elongation velocity was dose-dependent and a direct measure of the rate at which microtubules slide apart (Mallavarapu *et al.*, 1999). Our experiment therefore suggested that microtubule sliding gradually slowed down in response to a drug-induced reduction in microtubule growth velocity, thereby preventing loss of overlap. This form of feedback was best observed at 5 $\mu\text{g}/\text{ml}$ MBC for which sliding rates were more than halved whilst midzone length, visualized by the core midzone protein GFP-ase1 (Loiodice *et al.*, 2005), was remarkably unaffected (Figure 1D).

Klp9 is a bidirectional motor

We set out to reconstitute sliding with components from fission yeast spindles to ultimately investigate how coupling between growth and sliding is established. For

this we purified full-length klp9, a tetrameric kinesin that selectively interacts with the spindle during anaphase-B and which drives spindle elongation together with the kinesin-5 homologue cut7 (Fu *et al.*, 2009). To characterize its motor function we first performed an in vitro surface gliding assay with klp9 attached to the surface of a cover slip and GMPCPP-stabilized microtubules free in solution. Motors that were directly adsorbed onto the glass surface did not support motion, which was also reported for purified cut7 (Edamatsu, 2014). Only after his-tagged klp9 motors were bound to surface-adsorbed anti-his-antibodies microtubules bound to the surface and moved directionally (Figure 2). However, the interaction between motors and microtubules was weak since many microtubules in the sample were only partially attached to the surface even after the surface was incubated with a high motor con-

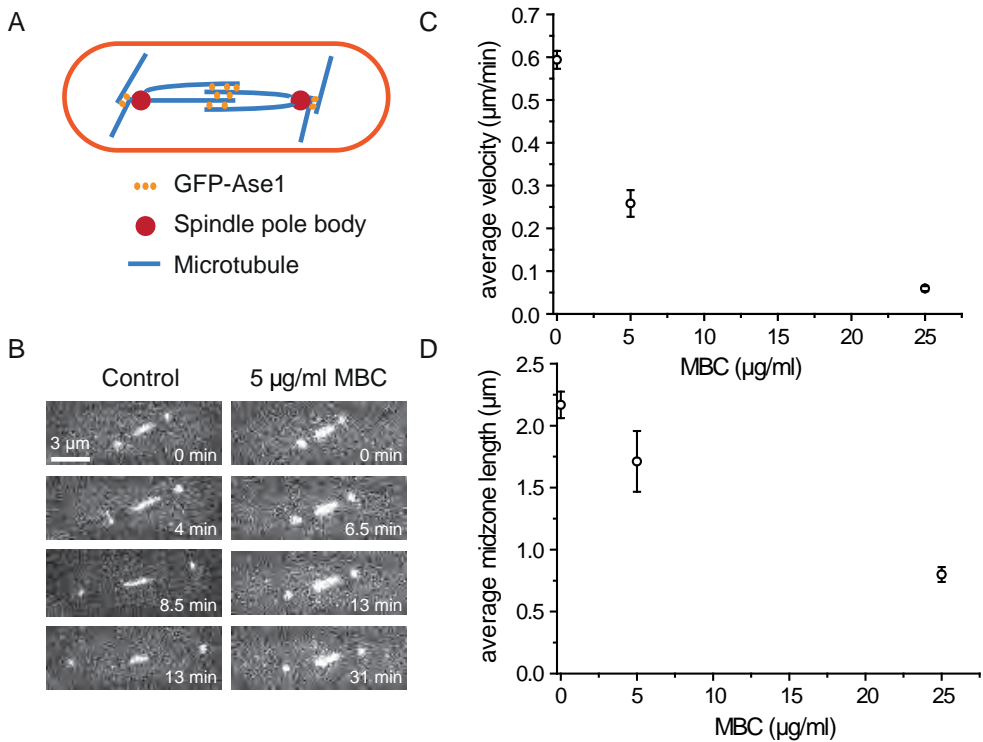


Figure 1 Dose-dependent decrease of spindle elongation velocity by MBC in fission yeast.

(A) A schematic representation of *S. pombe* mitosis. Ase1 is present on antiparallel interpolar microtubules within the spindle midzone and on astral microtubules near the spindle pole bodies. (B) Snapshots of anaphase-B cells expressing GFP-ase1 in absence of MBC (control) and with 5 µg/ml MBC. (C) Spindle elongation velocity at three different MBC concentrations. Error bars indicate SE ($n \geq 5$ spindles per condition). (D) Midzone length of spindles analysed in C. Error bars indicate SE.

centration of 1.5 μM . Strikingly, using polarity-marked microtubules we observed both minus-end and plus-end-directed motion of motors but no switches in directionality during the observation time of 10 min (Fig 2B). The velocity of gliding was slightly different for the two directions in our standard buffer containing MRB80 and 72mM KCl ($1.17 \pm 0.33 \mu\text{m}/\text{min}$; $\pm\text{SE}$; $N=37$ for plus-end directed and $1.49 \pm 0.53 \mu\text{m}/\text{min}$; $N=18$ for minus-end directed gliding; $p < 0.05$). Bidirectional gliding was earlier reported for kinesin-5 motors from budding and fission yeasts and similarly to *Sc-Cin8*, we observed that minus-end-directed motion became more prevalent at higher ionic strength (Figure 2C) (Gerson-Gurwitz *et al.*, 2011; Roostalu *et al.*, 2011; Fridman *et al.*, 2013; Edamatsu, 2014). Because recombinant N- and C-terminal fusions of GFP and klp9 were not motile we could not simply establish whether individual klp9 motors moved towards microtubule minus-ends like other kinesin-5 motors from yeasts. Nonetheless, our data showed that klp9, which was previously classified as a kinesin-6 motor based on the presence of extended loops in the N-terminal kinesin motor domain, has characteristics of kinesin-5 motor proteins (Fu *et al.*, 2009). We therefore reinvestigated the assignment and searched for homologies outside the motor domain. A BASS tetramerization domain was found in the C-terminus of klp9 that is a hallmark of kinesin-5 motors (Supplemental Figure 1) (Scholey *et al.*, 2014). Surprisingly, the catalytic motor domain of klp9 is directly connected by a short neck linker to the BASS domain without an intermediate neck coiled coil dimerization domain. The dimeric parallel coiled-coils at both ends of the BASS domain may have taken over their function, creating an atypically short kinesin-5 motor with a length of only 633 amino acids.

Klp9 induces relative sliding of microtubules

Next, we investigated the ability of klp9 to slide microtubules along each other in a relative sliding assay. We observed the interaction of short stabilized microtubules ('transport microtubules') with long surface-immobilized microtubules ('surface microtubules') in the presence of varying amounts of klp9 (Figure 3A-D). About 60 to 80 percent of the transport microtubules moved unidirectionally towards one end of the surface microtubule. A small percentage of transport microtubules alternated their direction while sliding and the remainder did not move. Mobile and immobile microtubules in relative sliding assays were previously shown to respectively correspond to an antiparallel and parallel geometry (Kapitein *et al.*, 2005; van den Wildenberg *et al.*, 2008; Hentrich and Surrey, 2010). In agreement we observed transport microtubules that flipped by 180° causing a switch from mobile to immobile or the reverse. The large percentage of mobile microtubules therefore indicated a preference for forming antiparallel microtubule pairs similar to what has been shown for the

kinesin-5 motor KLP61F (van den Wildenberg *et al.*, 2008). Interestingly, the sliding velocity for unidirectional moving microtubules increased from $1.12 \pm 0.21 \mu\text{m}/\text{min}$ at a *klp9* concentration of 150 nM to a plateau of around $2.7 \pm \mu\text{m}/\text{min}$ for concentrations above 1.5 μM (Figure 3E). This indicated that *klp9* motors acted cooperatively to generate sliding.

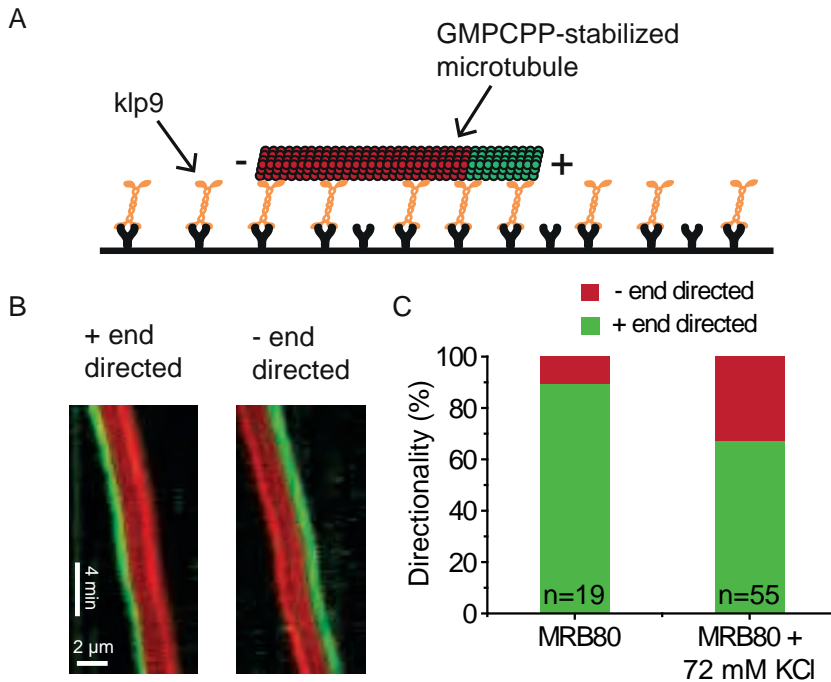


Figure 2 Bidirectional gliding of microtubules by *klp9*. (A) A schematic representation of the gliding assay with *klp9* (orange tetramer) attached to a glass surface via anti-his-antibodies (black Y) and a polarity-marked, GMPCPP-stabilized microtubule (red and green segment) gliding on top. (B) Kymographs of surface gliding events showing plus (left) and minus end-directed (right) motion of motors. The plus-ends of microtubules are marked in green. (C) Percentage of plus and minus end-directed events for different ionic strength buffers (n=19 MTs in MRB80, n=55 MTs in MRB80 + 72 mM KCl, difference is significant $p < 0.05$).

Ase1 increases and decreases sliding velocity depending on its concentration

We next introduced ase1 cross linkers to the relative sliding assay since we expected that its activity might be essential to explain our results in fission yeast. To investigate how sliding is affected by the presence of ase1 we added transport microtubules and klp9 (150nM) to surface microtubules that were covered with varying levels of ase1 (Figure 4A). The presence of ase1 at high levels (>10 nM) decreased the velocity of unidirectionally moving microtubules similar to what has been described for ncd-driven sliding in presence of ase1 (Figure 4E) (Braun *et al.*, 2011). However, the sliding velocity was surprisingly increased by low levels of ase1. At 3 nM ase1, the sliding velocity was 48% higher than in its absence ($p < 0.05$). A similar decrease in velocity was reported for microtubule sliding by ScCin8 in cell extracts lacking Scase1 (Gerson-Gurwitz *et al.*, 2011). Moreover, spindle elongation rates are lower in ase1 Δ cells (Loiodice *et al.*, 2005; Syrovatkina *et al.*, 2013). Ase1 may thus optimize motor action either by controlling the distance between overlapping microtubules or directly through its proposed binding to klp9 (Fu *et al.*, 2009).

Passive crosslinkers induce bidirectionality in klp9-driven sliding

The motion of transport microtubules was counted as bidirectional if they switched direction during the observation time of 20 minutes (Supplemental movie 1). This was not observed at a low level of klp9 in absence of ase1 (150 nM) (Figure 4D). Remarkably, for the same motor concentration in combination with a low amount of ase1 (3 nM), 23 % of the microtubules moved bidirectionally whilst at higher crosslinker levels (54 nM ase1) the phenomenon was absent again (Figure 4, B and D). Instead, at this higher concentration a larger fraction of immobile seeds was observed. Possibly, klp9 can generate less force towards minus ends and sliding in this direction may be selectively slowed down by increasing amounts of ase1. Since both ase1 and klp9 as well as their homologues in budding yeast reportedly interact with each other, we hypothesized that this interaction may stimulate bidirectional motion under the right conditions (Fu *et al.*, 2009; Khmelinskii *et al.*, 2009). Experiments with klp9 and AtMAP65-1 crosslinkers showed however a similar tendency for bidirectional motion (Figure 4, C and D). This related microtubule bundling protein from plants was not expected to associate with klp9 as it lacks homology with the C-terminus of ase1 containing the interaction domain (Fu *et al.*, 2009). The physical presence of crosslinkers may thus be sufficient to trigger bidirectional switching. Passive crosslinkers do therefore not just slow down motorized transport by klp9, but interfere in more intricate ways.

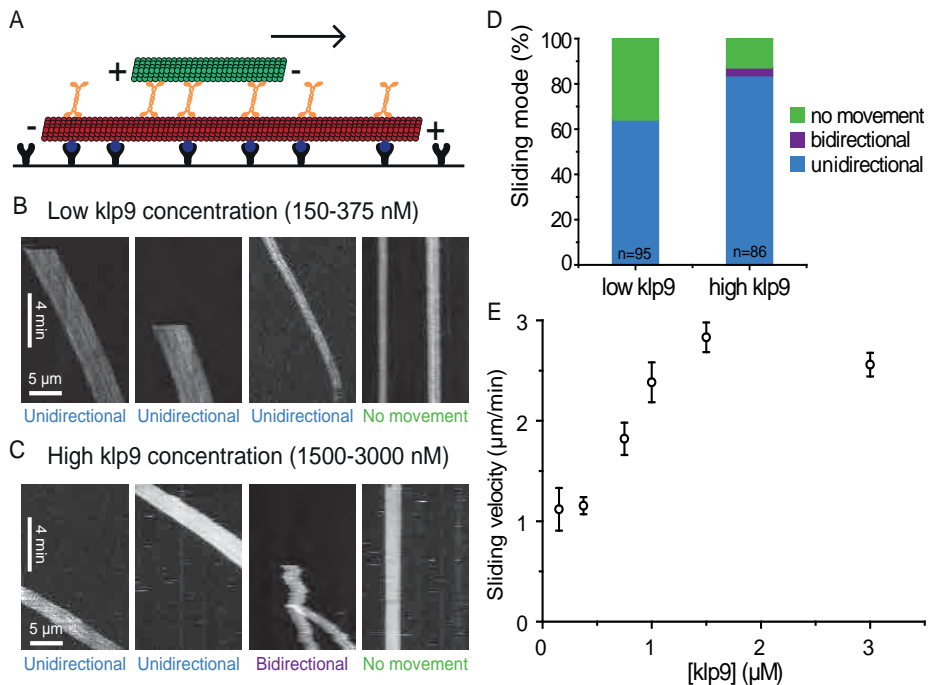


Figure 3 Klp9 drives relative microtubule sliding. (A) A schematic representation of the relative sliding assay. A long biotinylated microtubule (red with blue biotin, referred to as surface microtubule) is attached to the surface with antibodies against biotin (black Y). Klp9 (orange) transports a short microtubule (green, referred to as transport microtubule) over a longer surface-adhered microtubule. The surface microtubule is labelled with Alexa 647, the transport microtubule with Alexa 568 and klp9 is unlabelled. (B) and (C) Kymographs of relative sliding at low (150-375 nM) and high (1500-3000 nM) klp9. Surface microtubules are not shown. (D) Percentage of microtubules that did not move, moved unidirectionally or moved bidirectionally in relative sliding assays with either low (150-375 nM; n=95) or high (1500-3000 nM; n=86) concentrations of klp9. The difference in bidirectional switching was not significant ($p < 0.05$). (E) Sliding velocity of unidirectionally moving transport microtubules for different klp9 concentrations. Error bars indicate SE.

Ase1 prevents microtubule plus ends from sliding apart

Thus far we analysed the motion of transport microtubules whose length fully overlapped with the surface microtubule. We next observed partial overlaps that formed when unidirectionally sliding microtubules moved beyond the end of the underlying microtubules. But first we established the direction of sliding by using polarity-marked transport microtubules. Of the microtubules that moved unidirectionally, the majority (9 out of 10) moved with their minus-end leading indicating that the

formed partial overlaps primarily consisted of overlapping microtubule plus ends, as in spindles (Supplemental Figure 2). After microtubules started to slide apart we observed three possible outcomes: 1) sliding continued and the transport microtubule immediately detached after the overlap was reduced to zero length (detachment), 2) like 1, but the very ends of both microtubules remained attached for some time while the transport microtubule pivoted around the point of interaction, (pivoting) or 3)

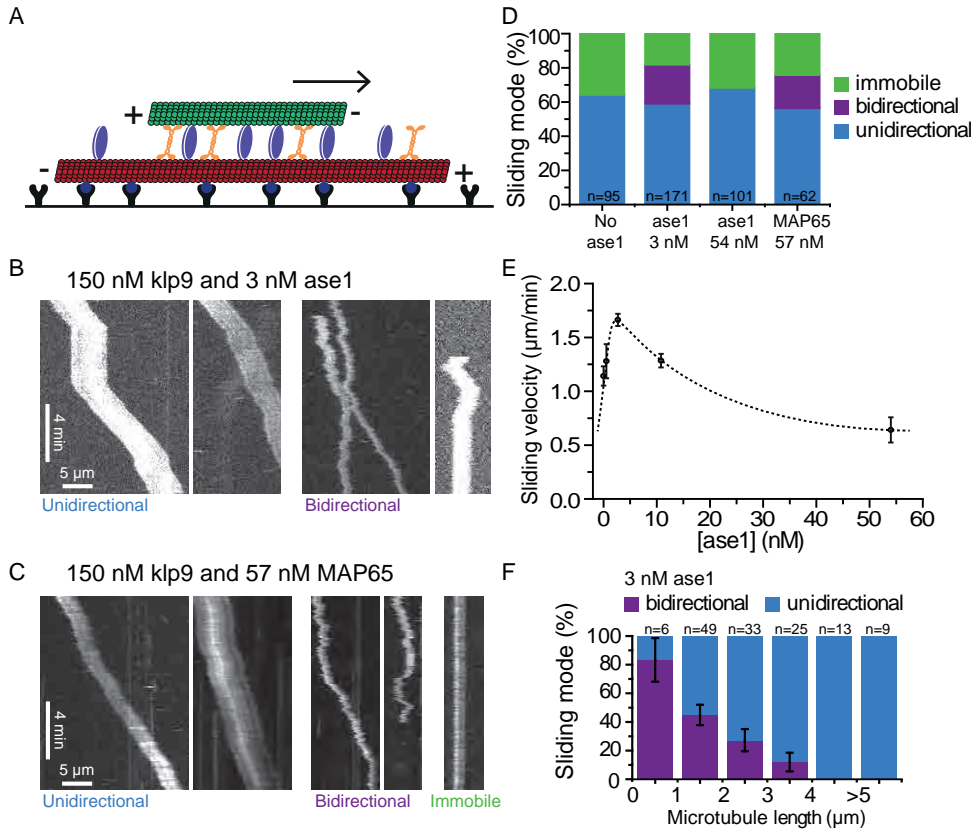


Figure 4 Relative sliding in presence of ase1. (A) A schematic representation as in figure 3A. Ase1 bundling proteins (blue) are simultaneously present. (B) and (C) Kymographs of sliding transport microtubules at 150 nM klp9 and 3 nM ase1 (B) or 57 nM MAP65 (C). Surface microtubules are not shown. (D) Percentage of microtubules that were immobile, moved unidirectionally or moved bidirectionally in relative sliding assays without bundling protein, with ase1 (3nM and 54 nM) and with MAP65 (57 nM). All experiments were done at a klp9 concentration of 150 nM. (E) Sliding velocity of unidirectional transport microtubules at increasing ase1 concentrations. Klp9 concentration was 150 nM. Error bars indicate SE. (F) A length histogram of transport microtubule that exhibited unidirectional or bidirectional sliding. Data from sliding experiments in the presence of 150 nM klp9 and 3 nM ase.

the transport microtubule switched its directionality frequently causing oscillations in overlap length (back and forth motion) (Figure 5, A-E and Supplemental movies 2-4). The relative occurrence of these three outcomes was compared for low klp9 concentrations (150 - 375 nM) in absence and presence of ase1 (3 nM) and for high klp9 concentrations (1500 -3000 nM) in absence of ase1. In all three cases, about 50-60% of the partial overlaps showed pivoting, a phenomenon previously observed for the *Xenopus* kinesin-5 Eg5 (Kapitein *et al.*, 2005). A striking difference was found in the probability of immediate detachment, which decreased from 25% in absence of ase1 to only 2% with ase1 present (Figure 5F). All three types of partial overlaps eventually ceased to exist when the transport microtubule disconnected or flipped over into a parallel configuration. Their average lifetime was increased about ten times by the presence of ase1 to a value of 47.5 minutes (Table 1). So although klp9 could sustain connections between microtubule plus ends by itself, the stability of the connection was greatly enhanced by the presence of ase1.

Directional switching correlates with overlap length

Back and forth motion of transport microtubules in partial overlaps was observed both in the presence (50% at 3 nM ase1) and absence of ase1 (13% and 32% respectively at low and high klp9 concentrations, Figure 5F). Backwards motion in partial overlaps was thus primarily driven by klp9 and not by ase1-generated forces (Lansky *et al.*, 2015). This notion was further supported by its velocity, $1.42 \pm 0.66 \mu\text{m}/\text{min}$

Table 1 Ase1 increases the life time of partial overlaps. Partial overlaps were formed when a transport microtubules reached the end of a surface microtubule (number of events from figure 5F). Partial overlaps ceased to exist when the transport microtubule disconnected or flipped over into a parallel configuration (number of partial overlap terminations). Sometimes overlaps terminated directly when they were formed and sometimes partial overlaps lasted until the end of the experiment. Both events were included in the analysis. The average lifetime of partial overlaps was calculated by dividing the total observation time of microtubules in the partial overlap state by the number of termination events. Conditions: low (150-375 nM) and high klp9 (1500-3000 nM) klp9 without ase1, and low klp9 (150 nM) and 3 nM ase1.

	Number of partial overlaps	Number of partial overlap terminations	Average attached time (min)
low klp9 3 nM Ase1	56	12	47.5
low klp9	16	11	5.3
high klp9	31	20	5.9

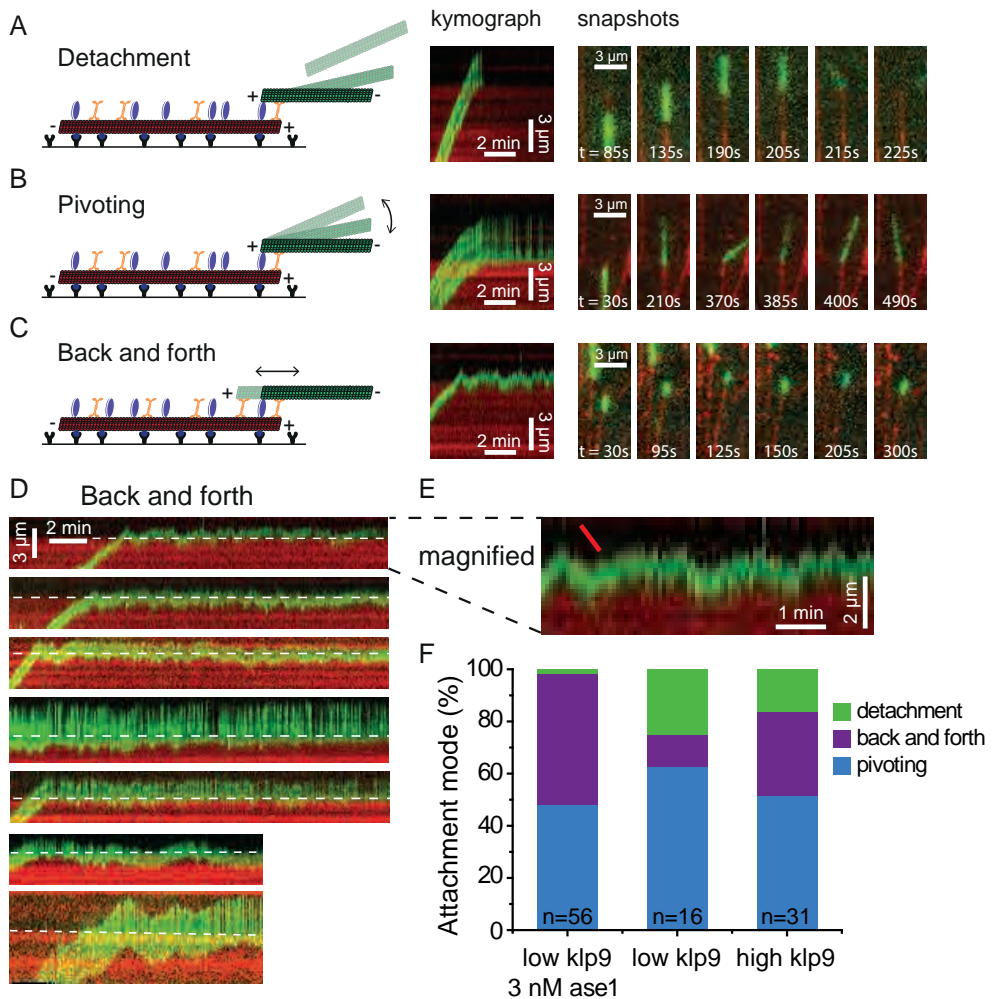


Figure 5 Ase1 prevents microtubule plus ends from sliding apart (A), (B) and (C) Schematic representation and an example of detachment (A), pivoting (B), and back and forth movement (C). For each event a kymograph and corresponding snapshots are shown. $t=0$ is the start of the kymograph. Transport microtubules are green and surface microtubules are red. Experiments were done at 150 nM klp9 and 3 nM ase1. (D) Several examples of back and forth events with 150 nM klp9 and 3 nM Ase1. The dashed lines indicate the end of the underlying microtubule. (E) Magnification of D showing backward sliding events. The red line indicates the average velocity of backwards sliding events in partial overlaps ($1.42 \pm 0.66 \mu\text{m}/\text{min}$; \pm SD; $N=24$ events from the kymographs in D). (F) Percentage of detachment, pivoting or back and forth motion in partial overlaps. Data are shown for experiments without ase1 at either low (150-375 nM) or high (1500-3000 nM) klp9 concentration, and experiments with 3 nM ase1 and 150 nM klp9.

(Figure 5E), which was in agreement with minus end-directed motion in our gliding assays. Directional switching in absence of *ase1* was only very rarely observed for transport microtubules that still overlapped fully with surface microtubules (Figure 3D). Apparently the shortening of partial overlaps provided a sufficient physical cue to activate directional switching under these conditions. To find further support for such a mechanism we reinvestigated directional switching observed in the “full overlap” geometry when *ase1* was present (Figure 4, B and D). This showed that the length of bidirectionally moving transport microtubules was significantly shorter compared to those that moved unidirectionally ($p < 0.05$) (Figure 4F). Directional switching therefore seems to be triggered by physical cues with both the presence of crosslinkers (*ase1* and *AtMap65-1*) and the length of overlaps as effectors.

Sliding is coupled to the dynamic state of microtubules

Now that we had established a system with *klp9* and *ase1* that efficiently prevented microtubule plus ends from sliding apart, we set out to investigate whether it could also couple the ends of dynamic microtubules, similar to a spindle midzone. For this we added dimly labelled free tubulin (15 μM) and GTP to the assay. The GMPCPP-stabilized sections of the transport and surface microtubules occasionally seeded microtubule growth (Figure 6A). These extensions dynamically switched between growth and shrinkage. The experiment proved to be very challenging but nonetheless we observed four partial overlaps in which growth and sliding occurred simultaneously (Figure 6, B and C). The brightly labelled seed section of the transport microtubules then continued to move outwards as growth enabled continuation of sliding. In these cases, the two seed sections became connected with a dynamic part. Frequently, the transport microtubule pivoted around the end of the seed section of the underlying microtubule (figure 6A and Supplemental movie 5). This indicated that the transport microtubule was growing whilst the surface microtubule was not. Moreover, it showed that sliding and growth occurred simultaneously while a minimal overlap length was maintained (Figure 6C). This was in agreement with the velocity of outward directed sliding ($1.57 \pm 0.46 \mu\text{m}/\text{min}$; $N=13$, time-weighted average \pm SD) being similar to the velocity of plus end growth at the used tubulin concentration ($1.42 \pm 0.21 \mu\text{m}/\text{min}$, $N=20$, time-weighted average \pm SD). Surprisingly, upon a catastrophe the overlap did not disappear, but the transport microtubule moved inwards again until the seed sections of both microtubules touched. Retraction was fast compared to outward sliding, and its average velocity of $10.14 \mu\text{m}/\text{min}$ ($N=6$) was in agreement with rates of microtubule shrinkage (Fygenson 1994). This type of motion was therefore likely driven by conformational changes of depolymerizing microtubule tips and facilitated by diffusing *ase1* proteins that fluidly link

microtubules (Grishchuk *et al.*, 2005; Kapitein *et al.*, 2005). After depolymerisation a new growth event could be initiated and several rounds of growth and shrinkage were observed before the overlap was lost. Our combined experiments thus demonstrate that the ends of passive, growing and shrinking microtubules remain connected in presence of klp9 and ase1 (Figure 5 and 6). Sliding is then respectively stagnating, outwards-directed or inwards-directed. We therefore show that sliding in partial overlaps is directly coupled to the dynamic state of microtubules.

Discussion

Essential to the proposed “growth-limited sliding” model for microtubule overlaps is the now demonstrated ability of microtubule plus ends to remain connected even when their rate of growth drops below the velocity of unrestrained sliding. Sliding can then stall when growth stalls and continuation of growth will fuel new sliding. Our relative sliding assay showed that separation of microtubules could be prevented if the direction of microtubule transport is switched when microtubules move apart (Figure 5). Overlaps then start to oscillate in length and the triggered change in motor activity may also contribute to the observed pivoting of microtubule ends. Directional switching of microtubule transport was previously observed in gliding assays with surface-adhered motors (Gerson-Gurwitz *et al.*, 2011; Roostalu *et al.*, 2011). We now show that the phenomenon also occurs in the biologically relevant sliding geometry in which two microtubules overlap and propose a function in regulating forces within overlaps of bipolar microtubule networks in cells. How directional switching is controlled is largely unknown. The team-size in which motors operate is a proposed effector (Roostalu *et al.*, 2011). Our results point in the same direction: when partial overlaps shorten by sliding they will likely shed motors and this may explain the observed oscillations in length (Figure 5). Switching is likely a cooperative process that requires a form of communication between motors. It will be interesting to find out how cooperative sliding (Figure 3E) and directional switching are related on a molecular level.

The ability for ends to remain connected within an overlap was demonstrated previously for non-dynamic microtubule minus ends that were moved apart by minus end-directed ncd motors in the presence of ase1 (Braun *et al.*, 2011; Lansky *et al.*, 2015). Here we demonstrate that plus ends can also stay connected and that ase1 prolongs this attachment as well. Forces generated by ase1 counteract sliding forces pro-

gressively when microtubules move apart. Since these forces are comparable in magnitude to forces generated by one to several kinesin-5 motors they may be required to increase the lifetime of overlaps for sliding by klp9 (Lansky *et al.*, 2015; Shimamoto *et al.*, 2015; Figure 6). An intriguing possibility is that forces by ase1 helped to trigger klp9 directional switching when microtubules moved apart. However, ase1 also increased the occurrence of directional switching in overlaps of constant length showing that cross linkers in general can sensitize klp9 for switching (Figure 4D). Clearly the presence of crosslinkers is an additional effector of directional switching.

Our analysis of spindle elongation in fission yeast suggested that the cellular rate of inter-microtubule sliding is dependent on microtubule growth. Growth-limited sliding in cells may act as a safeguard to preserve overlaps under challenged conditions in which microtubule growth rates are low. However, it may also be a way to regulate sliding under non-challenged conditions. This could explain the discrepancy between the rate of microtubule sliding by klp9 in *in vitro* assays and the slower rate of spindle elongation in cells (Figures 1C and 3E). On one hand, sliding may be slowed down in cells because forces are generated to push chromosomes apart. On the other hand, microtubule growth within the dense midzone of interdigitating microtubules might occur at rates that limit spindle elongation. During anaphase up to about 14 microtubules are packed in a square lattice in which the distance between antiparallel microtubules is approximately 20 nm and likely dictated by ase1 (Ding *et al.*, 1993). The motion of all microtubules is therefore coupled and one microtubule whose growth lags behind may slow down the sliding of all. It is worth noting that the short length of klp9 may have evolved to work in the compact lattice of anaphase-B spindles whilst its partner kinesin-5, cut7, may work preferentially on the more irregular spaced lattices of metaphase spindles. The length of the BASS domain in klp9 is 26 nm, whilst pairs of motor domains are spaced at 60 nm in *drosophila* KLP61F (Scholey *et al.*, 2014). The higher velocity of klp9-induced sliding in presence of small amounts of ase1 also hinted that the lengths of klp9 and ase1 may be tuned to each other (Figure 4E).

Our work suggests that cells may limit polymerization of interpolar microtubules to regulate rates of spindle elongation and spindle flux while maintaining their overlaps. Sliding would then be expected to speed up if growth is stimulated in the midzone. This provides an interesting explanation for the increased rate of poleward microtubule flux throughout anaphase in cells that lack the microtubule depolymerase kinesin-8 (Wang *et al.*, 2010). The concept of “growth-limited sliding” thus provides a new perspective for understanding the balance of forces in spindles.

Materials and methods

Protein purification

Recombinant histidine-tagged full-length *S. pombe* ase1 (pPT179, Fu *et al.*, 2009), klp9 (pPT200, Fu *et al.*, 2009) and *Arabidopsis thaliana* MAP65-1 (Stoppin-Mellet *et al.*, 2013) were expressed in *E. coli*. The proteins were immobilized on Ni-NTA agarose beads and eluted in 20 mM phosphate buffer with 500 mM NaCl and 500 mM imidazole. Porcine tubulin was purified as described previously (Castoldi and Popov, 2003) and labelled with Alexa Fluor® 568, Alexa Fluor® 647 and biotin (Fisher Scientific) (Hyman *et al.*, 1991; Peloquin *et al.*, 2005).

Microtubules

For short ‘transport’ microtubules and long ‘surface’ microtubules see chapter 2. Polarity marked microtubules were made from short microtubules labelled with Alexa 647. These microtubules were diluted 10x in MRB80 and 0.2 µM Alexa 568 tubulin and 0.2 µM GMPCPP were added. This mixture was again incubated for 30 min at 37 °C and centrifuged in a Beckman airfuge at 100,000g for 10 min. The pellet was re-suspended in 100 µl MRB80 with 1 mg/ml casein and the desired KCl concentration.

Gliding assays

A flow cell with silanized glass was incubated for 5 min with 20 µg/ml of 6x-His epitope tag monoclonal antibody (Fisher Scientific) in PBS. The flow cell was flushed with MRB80 and 1.5 µM his-tagged klp9 in MRB80. After 10 min, non-adsorbed klp9 was flushed out using MRB80 with the desired KCl concentration. Finally, polarity marked microtubules with 2 mM ATP (Jena Bioscience), 1 mg/ml casein and oxygen scavenging system (35 mM glucose, 16 µg/ml catalase, 166 µg/ml glucose oxidase) were flushed in.

Relative sliding assays

See chapter 2 for protocol. An objective heater kept the microscope objective at 30 °C for polymerization assays.

Fission yeast experiments

Cells expressing GFP-ase1 (PT738) were grown as described previously (Janson *et al.*, 2007). Spindle lengths were measured between the centres of the SPB-associated GFP-ase1 signals. Spindle elongation velocity was analysed over the time during which the spindle elongated from 5 µm to 7 µm. The length of the spindle midzone,

corresponding to the length of the central section of GFP-ase1, was measured when the spindle reached a length of 6 μm . For this a line scan of the fluorescence intensity was generated over each spindle (thickness 5 pixels). Intensity values were background-subtracted and normalized to the peak intensity in the midzone. The midzone length was measured in between the two points where the normalized intensity reached a value of 0.5.

Imaging

Flow cells were imaged by using an inverted fluorescence microscope (Nikon eclipse Ti) with a Nikon 100x oil immersion 1.49 NA TIRF objective in combination with an QuantEM:512C (Photometrics) EMCCD camera controlled by Metamorph image acquisition software (Molecular Devices Corporation). For TIRF illumination, three DPSS lasers were used: 473 nm (Cobolt Blues), 561 nm (Cobolt Jive), 638 nm (Lasos RLD-XT 38). Dual- or Tri-colour images were acquired sequentially through a quad-band dichroic mirror (zt473/561/633/748rpc-TIRF, Chroma Technology) and the appropriate bandpass filters. For gliding assays, the time between frames was 2 s, for relative sliding assays, it was 5s. Kymographs were made using imageJ image analysis software. Velocities were calculated by determining the slope of the moving microtubules in kymographs. For calculating backward sliding velocities (Figure 4E), only events of 5 frames or longer ($\geq 20\text{s}$) were taken into account.

Fission yeast cells were imaged with a Yokogawa CSUX1 spinning disk and Photometrics Evolve 512x512 camera attached to a Nikon eclipse Ti with a Nikon 100x oil immersion 1.45NA objective lens. A 491nm laser was used for excitation. Cells were imaged every 30 seconds. Shown are maximum projections of a 6-plane z-stack with 0.5 μm spacing.

Statistics

For comparing percentages, we tested the null hypothesis that the proportions are the same with a confidence interval of 95% ($p < 0.05$) using a binomial test (Figure 2C). Similarly, we tested the null hypothesis that the proportions of bidirectional switching are the same with a binomial test (Figure 3D). To compare velocities, an independent-samples Kruskal-Wallis test was performed in SPSS (gliding and Figure 4E). Microtubule lengths distributions were compared with an independent-samples Mann-Whitney U test in SPSS (Figure 4F).

Acknowledgements

We thank Karsten Kruse and Denis Johann for discussions, Zdenek Lansky for advice on the experiments, Juliane Teapal and Piotr Topolewski for performing exploratory experiments, and Virginie Stoppin-Mellet for providing the MAP65-1 expression plasmid. The work has been financially supported by HFSP grant RGP0026/2011 to MEJ.

Captions supplemental movies

Supplemental movie 1 Bidirectional and unidirectional sliding. Corresponds to Figure 4B. In the same sample unidirectional (bottom left) and bidirectional sliding (top right) are observed. Time is indicated in min:sec.

Supplemental movie 2 Detachment.

Corresponds to Figure 5A. Time is indicated in min:sec.

Supplemental movie 3 Pivoting.

Corresponds to Figure 5B. Time is indicated in min:sec.

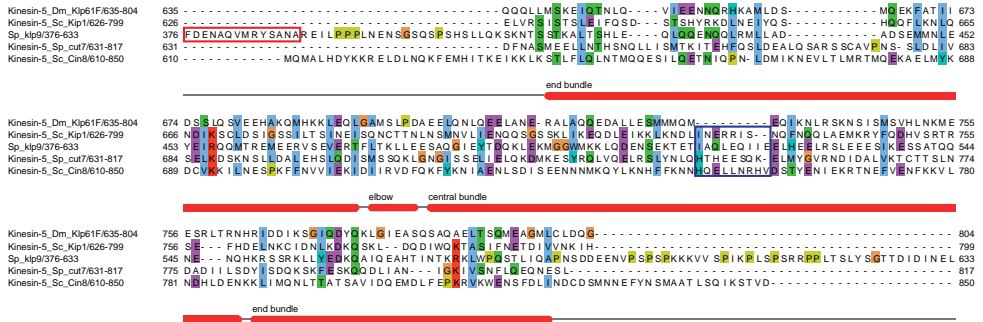
Supplemental movie 4 Back and forth.

Corresponds to Figure 5C. Time is indicated in min:sec.

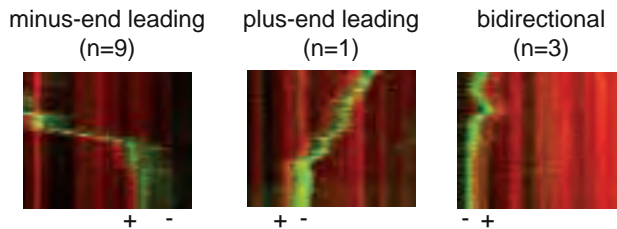
Supplemental movie 5 Dynamic relative sliding.

Corresponds to Figure 6, B and C. Time is indicated in min:sec.

Supplemental figures



Supplemental Figure 1 Multiple sequence alignment of Spklp9, three kinesin-5 motors from fission and budding yeast and the reference kinesin-5 klp61f from *D. melanogaster*. The N-termini of Spklp9 and Sccin8 were manually aligned to the alignment made by Scholey et al. for klp61f, Skip1 and Spcut7. The red box around the first residues from klp9 indicates the C-terminus of the motor domain. Many residues that form hydrophobic and ionic interfaces in the klp61f structure are conserved in the klp9 sequence (Scholey et al., 2014). A yeast specific feature, but also present in *X. Laevis* (not shown), is the 7-9 residue long insert in the middle of the central bundle.



Supplemental Figure 2 Kymographs of polarity-marked transport microtubules in a relative sliding assay with klp9 and ase1. Surface microtubules and plus-ends of transport microtubules are both shown in red. Transport with the minus or plus end leading indicates respectively plus end or minus end-directed motor action. The number of observed events are shown between brackets.

Chapter 5

Motor proteins influence ase1 localization on microtubules

Aniek Jongerius, Christopher Zapp and Marcel E. Janson

Abstract

In vivo, many microtubule associated proteins are active on the same microtubule. In this crowded environment, proteins could influence each other by occupying binding sites. Simulations showed before that motor proteins can influence diffusing proteins by introducing a bias in their diffusion. Ase1 is such a diffusive protein and we investigated the mutual interaction between ase1 and a motor protein on single microtubules. We see that ase1 can form accumulations at one microtubule end in presence of motor proteins. On the other hand, motor proteins are slowed down by ase1, but long processive runs are still possible. This shows that motors can influence the localization of diffusive proteins, which could be a method to prime microtubule ends for microtubule bundling in the case of ase1.

Introduction

In cells many different types of microtubule associated proteins (MAPs) bind simultaneously to microtubules. This results in a crowded microtubule lattice and steric interactions between different MAPs. When the density of MAPs is high enough we expect proteins to influence each other. In chapters 3 and 4 we created overlaps with multiple proteins, but it is not known if they influence each other's movement within these overlaps. Of special interest are interactions between active MAPs, i.e. motors that translocate in a directed manner by using ATP, and passive MAPs that bind to microtubules without directed motion. The effect of lattice crowding on motor proteins has been studied by creating 'roadblocks' on single microtubules in different ways. In general, roadblocks decrease motor velocity, but the molecular mechanisms may differ depending on the mode of attachment of the proteins that form the roadblock. As model roadblock streptavidin firmly adhered to biotin conjugated to tubulin was studied. Streptavidin introduces a pause in motor movement, after which some motors pass the obstacle (Korten and Diez, 2008). More recently it has become clear that many MAPs do not bind firmly to microtubules but instead have a diffusive mode of interaction (Asbury *et al.*, 2006; Kapitein *et al.*, 2008; Janning *et al.*, 2014). So perhaps the roadblock picture, a nonmobile object in the path of the motor protein, is not suited for these proteins. With diffusive proteins, the situation might be more like a traffic jam. An example is the neuronal MAP tau, a passively diffusing protein which has been observed to result in either motor detachment or directional reversal (Dixit *et al.*, 2008). Other examples of diffusive proteins that might influence motor behaviour are the MT bundling protein family PRC1/ase1/MAP65, and the microtubule-kinetochore anchoring protein dam1 (Asbury *et al.*, 2006; Kapitein *et al.*, 2008).

So far work combining passive and active MAPs focussed on the analysis of motor stepping in presence of potential roadblocks. How motor proteins on the other hand influence the motion of passively diffusing proteins like tau and PRC1/ase1/MAP65 is not known. When a motor protein is bound, it occupies a lattice site. On one hand, this site is not available for the attachment of proteins from solution. If a motor is capable of introducing a gradient in localization, this would affect MAP attachment inhomogeneously along the microtubule. On the other hand, we expect that a diffusing protein at a neighbouring site temporarily cannot move to the site occupied by the motor protein. Diffusing to the other side is possible, provided that this site is unoccupied. This is known as a totally asymmetric exclusion process TASEP (MacDonald *et al.*, 1968). Restricting the direction of diffusion potentially creates a bias

in the diffusive movement by introducing a ratchet effect. So far the implications of the site exclusion effect for MAPs on microtubules have only been explored using simulations. These simulations show that this effect can lead to an excess of the passive diffuser at the microtubule end towards which the motor is moving (Johann *et al.*, 2014). Thus, in theory, this can lead to a segregation of a passive diffuser and the motor proteins.

We performed in vitro experiments on surface attached microtubules using a motor protein and a diffusive MAP. The motor we used was DK4mer. This is a chimera consisting of the stalk with tetramerization domain of kinesin-5 motor eg5, and motor domains and linkers of kinesin-1 (Thiede *et al.*, 2013). The diffusive protein we used was ase1, the yeast homologue of the PRC1/ase1/MAP65 family. We investigated the mutual impact of kinesin and ase1 on velocity and localization of both proteins.

Results

DK4mer is slowed down by ase1 in a dose dependent manner

To observe how the passive linker ase1 affects motor motion, we studied ase1 and DK4mer on single microtubules. DK4mer was used as it is very processive, fast and plus end-directed because of the kinesin-1 motor heads, and tetrameric because of the eg5 stalk (Thiede *et al.*, 2013). The processivity simplified the analysis of motor motion and the tetramerization ensured that the motor is bulky and is likely to interact with other proteins via exclusion. We imaged single DK4mer-GFP proteins on single microtubules (Figure 1A) with varying concentrations of ase1.

Kymographs showed that the higher the ase1 concentration, the smaller the number of motor proteins that landed on the microtubule and made a run (Figure 1C). This indicated that ase1 binding can exclude motors from binding to the microtubule lattice. The K_D of ase1 on single microtubules is 5.5 nM (Lansky *et al.*, 2015), so at 54 and 270 nM, saturation of the microtubule lattice was expected. At 270 nM ase1, DK4mer-GFP traces showing directed motion were absent. The high amount of ase1 prevented DK4mer from binding to the microtubule. At 54 nM ase1, we also expected near saturation of ase1 on the microtubule. Surprisingly, motors landed on the microtubule and continued in processive runs. Even though the microtubule was expected to be crowded with ase1, motor runs were possible. This suggested that ase1 mainly excluded motors from binding the microtubule, but when motors did bind, the crowded ase1 environment did not prevent directed runs. At 5 nM ase1, where

about half the lattice sites is expected to be occupied with ase1, even more runs were observed. Without ase1 the number of DK4mer runs was clearly higher. This was consistent with motor exclusion by ase1 binding.

From the DK4mer-GFP traces in the kymographs the velocity was determined. When pauses and/or velocity changes occurred, the trace was divided into sections. The velocity in these sections was calculated and weighted with the duration of each section when calculating average values. Only motors that moved at some point were used in the analysis. Without ase1, DK4mer moved at an average velocity of $0.477 \pm 0.020 \mu\text{m/s}$ (weighted average \pm SD, $n=44$, stalls not included), which is similar to the velocity reported by Thiede *et al.*, 2013 ($0.500 \pm 0.010 \mu\text{m/s}$). The distribution of velocities in Figure 1D showed that we observed stalling events ($v < 0.1 \mu\text{m/s}$) in presence of motors alone. Increasing ase1 concentration resulted in lower average velocities (Figure 1B) and longer, although not more, stalling events (Figure 1D). The average velocity decreased to $0.432 \pm 0.013 \mu\text{m/s}$ (weighted average \pm SD, $n=48$, stalls not included) at 5 nM ase1 and even further to $0.331 \pm 0.016 \mu\text{m/s}$ (weighted average \pm SD, $n=36$, stalls not included) at 54 nM ase1. This showed that the presence of ase1 had a dose dependent effect on DK4mer velocity. While fast runs were still possible with ase1, the frequency of lower velocity runs increased. The undisturbed runs lasted longer than expected when single ase1 dimers would form roadblocks, given the crowded ase1 environment. Even at ase1 densities near saturation at 54 nM, the motor made fairly long runs. This suggested that motors are not hindered substantially by ase1.

Diffusion of ase1 seems not biased by motor proteins

Next, we looked at the ase1 diffusion in presence of motor proteins to see if directed motion of ase1 is observed. Kymographs were made of ase1-GFP in experiments with and without motors. Individual ase1-GFP proteins could not be tracked because the density was too high. Qualitatively, kymographs of ase1-GFP with and without motors looked similar (Figure 2, A and B). Single ase1-GFP proteins moved to both directions in both cases. Sporadically a trace with clear directionality was observed both with and without motor proteins present (Figure 2, A and B). From our experiments we cannot conclude without a more detailed analysis of diffusion that ase1 movement is affected by motor motion. This suggested that the effect of motor motion on ase1 can only be a small bias in diffusion, if present at all.

To gain more insight, we estimated the number of motor proteins from kymographs without ase1 as in Figure 1C. When extrapolated to the concentration DK4mer used

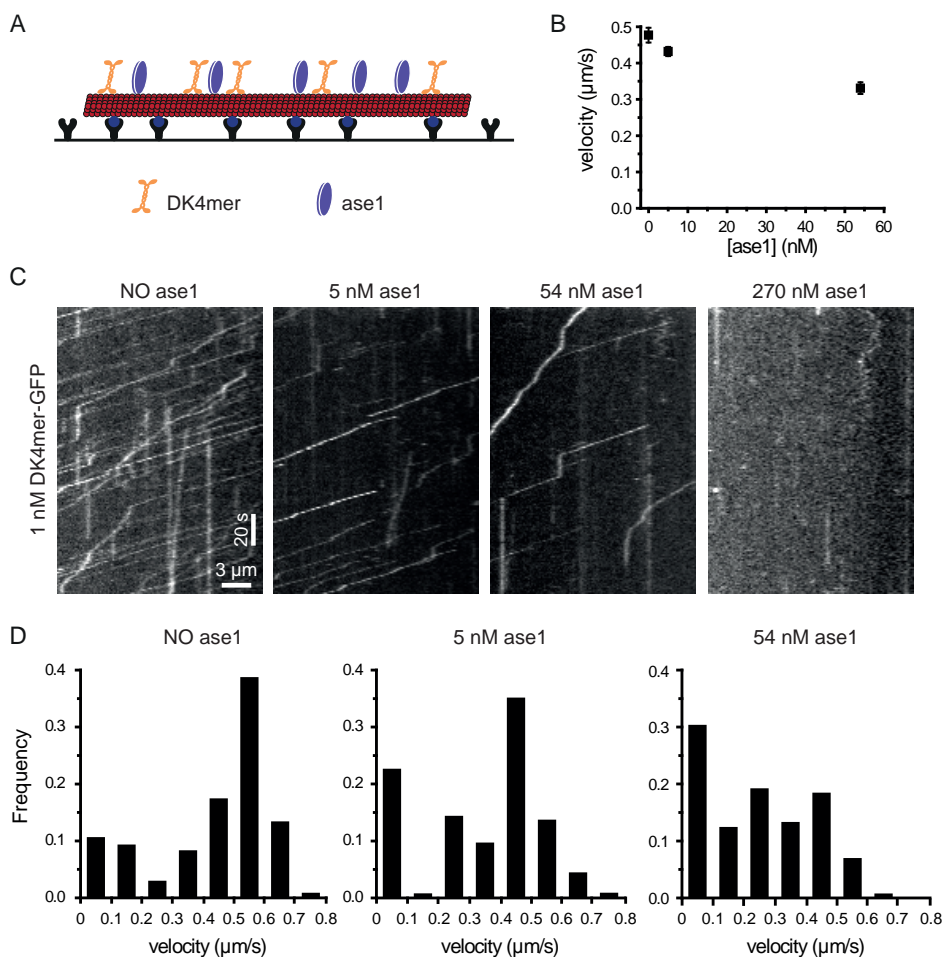


Figure 1 DK4mer-GFP slows down dependent on ase1. (A) A schematic representation of a single microtubule assay. A long biotinylated microtubule (red with blue conjugated biotin, referred to as surface microtubule) is attached to the surface with antibodies against biotin (black Y). Ase1 bundling proteins (blue) diffuse over the surface microtubule, while DK4mer-GFP (orange tetramer) walks unidirectionally to the microtubule plus end. (B) DK4mer-GFP weighted average velocity \pm SD as calculated from the histograms in D, excluding the stalls ($<0.1 \mu\text{m/s}$). (C) Kymographs of DK4mer-GFP on single microtubules. DK4mer concentration was 1nM and ase1 concentration varied from 0-270 nM. (D) Histograms of DK4mer-GFP velocities as measured from the first three kymographs of C, plus other kymographs from similar experiments. See materials and methods for details on the analysis. The total duration of measured traces was 1085s without ase1, 903s at 5 nM ase1 and 916s at 54 nM ase1. The frequency at which velocities occur was normalized to the total duration per ase1 concentration.

in presence of ase1, this resulted in approximately 5 motor proteins per micrometre microtubule. This estimation is an upper limit, since we do not correct for possible exclusion by ase1. A micrometre of microtubule contains over 1500 lattice sites, so the density of motor proteins is quite low. Probably, this concentration of motor proteins is not enough to influence ase1 diffusion since encounters would be rare. We could not further increase motor density in our assay, because at 190 nM DK4mer sliding and curving of microtubules along the surface was observed. Apparently motors bound to the surface as well. This means that we could not reach the high motor concentrations that are probably needed for measurable drift of ase1 in our assays.

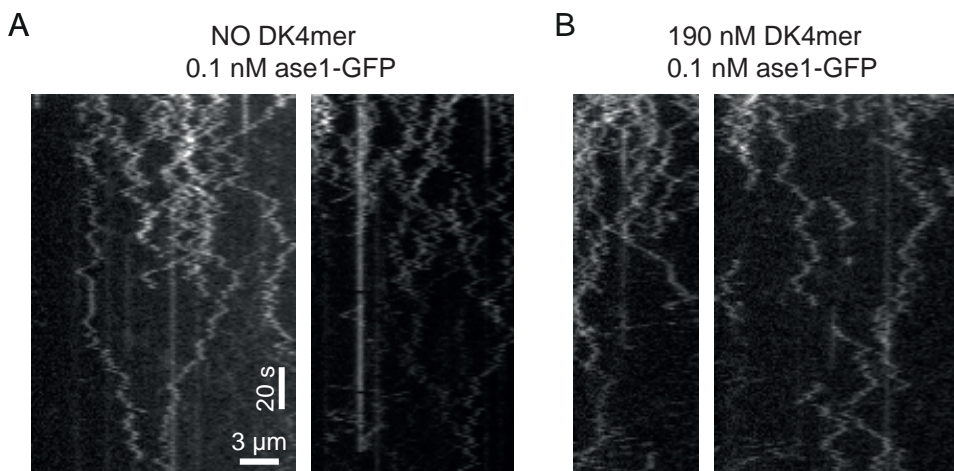


Figure 2 Ase1-GFP and DK4mer on single microtubules. (A) Representative kymograph of single microtubule assay with 0.1 nM ase1-GFP. (B) Representative kymograph of single microtubule assay with 0.1 nM ase1-GFP and 190 nM DK4mer.

DK4mer induces ase1 localization to the microtubule end

The kymographs of single ase1 mobility in presence of motor proteins did not show a clear drift induced by motor proteins. Simulations and theory predict that drift will cause a build-up of MAPs at microtubule plus ends in presence of plus end-directed motors because the ends of microtubules are diffusion barriers for ase1 motion. To find evidence for a drift we moved away from single molecule analysis and analysed the overall distribution of ase1 along microtubules. End accumulation of ase1-GFP became apparent when all frames of an image sequence (121 frames, 2 min total length) were averaged (Figure 3A). Not all experiments with exactly the same added protein concentrations showed end accumulation demonstrating that we were una-

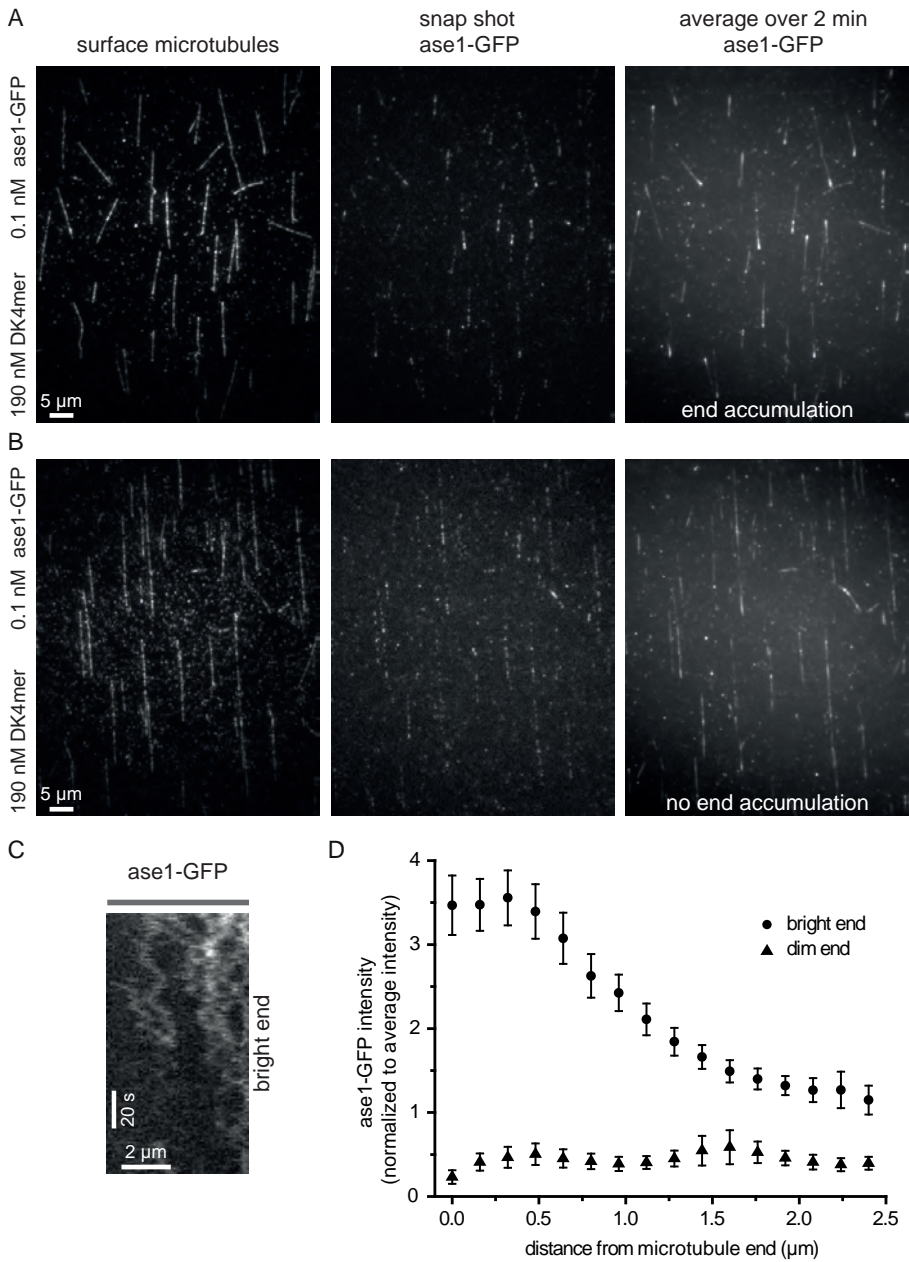


Figure 3 Ase1-GFP end accumulation with DK4mer. (A) and (B) Images of surface microtubules (Alexa 568) and ase1-GFP in single microtubule assays at 0.1 nM ase1-GFP and 190 nM DK4mer. The rightmost image is an average of 121 frames with 1s between frames of the ase1-GFP fluorescence. In A a clear end accumulation is seen, while in B end accumulation is not clear. (C) Kymograph showing ase1-GFP mobility on a microtubule in the experiment shown in A. The kymograph shows the full length of the microtubule. The bright end that is visible in the time-averaged image is on the right side. (D) Average ase1-GFP intensity \pm



ble to control experimental conditions, hindering reproducibility of the experiment (33% of the experiments showed end accumulation, Figure 3B). Nonetheless, in order to characterize the phenomenon we analysed many microtubules within one single movie that showed clear end accumulation to get a measure for the length scale of the accumulation. All microtubules over $5\ \mu\text{m}$ in this experiment were selected for analysis. First, the intensities along the line scans were time-averaged. Then, the fluorescence intensity of the brightest end and the adjacent $2.4\ \mu\text{m}$ of microtubule were averaged for all microtubules. The same was done for the other end of the microtubule. The resulting intensity plot showed a peak that was 3.5 times brighter than the average *ase1*-GFP intensity along the total length of the microtubule (Figure 3D). At the dimmer end, we saw a relatively flat curve at about 40% of the average intensity. Accumulation was much less evident from single frames of the movies (Figure 3A, B). Single *ase1*-GFP dimers diffuse near the bright microtubule ends indicating that end accumulations are dynamic steady state structures (Figure 3C).

To get a better understanding of how the motor can influence *ase1*, we looked at motor localization under similar conditions. DK4mer also accumulated at the microtubule end (Figure 4, A). The direction of motor movement showed that the motor accumulated at the microtubule plus end (Figure 4B). The accumulations were much more pronounced, with a peak of 7.7 times average intensity, and over a shorter length scale (Figure 4C). This experiment was done with a comparable (2-fold less) motor concentration as in Figure 3. Since *ase1* concentration is low in this experiment (1nM), we assumed that motors are not influenced by *ase1* presence, given our earlier results (Figure 1). Therefore, we expect the motor profiles in the experiment shown in Figure 3 to be similar, or slightly wider than that of the experiment in Figure 4C. Although we did not establish that *ase1* is accumulated at the microtubule plus end, we overlaid the *ase1* profile and motor profile to investigate how the two profiles may interrelate. We see that the *ase1* peak flattens in the region of the motor peak (Figure 5B). This suggested that the motor and *ase1* could be segregated at the microtubule plus end. A lot of motor protein is accumulated in the first half micron of the microtubule with an *ase1* tail that stretches to 1.5 micron from the microtubule plus end (Figure 5A). However, to confirm this, experiments with both labelled *ase1* and labelled motor are necessary.

SE along the two microtubule ends (length $2.4\ \mu\text{m}$) for the microtubules of the right image shown in A (linewidth 1 pixel). All microtubules over $5\ \mu\text{m}$ were selected for analysis ($N=31$). The fluorescence intensity over the first and last $2.4\ \mu\text{m}$ of the microtubule were averaged and compared. The microtubules were sorted with their brighter end to the same side and all line scans were normalized to the average intensity of the complete line scan. The fluorescence intensity in the first and last $2.4\ \mu\text{m}$ was averaged over all line scans for every pixel.

Discussion

Motors reportedly stall and detach when encountering an obstacle. Schneider *et al.*, 2015 report a waiting time of 0.4 s for kinesin-1 encountering immobilized motors after which motors frequently detach (70%) or circumvent the obstacle (30%). Similarly, kinesin-1 was shown to detach when encountering immobile clusters of the neuronal protein tau (Dixit *et al.*, 2008). We, on the other hand, see highly processive motion of DK4mer in presence of near-saturating levels of ase1, implying that detachment probability upon encountering ase1 is very rare. Also, the high velocity in presence of ase1 implicates that there is hardly a waiting time associated with a single interaction. The mobility of ase1 thus limits its effect on motors. Similarly, the high mobility of individual tau proteins has been put forward to explain why tau expression in cells has no large effect on neuronal transport (Janning *et al.*, 2014).

How can motors move within high densities of ase1? It was proposed that motors can sidestep to a neighbouring protofilament (Schneider *et al.*, 2015). Sidestepping is rare for kinesin walking on empty microtubules but was triggered by immobilized motor proteins. For the interaction with ase1 it seems more likely that ase1 diffuses out of the way of motors. Given the diffusion constant of ase1 on single microtubules, $5.5 \times 10^4 \pm 0.5 \text{ nm}^2 \text{ s}^{-1}$ (Kapitein *et al.*, 2008), the mean waiting time for stepping to a neighbouring lattice site on a protofilament is 0.6 ms. The motor makes these 8 nm steps approximately every 20 ms. So, unless the microtubule is very crowded with ase1, hindering its mobility, ase1 can only temporarily hinder the procession of a motor protein by occupying a lattice site. Accordingly, ase1 did not induce stalls in our assays. Stalls were observed in presence and absence of ase1 with equal occurrence. These stalls may therefore be triggered by imperfections in the microtubule lattice or temporarily inactivated motor domains. The duration of the stalls increased in presence of ase1. This suggested that lattice crowding increased the time necessary for overcoming temporary motor inactivity, but did not induce stalls.

An interesting aspect of our investigations is that motors walking on the microtubule might influence the diffusion of ase1. It was proposed that motile motors generate biased diffusion of ase1 based on simulations and theory (Johann *et al.*, 2014). During the binding time of about 1 minute for ase1 (Figure 2), motors easily traverse the length of a typical microtubule in our assay. If motion of both ase1 and DK4mer would be limited to a single protofilament, we would expect to see occasions in which ase1 traverses a microtubule length driven by motor motion. The complete absence of such events thus shows that ase1 and/or motor can switch between protofilaments.

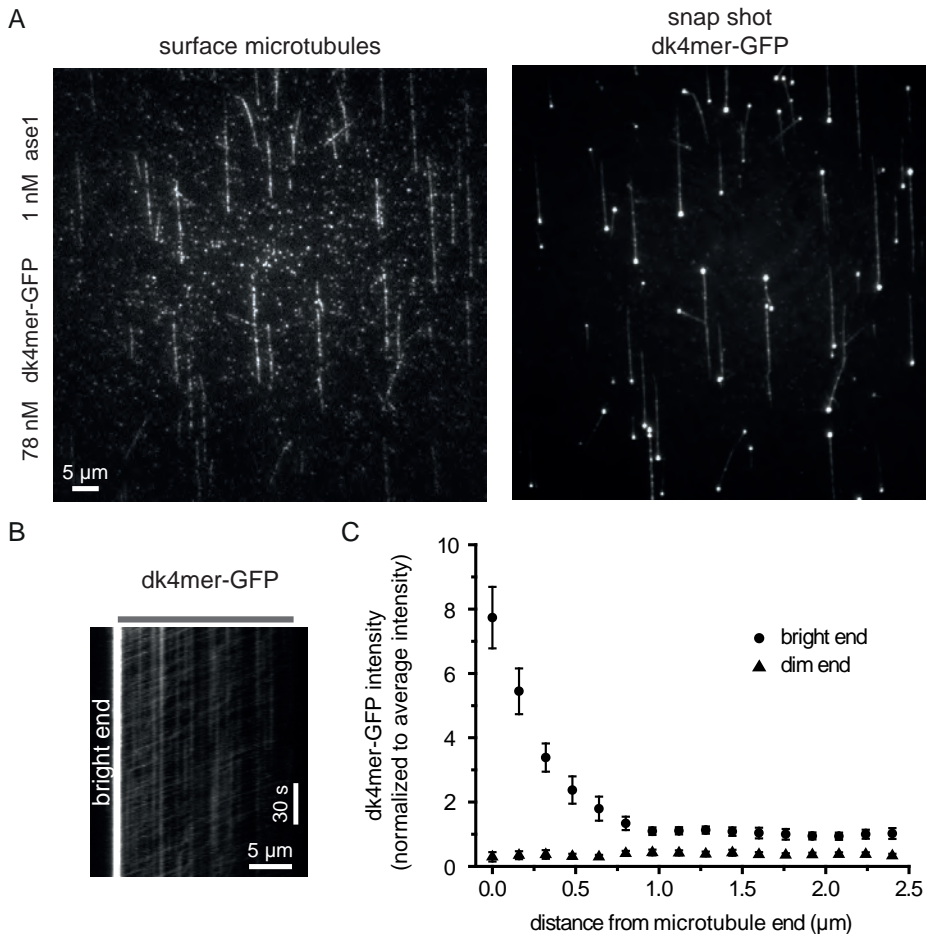


Figure 4 DK4mer-GFP end accumulation. (A) Images of surface microtubules (Alexa 568) and DK4mer-GFP in a single microtubule assay at 1 nM ase1-GFP and 78 nM DK4mer-GFP. (B) Kymograph showing DK4mer-GFP on a microtubule in the experiment as shown in A. The grey bar above denotes the position of the surface microtubule. The bright end is on the left side. (D) Average DK4mer-GFP intensity \pm SE at the first 2.4 μ m from the microtubule ends measured from the right image shown in A (line width 1 pixel). All microtubules over 5 μ m were selected for analysis (N=26). The fluorescence intensity over the first and last 2.4 μ m of the microtubule were averaged and compared. The microtubules were sorted with their brighter end to the same side and all line scans were normalized to the average intensity of the complete line scan. The fluorescence intensity in the first and last 2.4 μ m was averaged over all line scans for every pixel.

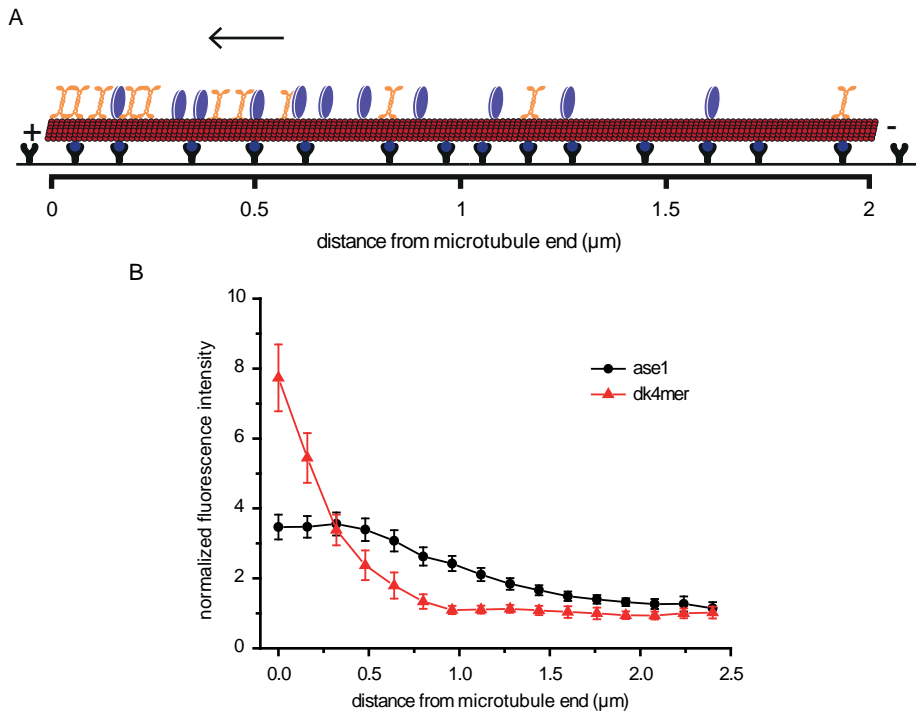


Figure 5 Combined ase1 and DK4mer end distribution along microtubule ends from different experiments. (A) A schematic representation of the localization of ase1 (blue) and DK4mer (orange) in a single microtubule assay. DK4mer localization increases all the way towards microtubule plus ends whereas the ase1 increase levels off near the end, possibly through exclusion by DK4mer. (B) Combined intensity plots of the first 2.4 μm of the microtubule bright end for ase1-GFP and DK4mer-GFP.

Moreover it shows that ase1 and DK4mer do not have direct binding interactions for a prolonged time, as is expected for these unrelated proteins. Nonetheless interactions through site exclusion may generate ase1 drift to a lesser extent which is not easily detected in kymographs. We found evidence for this in the accumulation of ase1 at microtubule ends.

To understand the distribution of ase1 and motors we first discuss the motors. Motors accumulated at plus ends, indicating that they remained associated with plus ends for some time (Varga *et al.*, 2006). These accumulated motors likely form traffic jams in which individual motors are nearly immobile. Such accumulations may locally prevent ase1 from binding. This is consistent with observed ase1 accumulations levelling off towards the microtubule end. Because motors traverse the full length

of microtubules, the number of moving motors increases steadily along the microtubule towards the plus end (Figure 1C). This is because most motors that bind will ultimately reach the plus end. Few motors, on the other hand, will pass a position that is very close to the minus end. The motor protein gradient depends on microtubule length. Therefore, it would be interesting to analyse the relation between end accumulations and microtubule length. Due to this gradient in active motors, any drift induced on *ase1* will also be graded. Hence we may expect substantial drift of *ase1* near plus ends whereas drift at minus ends is limited. Therefore, the accumulation of *ase1* (Figure 3D) at plus ends may be larger than the depletion of *ase1* at minus ends, as was observed. The approximate width of the observed accumulation (1 μm) is expected to be equal to the residence time of *ase1* on microtubules (1 minute) multiplied with the drift velocity near the microtubule end. The drift velocity in our experiment is thus predicted to be of order 1 $\mu\text{m}/\text{min}$. The MSD (mean squared displacement) caused by diffusion alone during the residence time is expected to be 3.3 μm^2 . Thus, the distance governed by diffusion is of similar order as the drift. This explains why drift is not directly observed in our kymographs.

The flattening of the *ase1* peak towards the microtubule end was also predicted by simulations under the condition that the microtubule end forms a mobility barrier for the motor proteins as well as for the diffuser (Johann *et al.*, 2014). This is the case in our experiments, since DK4mer forms end accumulations. While we found a weak segregation with the motor protein closest to the microtubule plus end, Johann *et al.* consistently see *ase1* leading with the motor proteins trailing. This difference is possibly explained by the fact that they model the motor with parameters of *eg5*. When using kinesin-1 parameters, with longer runs, higher velocities and different residence times, outcomes could differ. Furthermore, Johann *et al.* simulated only one protofilament, while on a microtubule 13 protofilaments are present. This introduces the possibility of side stepping and circumventions that are not accounted for in the simulations. The possibility to pass an *ase1* by side-stepping might be crucial to get motor accumulations in front of *ase1*.

Interestingly, similar intensity profiles were seen by Subramanian *et al.* where a similar assay with PRC1 and KIF4 was done. PRC1 gave an end accumulation of several microns in presence of the motor protein. KIF4 localized sharply at the tip without PRC1 and colocalized with PRC1 when present, elongating the end accumulation. The PRC1 localization was attributed to the direct interaction between the motor and the passive crosslinker. However, presented kymographs suggest that long-lasting complexes were not present, since PRC1 showed more diffusive behaviour, while

KIF4 showed long directed runs (Figure 3E and S6C Subramanian *et al.*, 2013). PRC1 clearly influenced kinesin-4 localization and vice versa, but this was possibly not because of the formation of long-lived complexes. Our results showed that a direct interaction is not essential for end accumulation, suggesting that interactions between PRC1 and KIF4 that are not necessarily in complexes can lead to end accumulation. Nevertheless, Subramanian's system seems to give end tags more robustly and the kinesin and PRC1 tags colocalize more accurately. These are possibly effects of the direct interaction. On the other hand, different motors react differently on different road-blocks/diffusing proteins (Schmidt *et al.*, 2012; Tarhan *et al.*, 2013). Likewise, it is probable that different diffusers react differently on motor proteins. So results cannot be generalized. However, an end accumulation was seen with both ase1/DK4mer and PRC1/KIF4 combinations. The combined results indicated that there may exist two end accumulation regimes. Strong interactions between motor and diffuser might result in perfect co-localization (Subramanian *et al.*, 2013) and no interactions might result in segregation of motor and diffuser (Johann *et al.*, 2014).

Our experiments did not always provide clear end accumulations of ase1. End accumulations were not observed in experiments at the same protein levels as those that showed end accumulation. When end accumulations appeared, almost all microtubules in the assay showed one brighter end. This suggested that the circumstances in the samples differed, although we took great care to standardize the protocol and experiments were repeated very carefully. The motor density was quite low with five motors per micron; this might be at the lower limit of motor protein density that allows for end accumulations. In further experiments, it will be interesting to look at experiments with higher motor densities as well as higher ase1 densities.

We showed that passive diffusers can accumulate at a microtubule end by influence of motor proteins. In cells, this can provide a method to localize and concentrate passive MAPs. Possibly activity gradients can be established in asters of microtubules and passive MAPs could reach a polarized localization in microtubule networks. In the case of ase1, this would be most important before microtubule overlaps are formed. When accumulating at the end of certain microtubules, bundling of these particular microtubules would be favoured (Subramanian *et al.*, 2013). Thus physical effects between proteins on crowded microtubules can play a role in the organization of microtubule networks.

Materials and methods

Protein purification

Recombinant histidine-tagged full-length *S. pombe* ase1 (pPT179, Fu *et al.*, 2009) and ase1-GFP (ase1 from pPT179 + GFP) were expressed in *E. coli* and cell extracts were made using a French press. The proteins were immobilized on Ni-NTA agarose beads and eluted in 20 mM phosphate buffer with 500 mM NaCl and 500 mM imidazole. DK4mer and GFP-DK4mer were purified from *E. coli* by Alice Wiesbaum (Schmidt lab, Göttingen) as described previously (Lakämper *et al.*, 2010; Thiede *et al.*, 2013). Porcine tubulin was purified as described previously (Castoldi and Popov, 2003) and labelled with Alexa Fluor® 647 and biotin (Fisher Scientific) (Hyman *et al.*, 1991; Peloquin *et al.*, 2005).

Single microtubule assays

A flow cell of silanized glass was incubated for 5 min with a 100 µg/ml goat anti-biotin antibody (Sigma Aldrich) in PBS and flushed with PBS afterwards. Then, surfaces were incubated with 1% pluronic F127 block copolymer in PBS for at least one hour. The sample was flushed with MRB80 and subsequently long microtubules (biotinylated) were bound to the surface via the anti-biotin antibodies. Unbound microtubules were immediately flushed out with MRB80 + 1 mg/ml casein (cas-MRB80). Finally, we flushed in a mix with ase1, dk4mer, 5 mM ATP and oxygen scavenging system (35 mM glucose, 16 µg/ml catalase, 166 µg/ml glucose oxidase) in cas-MRB80. Apart from unlabelled ase1 and DK4mer, GFP-labelled versions were used.

Imaging

Flow cells were imaged by using an inverted fluorescence microscope (Nikon eclipse Ti) with a Nikon 100x oil immersion 1.49 NA TIRF objective in combination with an QuantEM:512C (Photometrics) EMCCD camera controlled by Metamorph image acquisition software (Molecular Devices Corporation). For TIRF illumination, three DPSS lasers were used: 473 nm (Cobolt Blues), 561 nm (Cobolt Jive), 638 nm (Lasos RLD-XT 38). Dual- or Tri-colour images were acquired sequentially through a quad-band dichroic mirror (zt473/561/633/748rpc-TIRF, Chroma Technology) and appropriate band-pass filters.

Analysis

For the single microtubule assays, the time between frames was 1s. Kymographs were made using imageJ image analysis software. Velocities were calculated by determining the slope of the moving motors in kymographs. When pauses and/or velocity changes were present, the trace was divided into sections. The velocity in these sections was calculated and weighted with the duration of each section to calculate the weighted average. Motors that did not show any movement throughout their observation time were not used in the analysis as these events may correspond with partly denatured or otherwise non-functional motors.

Intensities were measured on line scans with a width of 1 pixel and background values were subtracted. All microtubules with lengths over 5 μm were selected for analysis. The bright end was determined by comparing the average intensity of the first 2.4 μm of both microtubule ends. The line scans were normalized to the average intensity of the complete microtubule. Then, the intensity was averaged over all line scans per pixel for the brighter and dimmer ends separately. This resulted in average intensity profiles of ase1 and DK4mer for the bright as well as the dim end.

The estimation of motor density was done using the most left kymograph in Figure 1C and three more kymographs from the same experiment. The combined observation time of DK4mer-GFP traces was divided by the total observation time and the total microtubule length of the combined kymographs. This resulted in an estimation of a DK4mer density of 0.0255 motors $\mu\text{m}^{-1} \text{nM}^{-1}$.

Chapter 6

General discussion

Abstract

The regulation and maintenance of antiparallel overlaps is very important. There are several mechanisms that could prevent the loss of overlap by establishing a feedback between growth and sliding. Some research points to the possibility of sliding-regulated growth, although this was not tested with sliding microtubules. We suggest that growth-limited sliding can maintain antiparallel overlaps. The requirements for growth-limited sliding are a motor protein that is sensitive to either *ase1* density or overlap length. The directional switching of *klp9* and other yeast kinesin-5 proteins seems to be optimized to maintain overlaps. Additionally, dynamic instability of microtubules has to be regulated. Since we could not induce rescues specifically at overlaps using *cls1* and *ase1*, another regulating mechanism might be required. Furthermore, we conclude that motors and diffusive proteins influence each other by occupying binding sites. This can lead to biased diffusion and end accumulations of the diffusive protein. In overlaps, the exclusion effect might be even larger. Most proteins we used are from fission yeast. However, these mechanisms can help to understand spindle organization in more complicated spindles from different organisms. Finally, we give some directions for future in vitro experiments and the implementation of our results into simulations.

General discussion

Function of antiparallel overlaps

Antiparallel microtubule overlaps are important features in bipolar microtubule arrays. Microtubules come from opposite sides and form an overlapping zone where microtubules meet. These microtubule overlaps are considered to be essential for formation and structural integrity of bipolar microtubule networks. When *ase1* is not present, antiparallel overlaps largely disappear. In anaphase, this results in monopolar spindles or the disconnection between the two spindle halves (Mollinari *et al.*, 2002; Loiodice *et al.*, 2005; Wang *et al.*, 2015). The loss of the midzone hinders the separation of the two nuclei, as overlaps are the site where kinesins generate forces to accommodate spindle elongation. Furthermore overlaps are necessary to withstand forces produced at the kinetochores. The unique position of the midzone that marks the middle of the spindle can be used as a landmark, for instance, Aurora B is present at the midzone and creates a phosphorylation gradient from there (Fuller *et al.*, 2008). The gradient of phosphorylated proteins provides spatial information that can influence anaphase and cytokinesis. When the midzone is disturbed, this will affect the positioning of the gradient. Although the position of the overlap is used to give spatial cues inside the cell, it is not known how the midzone is centred in the spindle. Therefore, it is important to understand mechanisms that regulate the formation and maintenance of the midzone in order to understand how all functions of the spindle are tied together. What is happening in the midzone has consequences throughout the spindle, either via force production or via signalling. Our results show some possible regulation mechanisms on overlaps and we will discuss what our results imply for spindle organization.

More recently it has been recognized that the midzone has important signalling roles in cytokinesis. Antiparallel microtubule overlaps are involved in setting up spatial activity gradients and in the coordination of membrane and cytoskeletal systems. In the later stages of the animal spindle and in the plant phragmoplast, a regular array of short antiparallel overlaps is necessary for successful cytokinesis (Mollinari *et al.*, 2002; Verni *et al.*, 2004; Zhu and Jiang, 2004; Hu *et al.*, 2011; Kong *et al.*, 2015; de Keijzer *et al.*, 2017). The site of cytokinesis is directly linked to the site of overlaps. When overlap length is not regulated correctly, this causes problems in cell wall formation. In plants, the formation of longer overlaps results in irregular, thick cell walls, because vesicles with cell wall material are directed to the microtubule overlaps specifically (de Keijzer *et al.*, 2017). In animal cytokinesis centralspindlin is involved in anchoring the microtubule overlaps to the plasma membrane (Lekomtsev *et al.*,

2012). Here the site of the midzone regulates where the membrane ingresses. The link between cytokinesis site and antiparallel overlaps is not well-studied, apart from these two described mechanisms. However, it is clear that antiparallel overlaps play a key role in cytokinesis. Thus, overlap length and position have to be regulated and overlaps have to be maintained for proper cell division.

Our work gives insight into how overlap length could be regulated and how processes like spindle flux and spindle elongation may be related to what is happening in the midzone (Chapter 4). Moreover we investigated how the lifetime of overlaps can be extended by regulating microtubule dynamics (Chapter 3). Lastly we show that purely physical interactions between the proteins along microtubules may affect the functioning and localization of individual components (Chapter 5).

Feedback of growth on sliding and vice versa

To maintain overlap stability in the midzone throughout mitosis, sliding and growth need to be coordinated. Sliding and growth affect overlap length by respectively decreasing and increasing it. Somehow feedback needs to be established between both activities. One possibility to maintain overlap length is a mechanism with sliding-limited growth. When sliding is affecting growth, faster sliding will increase microtubule growth velocity so that overlaps are not lost. When sliding stops, microtubules stop growing as not to increase overlap length. The other way around, when sliding is limited by the velocity of microtubule growth this is called growth-limited sliding. This means that motor proteins can slide only as fast as the microtubules are growing. Klp9 maximal velocity is four times faster *in vitro* than the elongation velocity *in vivo* (Fu *et al.*, 2009; Chapter 4). This suggests that growth rate is limiting klp9 sliding *in vivo*. Furthermore, from our *in vitro* experiments in chapter 4 we learned that relative sliding by klp9 in presence of ase1 was coupled to the dynamic state of microtubules. When microtubules are sliding apart, directional switching prevents complete loss of overlap in the case of stabilized microtubules. Dynamic microtubules slide apart while growing and are tethered back while shrinking (Chapter 4). Also *in vivo*, we found that decreased polymerization resulted in a decreased sliding velocity (Chapter 4). Therefore, we suggest that one way to regulate overlap length is by growth-limited sliding.

There is also research that points to a sliding-limited growth mechanism. In higher eukaryotes, PRC1 bundling proteins interact with kinesin-4 motors that slow microtubule growth. Kinesin-4 inhibits microtubule growth and its localization is regulated by PRC1, so it is mainly active on antiparallel overlaps (Kurasawa *et al.*,

2004; Hu *et al.*, 2011; de Keijzer *et al.*, 2017). Also here, regulation is crucial and feedback between sliding and growth is required. The recruitment of kinesin-4 to overlaps by PRC1 is not sufficient to explain length regulation. In vitro experiments with PRC1 and kinesin-4 showed an interesting feedback mechanism in which overlap length and the mobility of proteins play a role in an antenna mechanism (Bieling *et al.*, 2010). In this mechanism, the length of the overlaps dictates the amount of kinesin-4 that binds there. Kinesin-4 that binds to the overlap moves to the edges of the overlap, where it inhibits microtubule growth. This results in larger accumulations of kinesin-4 in longer overlaps and smaller accumulations in shorter overlaps. Since kinesin-4 is suppressing microtubule growth, Bieling *et al.* propose that growth is adapted to overlap length. However, Bieling *et al.* did not introduce sliding, so it is not clear if the mechanism would hold up under sliding conditions. When sliding would be introduced, overlaps would shrink when sliding apart. This would decrease kinesin-4 accumulations and increase microtubule growth so that the overlap is not lost. This implies a sliding-limited growth mechanism. This would only work when the sliding velocity does not exceed twice (for both microtubules in the bundle) the maximum growth velocity of the microtubules. Depending on the motor used, the sliding might be limited by growth of the overlap. So, growth-limited sliding and sliding-limited growth might therefore not be mutually exclusive. It would be interesting to see how this intricate feedback would function. How motor sliding and microtubule dynamics regulators work together is not yet clear. Many motor proteins are active in spindle midzones, including some that regulate microtubule dynamics (Gatlin and Bloom, 2010; Miki *et al.*, 2014). Cells might use one mechanism or the other depending on the specific requirements in different species.

Observations by the Scholey lab can be explained with the growth-limited sliding mechanism we propose. They show that a depletion of kinesin-8, which depolymerizes microtubules, changes flux rate and spindle elongation rate in *Drosophila* (Wang *et al.*, 2010). Both flux and spindle elongation are the result of relative sliding in the midzone. Kinesin-8 depletion promotes microtubule growth and induces faster flux and spindle elongation. This is in agreement with our yeast experiments from chapter 4 where microtubule growth is decreased and spindle elongation decreases accordingly. This shows that the growth-limited sliding mechanism is more universal, and not only present in yeast. In general growth-limited sliding forms an alternative way to change spindle elongation rate, the regulation of growth velocity is regulated instead of directly regulating motor velocity. In sliding-limited growth on the other hand, sliding velocity is not regulated. We are inclined to investigate motor proteins with a sliding function to understand the regulation of spindle elongation. However,

the concept of feedback shows that cells may alternatively change dynamics of microtubules in overlaps to regulate spindle elongation. Awareness of this insight may lead to more research on regulators of microtubule dynamics in the spindle and particularly their regulation and localization. Possibly, this will increase our understanding of the regulation of spindle elongation and spindle flux.

Requirements for growth-limited sliding

How is the feedback of growth on sliding achieved? Overlaps will decrease in length when motorized sliding is faster than the combined growth of the two overlapping microtubules. A mechanism is required that slows sliding when overlaps become too short and microtubules are at risk of disconnecting. Braun *et al.* and Lansky *et al.* showed how this can be done using *ase1*, the yeast homolog of PRC1/*ase1*/MAP65, as modulator of sliding velocity (Braun *et al.*, 2011; Lansky *et al.*, 2015). For adaptive braking as well as entropic forces to oppose overlap shortening, *ase1* has to accumulate in shortening overlaps. In adaptive braking, the changing ratio of *ase1* and motor proteins reduces the velocity in decreasing overlaps. At the same time, accumulated *ase1* induces sliding that opposes a decrease in overlap length because longer overlaps are entropically more favourable. However, the question is if these mechanisms are broadly relevant. Although sliding is mildly slowed down by PRC1, the mammalian homolog of PRC1/*ase1*/MAP65, PRC1 does not trigger a decrease in sliding velocity when Eg5 is used to slide microtubules apart (Subramanian *et al.*, 2010). PRC1 does not accumulate when overlaps decrease in size as *ase1* is doing. Instead, the number of PRC1 cross linkers in the overlap decreases proportionally with the reduction in overlap length (Subramanian *et al.*, 2010). This difference might be caused by a difference in microtubule binding properties between PRC1 and *ase1*. The residence time of PRC1, that has a half-life of 1 second in microtubule overlaps, is much shorter than that of *ase1*, that has an average interaction time of at least 22 seconds in overlaps (Kapitein *et al.*, 2008; Bieling *et al.*, 2010). Furthermore, it is unclear to which extent the microtubule ends form a diffusive barrier for PRC1. Thus, although accumulation of *ase1* in overlaps might result in an increased friction that slows down antiparallel sliding, the *ase1* homologs PRC1 and MAP65 do not necessarily show such an effect. Furthermore, different motor proteins might react differently to the increase in friction. While the minus end directed motor *ncd* is slowed down by an accumulation of *ase1* in overlaps (Braun *et al.*, 2011), we do not see such an adaptive braking effect on *klp9* (Chapter 4). Possibly, the directional switching of *klp9* conceals adaptive braking in our experiments. We also see directional switching of *klp9* in combination with MAP65 instead of *ase1* (Chapter 4). Therefore, we conclude that a general property of the bundling protein induces the directional switch.

We now show, that not only properties of *ase1* but also the directional switching of kinesin-5 may be optimized for maintaining antiparallel overlaps. We observe directional switching in relative sliding assays with *klp9* and the occurrence increases in presence of *ase1* and within decreasing overlap length (Chapter 4). Note that although directional switching of yeast kinesin-5 proteins has been observed before, the cellular function of switching was not understood. So far only yeast kinesin-5 and yeast and *Aspergillus* kinesin-14 were observed to switch directionality (Roostalu *et al.*, 2011; Thiede *et al.*, 2012; Fridman *et al.*, 2013; Edamatsu, 2014; Molodtsov *et al.*, 2016; Popchock *et al.*, 2016). Furthermore, *Xenopus* kinesin-5, Eg5, is known to switch between diffusive and directional modes (Kwok *et al.*, 2006). In yeast, kinesin-5 switching is thought to depend on whether the motor is bound to single microtubules or overlapping microtubules (Gerson-Gurwitz *et al.*, 2011; Thiede *et al.*, 2012). Alternatively, the number of motor proteins is thought to trigger kinesin-5 switching through motor coupling (Roostalu *et al.*, 2011; Fridman *et al.*, 2013). *Aspergillus* kinesin-14 switching is dependent on a nonmotor microtubule binding domain. If this domain binds to the same microtubule as the heads, this results in minus end-directed movement. On the other hand, if this domain detaches it leads to plus end-directed motion (Popchock *et al.*, 2016). In practice, this results in minus-end directed motion on single microtubules and in plus end-directed motion when sliding a pair of microtubules. Another mechanism is found in budding yeast. There, the directional switch of the normally minus end-directed kinesin-14 is induced by an opposing force. When the motor is linked to a growing plus end by EB1, the force of the growing microtubule induces plus end-directed motion. Given the results on yeast it will be interesting to investigate whether the switch to a diffusive mode by Eg5 can also be triggered depending on overlap length. A switch to diffusive instead of directional movement might be enough to maintain overlaps.

Importantly, we show for the first time that overlap lifetime can be prolonged by passive cross linkers in the case of plus-end directed motors (Chapter 4). This was so far only demonstrated for *ncd* (Braun *et al.*, 2011). At this time we do not understand how switching is triggered when microtubules slide apart. One interesting possibility is that the motor is poised to respond to counteracting forces generated by the passive linkers. This would be similar to the mechanism that induces adaptive braking by a change in ratio of motors to *ase1*. The presence of the linkers alone induces motor switching in 20% of the bundles even in overlaps that do not shrink (Chapter 4), which would imply that friction caused by *ase1* can trigger switching. On the other hand, switching is triggered by decreasing overlap length without *ase1*,

possibly because of the decreasing number of motor proteins in the overlap. When the overlap lengthens by growth, the microtubules can slide apart again. This switch back to directional sliding could be linked to the possibility of new motors to attach to the overlap. This could change the balance between *ase1* and *klp9*, favouring relative sliding with relatively more motor proteins. When more motors are present, the friction caused by *ase1* is spread over more motor proteins. Since every motor now experiences less friction, switching to relative sliding can be triggered. Alternatively, the increased amount of motor protein can lead to a switch back to the forward direction because of the team size. More research on the behaviour of individual motor proteins sliding within decreasing overlaps should give more insight, preferably in presence of a diffusive cross linker. It would be very interesting to see if *ase1* can affect the other bidirectional yeast kinesin-5 proteins in similar ways.

Another mechanism for generating growth-limited sliding was suggested by Wang *et al.* to explain how kinesin-8 depletion can induce faster spindle elongation (Wang *et al.*, 2010). One of their hypotheses is that an increase in overlap length results in an increase of motor proteins in the overlap and thereby induces faster sliding. They propose that with more motor proteins, the load per motor is lower so velocity increases. This implies that motors are working against a load, while previous research showed that kinesins work unloaded in *Drosophila* anaphase B (Brust-Mascher *et al.*, 2004, 2009). We propose a dependency of the motor protein directionality on overlap length and we suggest that the load or friction the motor feels might induce a directional switch in motor activity (Chapter 4). This both results in slower motor function in shorter overlaps. From the work of Wang *et al.* it is not clear which mechanisms are at work to generate growth-limited sliding while we propose that *ase1* bundling proteins and a bidirectional kinesin-5 can regulate overlap length dependent on microtubule growth.

Regulation of catastrophes

Microtubules can switch to a state of rapid shrinkage. Our results show that the ends of shrinking microtubules remain attached in the presence of *ase1* and *klp9* (Chapter 4). It is not clear whether this mechanism is enough to maintain overlaps in the context of the spindle, where minus ends are fixed at the poles. A catastrophe potentially disengages two overlapping microtubules. In *S. pombe* the whole apparatus consists of approximately 20 microtubules and the antiparallel microtubules are clustered in the midzone (Ding *et al.*, 1993). One set of interpolar microtubules shrinking back while maintaining the overlap is probably not possible within this microtubule network. The fixed minus ends at the spindle pole do not allow short-

ening of the complete length of one set of inter-polar microtubules while another set of inter-polar microtubules maintains a constant length (Figure 1A). To maintain the overlap, a catastrophe must be followed by a rescue. Rescues should be triggered at the overlaps, where shrinkage into the midzone has to be prevented. Cls1 has been proposed to perform this role in yeast. Ase1 recruits cls1 to the midzone, where cls1 can induce rescues (Bratman and Chang, 2007). The interaction between CLASP and PRC1 suggests that a similar mechanism is present in animal cells (Liu *et al.*, 2009). In higher eukaryotes kinesin-4 regulates the dynamics of microtubule overlaps additionally (Kurasawa *et al.*, 2004; Bieling *et al.*, 2007; Hu *et al.*, 2011; de Keijzer *et al.*, 2017). When overlap length decreases, the decrease in kinesin-4 will induce extra microtubule growth. So microtubule dynamics can be regulated at multiple levels in order to fine tune overlap length and life time.

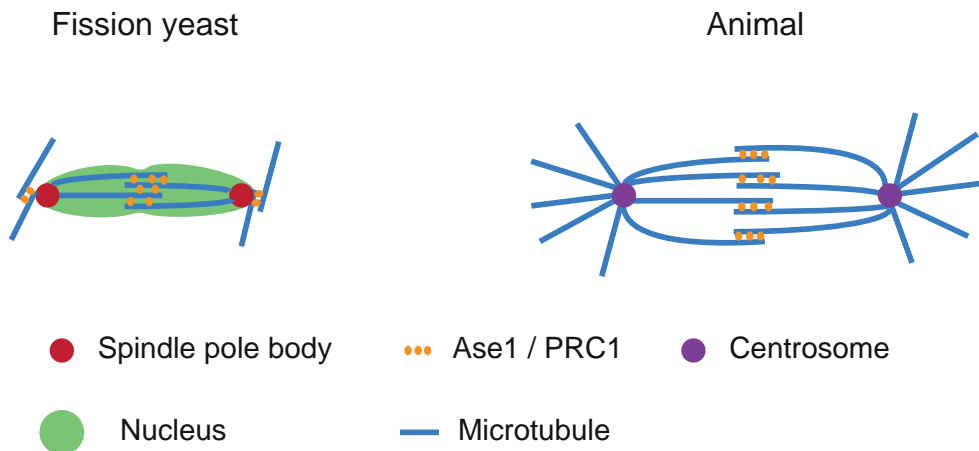


Figure 1 A schematic representation of the microtubule organization in the mitotic spindle of fission yeast and animal cells.

In chapter 3 we reconstitute the recruitment of cls1 to ase1 overlaps and we show that a direct interaction is responsible for this recruitment. However, we did not succeed yet in restricting rescues to overlaps. We did not find a concentration at which cls1 is solely located to the overlaps and not to single microtubules (Chapter 3). The two component system with cls1 and ase1 possibly needs additional regulation mechanisms to confine rescues to the overlaps. Apparently, the concentrations of cls1 and ase1 have to be fine-tuned quite strictly. An interesting next step would be to limit the amount of cls1 and ase1. What is often neglected is that cells may have limiting pools of components like tubulin, CLASP and ase1. Competition for these components may facilitate regulatory mechanisms. A limited protein pool might explain why the

zone of overlap does not expand maximally in the presence of *ase1/cls1* modules. When concentrations are not limiting, pioneering microtubules that grow away from the midzone could recruit more *ase1* and *cls1*, which would cause overextension of the overlap. This notion is supported by overexpression of *cls1* in yeast, that yields extended overlaps (Bratman and Chang, 2007). However, at endogenous *cls1* concentration, microtubules do grow away from the midzone but frequently have catastrophes. Subsequently the shrinking microtubule is rescued at the midzone (Sagolla *et al.*, 2003). So the midzone overlap has different properties than the overlap that is formed by pioneering microtubules growing from the midzone. How this is regulated is not known. A limiting amount of CLASP may prevent the formation of an overly long hyper-stabilized midzone. In that case, when all overlaps are long, this results in an overall lower CLASP density. This would destabilize the long overlaps as they are less often rescued. Furthermore, Bratman and Chang estimated the amount of *cls1* to be approximately 11 *cls1* molecules per microtubule in the spindle. In our current experiments, the concentration of CLASP is not limiting. Therefore, it will be interesting to study this interaction network within the bounds of a confined geometry, such as a micro-fabricated chamber.

Difference between yeast spindles and animal spindles

We tried to reconstitute some features of the spindle midzone with components from fission yeast. The components we use are conserved in animal cells.

Ase1 and *PRC1* both localize to the spindle midzone in yeast and animal cells respectively (Duellberg *et al.*, 2013). *PRC1* bundles antiparallel microtubules and is essential for spindle stability (Mollinari *et al.*, 2002; Subramanian *et al.*, 2010).

The motor we use is *klp9*, a kinesin-5. In yeast, kinesin-5 localizes to the midzone (Hagan and Yanagida, 1992; Fu *et al.*, 2009; Khmelinskii *et al.*, 2009; Fridman *et al.*, 2013). Kinesin-5 is found throughout the spindle in animal cells and is enriched at the spindle poles (Kwok *et al.*, 2006; Ferenz *et al.*, 2010; Ma *et al.*, 2011). Though in yeast kinesin-5 has a direct interaction with *ase1*, this is not the case in animal cells (Fu *et al.*, 2009). Despite its different localization, in most animal cell types kinesin-5 is responsible for spindle elongation (Sawin *et al.*, 1992; Sharp *et al.*, 2000; Brust-Mascher *et al.*, 2009), while in other cells elongation is slowed by kinesin-5 (Saunders *et al.*, 2007, *C. elegans* embryos; Collins *et al.*, 2014, LLC-Pk1 epithelial cells). It has been proposed that *Eg5* acts like a brake in these cases and sets the pace at which spindles elongate (Saunders *et al.*, 2007). The microtubule dynamics regulator we use is *cls1*, a homolog of CLASP. CLASP is found to localize to kinetochores and the spindle midzone in animal cells (Maiato *et al.*, 2003; Liu *et al.*, 2009). *PRC1* was seen to recruit CLASP to the antiparallel overlaps in the midzone in HeLa cells (Liu *et al.*,

2009), which is similar to *cls1* that has a direct interaction with *ase1* (Bratman and Chang, 2007). CLASP induces rescues in both yeast and animal cells (Maiato *et al.*, 2003; Liu *et al.*, 2009; Al-Bassam and Chang, 2011).

While there are many similarities, the spindle differs between yeast and animals at some other points. Yeast spindles consist of approximately 20 microtubules, while mammalian spindles can consist of hundreds of microtubules (Ding *et al.*, 1993; Mitchison *et al.*, 2004). So while all being bipolar networks of microtubules, mitotic spindles can differ substantially in architecture of the microtubule network (Figure 1, A and B). The number of interpolar microtubules at the midzone can greatly differ. Animal cells have many more overlaps that all have to be synchronized. When the spindle elongates, all interpolar microtubules have to slide at the same pace. They also may need to prevent merging of neighbouring overlaps, while the yeast midzone consists of one dense cluster of bundled microtubules (Ding *et al.*, 1993, Figure 1). This sets requirements in animal cells that may not be present in yeast and suggests that different regulation mechanisms play a role in the positioning of overlaps relative to each other.

Another difference is the spindle organization at the poles. In animal cells, the poles of the spindle are governed by centrosomes, while yeast has spindle pole bodies at the poles. Astral microtubules that emanate from these structures towards the outer parts of the cell play different roles in animal and yeast cells. While yeast spindles are under external pushing forces of the astral microtubules (Khodjakov *et al.*, 2004; Tolic-Nørrelykke *et al.*, 2004), astral microtubules help pulling to elongate the spindle in animal cells (Aist *et al.*, 1993), although some research shows that the astral pulling force does not play a role in anaphase B (Brust-Mascher *et al.*, 2009). This sets different conditions under which the spindle has to function. In yeast, the function of a well-organized spindle midzone was proposed to be a primarily a mechanical one to resist the compressive force (Khodjakov *et al.*, 2004; Ward *et al.*, 2014). Animal spindles do not have to resist such forces and might be more important in signalling roles. It is, therefore, not surprising that animal and yeast spindles evolved different systems to control the stability of the spindle midzone. Also the signalling function of the antiparallel overlaps is different between yeast and animal cells. Other than in mammalian and plant cells (Lekomtsev *et al.*, 2012; de Keijzer *et al.*, 2014), so far the position or length of the midzone in yeast has not been linked directly to the site of cytokinesis. The location of septum formation in yeast is thought to be derived from the position of the interphase nucleus instead (Gould and Simanis, 1997). As a result of the different design requirements a different set of proteins might be required in

different cell types. For instance in animal cells, kinesin-4 is a regulator of antiparallel overlap length. Kinesin-4 has a direct interaction with PRC1 and regulates microtubule growth at the midzone (Kurasawa *et al.*, 2004; Hu *et al.*, 2011). However, kinesin-4 is not present in yeast. Apparently *cls1* is sufficient in yeast to regulate microtubule dynamics in the spindle.

Observing different types of spindles may highlight core mechanisms and may shine light on how functioning of bipolar networks can be adapted to serve different roles in different organism and at different settings (mitosis, meiosis, cytokinesis). Animal spindles are highly complex and it is difficult to extract mechanisms from them. On the other hand, yeast spindles are relatively simple as there are less microtubules and MAPs. Mechanisms found in yeast cells and verified with in vitro experiments can help in understanding animal spindles. Motor proteins, bundlers and microtubule dynamics regulators are present in both animals and yeast. Thus, although yeast proteins are used to identify a mechanism, this mechanism could be relevant in other species as different proteins have similar roles there. Taking found mechanisms into account can shed a new light on the more complex organization of the animal spindle.

Biased diffusion and crowding on microtubules

Recently it has become clear that many MAPs do not bind firmly to microtubules but instead have a diffusive mode of interaction (Asbury *et al.*, 2006; Helenius *et al.*, 2006; Kwok *et al.*, 2006; Kapitein *et al.*, 2008). This seems to be specific for microtubule-bound proteins and is not seen with proteins that interact with actin. These diffusive proteins act in very different situations. For cross linkers like *ase1*, the diffusive mode might be necessary in order not to hinder motor proteins. Examples of proteins that have such a diffusive mode of interaction are *Dam1*, which is thought to use the diffusive mode to track shrinking microtubule ends (Asbury *et al.*, 2006), and *MCAK*, which diffuses over the microtubule and targets microtubule ends efficiently in this way (Helenius *et al.*, 2006). Since microtubules are crowded with diffusive MAPs as well as motors, it would be interesting to know how they influence each other's behaviour.

Simulations by Johann *et al.* suggested that motor proteins could influence localization of proteins that are diffusely bound to microtubules. In vitro assays are the preferred method to verify the feasibility of such a physical mechanism. Such an approach makes us aware of mechanisms that could play a role in vivo. Importantly, in vitro experiments allow us to vary concentrations and conditions that allows us

to characterize a mechanism in detail. Especially in vitro experiments with combinations of MAPs are interesting, since many microtubule associated proteins work together in vivo. Our experiments show that spatial ordering can emerge from the physical interaction of passive and active cross linkers as predicted (Chapter 5). The combination of motor proteins and ase1 resulted in end accumulations of ase1. However, we observe that complete segregation, with all ase1 at the microtubule end and the motors behind them, as predicted in the simulations, is not achieved under the tested circumstances. While no directional ase1 runs were observed, ase1 did accumulate at one microtubule end. This suggests that side-stepping, by motors or ase1, to bypass other proteins influences the interactions between proteins on a microtubule (Chapter 5). Therefore, more research is needed on protofilament switching of motor proteins as well as diffusive proteins. The mechanism we found can be used to explain existing experiments in an alternative way. Ase1 and DK4mer do not have a direct interaction with each other. Nevertheless the combination of these proteins results in ase1 end accumulations. Therefore, care should be taken when interpreting the role of direct protein interactions as reported for KIF4 and PRC1 (Subramanian *et al.*, 2013). In these experiments, end accumulations of PRC1 are attributed to the direct interaction between the motor and PRC1, while we show that non-interacting proteins can lead to similar end accumulations.

Biased diffusion of diffusely-bound MAPs may arise when motors and MAPs compete for the same binding sites along microtubules. In vivo, microtubules are expected to be crowded with many different MAPs. Thus, what are the implications of this mutual influence of motors and diffusers in vivo? We show that motor proteins slow down on microtubules that are crowded with ase1 (Chapter 5). Although the motor proteins do not have to generate forces, their velocity is decreased because from time to time the next lattice site is occupied. We study this on single microtubules, but the same should hold for motor proteins like kinesin-5 or ncd in microtubule overlaps. Until now, the decreased sliding velocity of microtubules in presence of ase1 was assigned to friction caused by ase1 (Braun *et al.*, 2011). However, we now show that a decrease in velocity could also be achieved by a competition for binding sites. Mechanisms like adaptive braking, where ase1 brakes motor proteins in shortening overlaps can also be explained by this alternative mechanism. Possibly, crowding has an even larger effect on motor proteins in overlaps. Our experiments suggest that ase1 can diffuse out of the way of motor proteins (Chapter 5). However, in overlaps cross linkers are bound to two microtubules. Since both ends of the protein have to be coordinated it might take longer to diffuse away. This would increase the impact of cross linker presence on motor velocity. Furthermore, we have seen that high ase1



concentrations prevent motor proteins from binding (Chapter 5). The high density of *ase1* in overlaps might thus prevent motor binding. This exclusion of motors from overlaps could decrease the ratio between motor proteins and *ase1* even more. This would increase the effect of adaptive braking. However, the effects of crowding in overlaps were not investigated in depth before. Further research should give more insight in the consequences of densely packed overlaps.

Future research directions

The ultimate goal is to understand how processes cooperate in the spindle. We hope to get a better understanding of the functioning of the spindle and how the spindle has evolved into more complex spindles. Now that we start to understand some mechanisms that are responsible for maintenance of the spindle midzone, it would be interesting to combine them. We combine bundling, sliding and microtubule growth in our assays (Chapter 4) and it would be interesting to also include rescue activity (Chapter 3). Is the combination of a motor protein, a bundler and a dynamics regulator enough to form stable overlaps or are we missing something? Do the overlaps get overextended or do sliding and growth balance each other in presence of *cls1*? These questions could be answered with complicated *in vitro* experiments in which several proteins with different functions are combined. This type of experiments will increase our understanding of the mechanisms needed for overlap length regulation under sliding conditions.

Another method to gain insight in how activities cooperate is the use of computer simulations. In simulations, a wide range of concentrations can be tested relatively quickly, whereas it would take very long to test all combinations *in vitro*. This could shorten the way to a working *in vitro* system. On the other hand, a verification of the simulated mechanism is needed as one can never know all properties of the proteins involved and important properties might be overlooked. Unexpected results from *in vitro* experiments might lead to surprising insights. The results we have found could be implemented in existing simulations and models. For instance, we suggest that biased *ase1* diffusion could be graded along the microtubule when motor proteins have long run lengths. This could be incorporated in the model by Johann *et al.* to see if this alters end accumulation. Also multiple protofilaments that allow for side-stepping could be incorporated. Another model, simulating a complete spindle in 2D, would also be interesting for implementing some of our results. In the simulations of Loughlin *et al.* a spindle is formed using approximately 200 dynamic microtubules, a cross linking force and kinesin-5 (Loughlin *et al.*, 2010). This leads to simulated spindle elongation. It would be interesting to introduce explicit bundling proteins

with the properties of *ase1*, as bundling is now simulated implicitly as a force between microtubules that are close to each other. If this is enough to create a clearly defined midzone it would be interesting to additionally add *cls1*, recruited by *ase1*. These simulations could give insight into midzone formation and maintenance. Including the mechanisms we found into simulations could help to find interesting relations and possibly surprising outcomes that can help us further to understand microtubule overlaps.

To answer questions about the coordination of multiple overlaps, and to increase our overall understanding of the spindle it would be interesting to introduce our proteins into more realistic spindles. A very interesting in vitro spindle-like structure is made by Vleugel *et al.*, 2016. They capture centrosomes and tubulin in water-in-oil droplets, which creates basic mitotic spindles in a confined 3D environment. Adding *ase1* and motor proteins would be an interesting next step that they already incorporated into this spindle model (Vleugel *et al.*, 2016). Results of these experiments are not yet published. The formation of a midzone in these spindles would create an environment to test more mechanisms, like *cls1* rescue induction and *klp9* spindle elongation. Ultimately, a combination of in vitro experiments, which combine multiple MAPs, and computer simulations will hopefully lead to insight in midzone length regulation and maintenance in vivo.

Bibliography

- Aist, J. R., Liang, H., and Berns, M. W. (1993). Astral and spindle forces in PtK2 cells during anaphase B: a laser microbeam study. *J. Cell Sci.* *104* (Pt 4, 1207–1216).
- Akera, T., Sato, M., and Yamamoto, M. (2012). Interpolar microtubules are dispensable in fission yeast meiosis II. *Nat. Commun.* *3*, 695.
- Al-Bassam, J. (2014). Reconstituting dynamic microtubule polymerization regulation by TOG domain proteins, Elsevier Inc.
- Al-Bassam, J., and Chang, F. (2011). Regulation of microtubule dynamics by TOG-domain proteins XMAP215/Dis1 and CLASP. *Trends Cell Biol.* *21*, 604–614.
- Al-bassam, J., Kim, H., Brouhard, G., Oijen, A. Van, Harrison, S. C., and Chang, F. (2010). Article CLASP Promotes Microtubule Rescue by Recruiting Tubulin Dimers to the Microtubule. *Dev. Cell* *19*, 245–258.
- Asbury, C. L., Gestaut, D. R., Powers, A. F., Franck, A. D., and Davis, T. N. (2006). The Dam1 kinetochore complex harnesses microtubule dynamics to produce force and movement. *Proc. Natl. Acad. Sci. U. S. A.* *103*, 9873–9878.
- Baumann, H., and Surrey, T. (2015). Self-organization of motors and microtubules in lipid-monolayered droplets, Elsevier Ltd.
- Berlier, J. E. *et al.* (2003). Quantitative comparison of long-wavelength Alexa Fluor dyes to Cy dyes: fluorescence of the dyes and their bioconjugates. *J. Histochem. Cytochem.* *51*, 1699–1712.
- Bieling, P., Laan, L., Schek, H., Munteanu, E. L., Sandblad, L., Dogterom, M., Brunner, D., and Surrey, T. (2007). Reconstitution of a microtubule plus-end tracking system in vitro. *Nature* *450*, 1100–1105.
- Bieling, P., Telley, I. A., and Surrey, T. (2010). A minimal midzone protein module controls formation and length of antiparallel microtubule overlaps. *Cell* *142*, 420–432.
- Bratman, S. V., and Chang, F. (2007). Stabilization of Overlapping Microtubules by Fission Yeast CLASP. *Dev. Cell* *13*, 812–827.
- Braun, M., Lansky, Z., Fink, G., Ruhnnow, F., Diez, S., and Janson, M. E. (2011). Adaptive braking by Ase1 prevents overlapping microtubules from sliding completely apart. *Nat. Cell Biol.* *13*, 1259–1264.
- Brust-Mascher, I., Civelekoglu-Scholey, G., Kwon, M., Mogilner, A., and Scholey, J. M. (2004). Model for anaphase B: role of three mitotic motors in a switch from poleward flux to spindle elongation. *Proc. Natl. Acad. Sci. U. S. A.* *101*, 15938–15943.
- Brust-Mascher, I., Sommi, P., Cheerambathur, D. K., and Scholey, J. M. (2009). Kinesin-5-dependent Poleward Flux and Spindle Length Control in *Drosophila* Embryo Mitosis. *Mol. Biol. Cell* *20*, 1749–1762.
- Caplow, M., Shanks, J., and Ruhlen, R. (1994). How taxol modulates microtubule disassembly. *J. Biol. Chem.* *269*, 23399–23402.
- Castoldi, M., and Popov, A. V. (2003). Purification of brain tubulin through two cycles of polymerization-depolymerization in a high-molarity buffer. *Protein Expr. Purif.* *32*, 83–88.
- Collins, E., Mann, B. J., and Wadsworth, P. (2014). Eg5 restricts anaphase B spindle elongation in mammalian cells. *Cytoskeleton* *71*, 136–144.
- Compton, D. A. (1998). Focusing on spindle poles. *J. Cell Sci.* *111* (Pt 1, 1477–1481).

-
- Ding, R., McDonald, K. L., and McIntosh, J. R. (1993). Three-dimensional reconstruction and analysis of mitotic spindles from the yeast, *Schizosaccharomyces pombe*. *J. Cell Biol.* *120*, 141–151.
- Dixit, R., Ross, J. L., Goldman, Y. E., and Holzbaaur, E. L. F. (2008). Differential Regulation of Dynein and Kinesin Motor Proteins by Tau. *Science* *319*, 1086–1089.
- Duellberg, C., Fourniol, F. J., Maurer, S. P., Roostalu, J., and Surrey, T. (2013). End-binding proteins and Ase1 / PRC1 define local functionality of structurally distinct parts of the microtubule cytoskeleton. *Trends Cell Biol.* *23*, 54–63.
- Edamatsu, M. (2014). Bidirectional motility of the fission yeast kinesin-5, Cut7. *Biochem. Biophys. Res. Commun.* *446*, 231–234.
- Erent, M., Drummond, D. R., and Cross, R. A. (2012). *S. pombe* kinesins-8 promote both nucleation and catastrophe of microtubules. *PLoS One* *7*.
- Fache, V., Gaillard, J., van Damme, D., Geelen, D., Neumann, E., Stoppin-Mellet, V., and Vantard, M. (2010). Arabidopsis Kinetochore Fiber-Associated MAP65-4 Cross-Links Microtubules and Promotes Microtubule Bundle Elongation. *Plant Cell* *22*, 3804–3815.
- Ferenz, N. P., Gable, A., and Wadsworth, P. (2010). Mitotic functions of kinesin-5. *Semin. Cell Dev. Biol.* *21*, 255–259.
- Fink, G., Hajdo, L., Skowronek, K. J., Reuther, C., Kasprzak, A. A., and Diez, S. (2009). The mitotic kinesin-14 Ncd drives directional microtubule-microtubule sliding. *Nat. Cell Biol.* *11*, 717–723.
- Fourniol, F. J., Li, T. De, Bieling, P., Mullins, R. D., Fletcher, D. A., and Surrey, T. (2014). Micropattern-guided assembly of overlapping pairs of dynamic microtubules, Elsevier Inc.
- Fridman, V., Gerson-Gurwitz, A., Shapira, O., Movshovich, N., Lakämper, S., Schmidt, C. F., and Gheber, L. (2013). Kinesin-5 Kip1 is a bi-directional motor that stabilizes microtubules and tracks their plus-ends in vivo. *J. Cell Sci.* *126*, 4147–4159.
- Fu, C., Ward, J. J., Loiodice, I., Velve-Casquilas, G., Nedelec, F. J., and Tran, P. T. (2009). Phospho-Regulated Interaction between Kinesin-6 Klp9p and Microtubule Bundler Ase1p Promotes Spindle Elongation. *Dev. Cell* *17*, 257–267.
- Fuller, B. G., Lampson, M. A., Foley, E. A., Rosasco-Nitcher, S., Le, K. V, Tobelmann, P., Brautigan, D. L., Stukenberg, P. T., and Kapoor, T. M. (2008). Midzone activation of aurora B in anaphase produces an intracellular phosphorylation gradient. *Nature* *453*, 1132–1136.
- Fygenon, D. K., Braun, E., and Libchaber, A. (1994). Phase diagram of microtubules. *Phys. Rev. E* *50*, 1579–1588.
- Gaetz, J., and Kapoor, T. M. (2004). Dynein/dynactin regulate metaphase spindle length by targeting depolymerizing activities to spindle poles. *J. Cell Biol.* *166*, 465–471.
- Gaillard, J., Neumann, E., Damme, D. Van, Stoppin-Mellet, V., Ebel, C., Barbier, E., Geelen, D., and Vantard, M. (2008). Two Microtubule-associated Proteins of Arabidopsis MAP65s Promote Antiparallel Microtubule Bundling. *Mol. Biol. Cell* *19*, 4534–4544.
- Gatlin, J. C., and Bloom, K. (2010). Microtubule motors in eukaryotic spindle assembly and maintenance. *Semin. Cell Dev. Biol.* *21*, 248–254.
- Gell, C. *et al.* (2010). Microtubule dynamics reconstituted in vitro and imaged by single-molecule fluorescence microscopy, Elsevier.

- Gerson-Gurwitz, A., Thiede, C., Movshovich, N., Fridman, V., Podolskaya, M., Danieli, T., Lakämper, S., Klopfenstein, D. R., Schmidt, C. F., and Gheber, L. (2011). Directionality of individual kinesin-5 Cin8 motors is modulated by loop 8, ionic strength and microtubule geometry. *EMBO J.* 30, 4942–4954.
- Gordon, D. M., and Roof, D. M. (1999). The kinesin-related protein Kip1p of *Saccharomyces cerevisiae* is bipolar. *J. Biol. Chem.* 274, 28779–28786.
- Goshima, G., and Scholey, J. M. (2010). Control of mitotic spindle length. *Ann. Rev. Cell Dev. Biol.* 26, 21–57.
- Gould, K. L., and Simanis, V. (1997). The control of septum formation in fission yeast. *Genes Dev.* 11, 2939–2951.
- Grishchuk, E. L., Molodtsov, M. I., Ataullakhanov, F. I., and McIntosh, J. R. (2005). Force production by disassembling microtubules. *Nature* 438, 384–388.
- Hagan, I., and Yanagida, M. (1992). Kinesin-related cut7 protein associates with mitotic and meiotic spindles in fission yeast. *Lett. to Nat.* 356, 74–76.
- Heald, R., Tournebize, R., Habermann, A., Karsenti, E., and Hyman, A. (1997). Spindle Assembly in *Xenopus* Egg Extracts: Respective Roles of Centrosomes and Microtubule Self-Organization. *J. Cell Biol.* 138, 615–628.
- Helenius, J., Brouhard, G., Kalaidzidis, Y., Diez, S., and Howard, J. (2006). The depolymerizing kinesin MCAK uses lattice diffusion to rapidly target microtubule ends. *Nature* 441, 115–119.
- Hentrich, C., and Surrey, T. (2010). Microtubule organization by the antagonistic mitotic motors kinesin-5 and kinesin-14. *J. Cell Biol.* 189, 465–480.
- Hu, C. K., Coughlin, M., Field, C. M., and Mitchison, T. J. (2011). KIF4 regulates midzone length during cytokinesis. *Curr. Biol.* 21, 815–824.
- Hyman, A. A., Salser, S., Drechsel, D. N., Unwin, N., and Mitchison, T. J. (1992). Role of GTP hydrolysis in microtubule dynamics: information from a slowly hydrolyzable analogue, GMPCPP. *Mol. Biol. Cell* 3, 1155–1167.
- Hyman, a, Drechsel, D., Kellogg, D., Salser, S., Sawin, K., Steffen, P., Wordeman, L., and Mitchison, T. (1991). Preparation of modified tubulins. *Methods Enzymol.* 196, 478–485.
- Janning, D., Igaev, M., Sundermann, F., Bruchmann, J., Beutel, O., Heinisch, J. J., Bakotta, L., Piehler, J., Junge, W., and Brandt, R. (2014). Single-molecule tracking of tau reveals fast kiss-and-hop interaction with microtubules in living neurons. *Mol. Biol. Cell* 25, 3541–3551.
- Janson, M. E., Loughlin, R., Loiodice, I., Fu, C., Brunner, D., Nédélec, F. J., and Tran, P. T. (2007). Crosslinkers and Motors Organize Dynamic Microtubules to Form Stable Bipolar Arrays in Fission Yeast. *Cell* 128, 357–368.
- Jeon, S. I., and Andrade, J. D. (1991). Protein-Surface Interactions in the Presence of Polyethylene Oxide. *J. Colloid Interphase Sci.* 142, 159–166.
- Johann, D., Goswami, D., and Kruse, K. (2014). Segregation of diffusible and directionally moving particles on a polar filament. *Phys. Rev. E* 42713, 1–6.
- Kajtez, J. *et al.* (2016). Overlap microtubules link sister k-fibres and balance the forces on bi-oriented kinetochores. *Nat. Commun.* 7, 10298.

-
- Kapitein, L. C., Janson, M. E., Wildenberg, S. M. J. L. Van Den, Hoogenraad, C. C., Schmidt, C. F., Peterman, E. J. G., and Mc, E. (2008). Report Microtubule-Driven Multimerization Recruits ase1p onto Overlapping Microtubules. *Curr. Biol.* 18, 1713–1717.
- Kapitein, L. C., Peterman, E. J. G., Kwok, B. H., Kim, J. H., Kapoor, T. M., and Schmidt, C. F. (2005). The bipolar mitotic kinesin Eg5 moves on both microtubules that it crosslinks. *Nature* 435, 114–118.
- de Keijzer, J., Kieft, H., Ketelaar, T., Goshima, G., and Janson, M. E. (2017). Shortening of Microtubule Overlap Regions Defines Membrane Delivery Sites during Plant Cytokinesis. *Curr. Biol.* 27, 514–520.
- de Keijzer, J., Mulder, B. M., and Janson, M. E. (2014). Microtubule networks for plant cell division. *Syst. Synth. Biol.* 8, 187–194.
- Khmelninskii, A., Roostalu, J., Roque, H., Antony, C., and Schiebel, E. (2009). Phosphorylation-Dependent Protein Interactions at the Spindle Midzone Mediate Cell Cycle Regulation of Spindle Elongation. *Dev. Cell* 17, 244–256.
- Khodjakov, A., La Terra, S., and Chang, F. (2004). Laser Microsurgery in Fission Yeast: Role of the Mitotic Spindle Midzone in Anaphase B Alexey. *Can. Field-Naturalist* 14, 1330–1340.
- Kong, Z. *et al.* (2015). Kinesin-4 Functions in Vesicular Transport on Cortical Microtubules and Regulates Cell Wall Mechanics during Cell Elongation in Plants. *Mol. Plant* 8, 1011–1023.
- Korten, T., and Diez, S. (2008). Setting up roadblocks for kinesin-1 : mechanism for the selective speed control of cargo carrying microtubules †. *Lab Chip* 8, 1441–1447.
- Kurasawa, Y., Earnshaw, W. C., Mochizuki, Y., Dohmae, N., and Todokoro, K. (2004). Essential roles of KIF4 and its binding partner PRC1 in organized central spindle midzone formation. *EMBO J.* 23, 3237–3248.
- Kwok, B. H., Kapitein, L. C., Kim, J. H., Peterman, E. J. G., Schmidt, C. F., and Kapoor, T. M. (2006). Allosteric inhibition of kinesin-5 modulates its processive directional motility. *Nat. Chem. Biol.* 2, 480–485.
- Laan, L., and Dogterom, M. (2010). In vitro assays to study force generation at dynamic microtubule ends, Elsevier.
- Lakämper, S., Thiede, C., Düselder, A., Reiter, S., Korneev, M. J., Kapitein, L. C., Peterman, E. J. G., and Schmidt, C. F. (2010). The effect of monastrol on the processive motility of a dimeric kinesin-5 head/kinesin-1 stalk chimera. *J. Mol. Biol.* 399, 1–8.
- Lansky, Z., Braun, M., L??decke, A., Schlierf, M., Ten Wolde, P. R., Janson, M. E., and Diez, S. (2015). Diffusible crosslinkers generate directed forces in microtubule networks. *Cell* 160, 1159–1168.
- Lekomtsev, S., Su, K.-C., Pye, V. E., Blight, K., Sundaramoorthy, S., Takaki, T., Collinson, L. M., Cherepanov, P., Divecha, N., and Petronczki, M. (2012). Centralspindlin links the mitotic spindle to the plasma membrane during cytokinesis. *Nature* 492, 276–279.
- Liu, J. *et al.* (2009). PRC1 Cooperates with CLASP1 to Organize Central Spindle Plasticity in Mitosis. *J. Biol. Chem.* 284, 23059–23071.
- Loiodice, I., Staub, J., Setty, T. G., Nguyen, N.-P. T., Paoletti, A., and Tran, P. T. (2005). Ase1p organizes antiparallel microtubule arrays during interphase and mitosis in fission yeast. *Mol. Biol. Cell* 16, 1756–1768.
- Loughlin, R., Heald, R., and Nédélec, F. (2010). A computational model predicts *Xenopus* meiotic spindle organization. *J. Cell Biol.* 191, 1239–1249.

- Ma, N., Titus, J., Gable, A., Ross, J. L., and Wadsworth, P. (2011). TPX2 regulates the localization and activity of Eg5 in the mammalian mitotic spindle. *J. Cell Biol.* 195, 87–98.
- MacDonald, C. T., Gibbs, J. H., and Pipkin, A. C. (1968). Kinetics of biopolymerization on nucleic acid templates. *Biopolymers* 6, 1–25.
- Maiato, H., Fairley, E. A. L., Rieder, C. L., Swedlow, J. R., Sunkel, C. E., and Earnshaw, W. C. (2003). Human CLASP1 is an outer kinetochore component that regulates spindle microtubule dynamics. *Cell* 113, 891–904.
- Mallavarapu, A., Sawin, K., and Mitchison, T. (1999). A switch in microtubule dynamics at the onset of anaphase B in the mitotic spindle of *Schizosaccharomyces pombe*. *Curr. Biol.* 9, 1423–1426.
- Matthies, H. J. G., McDonald, H. B., Goldstein, L. S. B., and Theurkauf, W. E. (1996). Anastral meiotic spindle morphogenesis: Role of the non-claret disjunctional kinesin-like protein. *J. Cell Biol.* 134, 455–464.
- Miki, T., Naito, H., Nishina, M., and Goshima, G. (2014). Endogenous localizome identifies 43 mitotic kinesins in a plant cell. *Proc. Natl. Acad. Sci. U. S. A.*, 1311243111-.
- Mitchison, T., Maddox, P., Groen, A., Cameron, L., Perlman, Z., Ohi, R., Desai, A., Salmon, E., and Kapoor, T. (2004). Bipolarization and Poleward Flux Correlate during *Xenopus* Extract Spindle Assembly. *Mol. Biol. Cell* 15, 5603–5615.
- Miyamoto, D. T., Perlman, Z. E., Burbank, K. S., Groen, A. C., and Mitchison, T. J. (2004). The kinesin Eg5 drives poleward microtubule flux in *Xenopus laevis* egg extract spindles. *J. Cell Biol.* 167, 813–818.
- Mollinari, C., Kleman, J. P., Jiang, W., Schoehn, G., Hunter, T., and Margolis, R. L. (2002). PRC1 is a microtubule binding and bundling protein essential to maintain the mitotic spindle midzone. *J. Cell Biol.* 157, 1175–1186.
- Molodtsov, M. I., Mieck, C., Dobbelaere, J., Dammermann, A., Westermann, S., and Vaziri, A. (2016). A Force-Induced Directional Switch of a Molecular Motor Enables Parallel Microtubule Bundle Formation. *Cell* 167, 539–552.e14.
- Mountain, V., Simerly, C., Howard, L., Ando, A., Schatten, G., and Compton, D. A. (1999). Cross-links Microtubules in the Mammalian Mitotic Spindle. *J. Cell Biol.* 147, 351–365.
- O’Connell, M. J., Meluh, P. B., Rose, M. D., and Morris, N. R. (1993). Suppression of the bimC4 Mitotic Spindle Defect by Deletion of klpA, a Gene Encoding a KAR3-related Kinesin-like Protein in *Aspergillus nidulans*. *J. Cell Biol.* 120, 153–162.
- Peloquin, J., Komarova, Y., and Borisy, G. (2005). Conjugation of fluorophores to tubulin. *Nat. Methods* 2, 299–303.
- Popchock, A. R., Tseng, K.-F., Wang, P., Karplus, P. A., Xiang, X., and Qiu, W. (2016). The mitotic kinesin-14 KlpA contains a context-dependent directionality switch. *Nat. Commun.* 7, 1–9.
- Rogers, G. C., Rogers, S. L., and Sharp, D. J. (2005). Spindle microtubules in flux. *J. Cell Sci.* 118, 1105–1116.
- Roostalu, J., Hentrich, C., Bieling, P., Tolley, I. a, Schiebel, E., and Surrey, T. (2011). Directional switching of the kinesin Cin8 through motor coupling. *Science* 332, 94–99.



-
- Sagolla, M. J., Uzawa, S., and Cande, W. Z. (2003). Individual microtubule dynamics contribute to the function of mitotic and cytoplasmic arrays in fission yeast. *J. Cell Sci.* *116*, 4891–4903.
- Saunders, A. M., Powers, J., Strome, S., and Saxton, W. M. (2007). Kinesin-5 acts as a brake in anaphase spindle elongation. *Curr. Biol.* *17*, R453–4.
- Saunders, W. S., and Hoyt, M. A. (1992). Kinesin-related proteins required for Assembly of the Mitotic Spindle. *Cell* *70*, 451–458.
- Sawin, K. E., LeGuellec, K., Philippe, M., and Mitchison, T. J. (1992). Mitotic spindle organization by a plus-end-directed microtubule motor. *Nature* *359*, 540–543.
- Sawin, K. E., and Mitchison, T. J. (1995). Mutations in the kinesin-like protein Eg5 disrupting localization to the mitotic spindle. *Proc. Natl. Acad. Sci. U. S. A.* *92*, 4289–4293.
- Schmidt, C., Kim, B., Grabner, H., Ries, J., Kulomaa, M., and Vogel, V. (2012). Tuning the “ Roadblock ” Effect in Kinesin-Based Transport. *Nano Lett.* *12*, 3466–3471.
- Schneider, R., Korten, T., Walter, W. J., and Diez, S. (2015). Article Kinesin-1 Motors Can Circumvent Permanent Roadblocks by Side-Shifting to Neighboring Protofilaments. *Biophys. J.* *108*, 2249–2257.
- Scholey, J. E., Nithianantham, S., Scholey, J. M., and Al-Bassam, J. (2014). Structural basis for the assembly of the mitotic motor Kinesin-5 into bipolar tetramers. *Elife* *3*, e02217.
- Sharp, D. J., McDonald, K. L., Brown, H. M., Matthies, H. J., Walczak, C., Vale, R. D., Mitchison, T. J., and Scholey, J. M. (1999). The bipolar kinesin, KLP61F, cross-links microtubules within interpolar microtubule bundles of *Drosophila* embryonic mitotic spindles. *J. Cell Biol.* *144*, 125–138.
- Sharp, D. J., Rogers, G. C., and Scholey, J. M. (2000). Microtubule motors in mitosis. *Nature* *407*, 41–47.
- Shimamoto, Y., Forth, S., and Kapoor, T. M. (2015). Measuring Pushing and Braking Forces Generated by Ensembles of Kinesin-5 Crosslinking Two Microtubules. *Dev. Cell* *34*, 669–681.
- Shirasu-Hiza, M., Perlman, Z. E., Wittmann, T., Karsenti, E., and Mitchison, T. J. (2004). Eg5 Causes Elongation of Meiotic Spindles When Flux-Associated Microtubule Depolymerization Is Blocked. *Curr. Biol.* *14*, 1941–1945.
- Stanhope, K. T., and Ross, J. L. (2015). Microtubules, MAPs, and motor patterns, Elsevier Ltd.
- Stoppin-Mellet, V., Fache, V., Portran, D., Martiel, J. L., and Vantard, M. (2013). MAP65 Coordinate Microtubule Growth during Bundle Formation. *PLoS One* *8*.
- Su, X., Arellano-Santoyo, H., Portran, D., Gaillard, J., Vantard, M., Thery, M., and Pellman, D. (2013). Microtubule-sliding activity of a kinesin-8 promotes spindle assembly and spindle-length control. *Nat. Cell Biol.* *15*, 948–957.
- Subramanian, R., and Kapoor, T. M. (2012). Building Complexity: Insights into Self-Organized Assembly of Microtubule-Based Architectures. *Dev. Cell* *23*, 874–885.
- Subramanian, R., Ti, S., Tan, L., Darst, S. A., and Kapoor, T. M. (2013). Marking and Measuring Single Microtubules by PRC1 and Kinesin-4. *Cell* *154*, 377–390.
- Subramanian, R., Wilson-kubalek, E. M., Arthur, C. P., Bick, M. J., Campbell, E. A., Darst, S. A., Milligan, R. A., and Kapoor, T. M. (2010). Insights into Antiparallel Microtubule Crosslinking by PRC1 , a Conserved Nonmotor Microtubule Binding Protein. *Cell* *142*, 433–443.

- Sullivan, K. F. (1988). Structure and utilization of tubulin isotypes. *Annu. Rev. Cell Biol.* 4, 687–716.
- Surrey, T., Nédélec, F., Leibler, S., and Karsenti, E. (2001). Physical Properties Determining of Motors Self-Organization and. *Science* (80-.). 292, 1167–1171.
- Syrovatkina, V., Fu, C., and Tran, P. T. (2013). Antagonistic spindle motors and MAPs regulate metaphase spindle length and chromosome segregation. *Curr. Biol.* 23, 2423–2429.
- Szollosi, D., Calarco, P., and Donahue, R. P. (1972). Absence of centrioles in the first and second meiotic spindles of mouse oocytes. *J. Cell Sci.* 11, 521–541.
- Tanenbaum, M. E., Macůrek, L., Janssen, A., Geers, E. F., Alvarez-Fernández, M., and Medema, R. H. (2009). Kif15 Cooperates with Eg5 to Promote Bipolar Spindle Assembly. *Curr. Biol.* 19, 1703–1711.
- Tanenbaum, M. E., Vale, R. D., and McKenney, R. J. (2013). Cytoplasmic dynein crosslinks and slides anti-parallel microtubules using its two motor domains. *Elife* 2013, 1–20.
- Tao, L., Mogilner, A., Civelekoglu-Scholey, G., Wollman, R., Evans, J., Stahlberg, H., and Scholey, J. M. (2006). A Homotetrameric Kinesin-5, KLP61F, Bundles Microtubules and Antagonizes Ncd in Motility Assays. *Curr. Biol.* 16, 2293–2302.
- Tarhan, M. C., Orazov, Y., Yokokawa, R., Karsten, S. L., and Fujita, H. (2013). Biosensing MAPs as “roadblocks”: kinesin-based functional analysis of tau protein isoforms and mutants using suspended microtubules (sMTs). *Lab Chip* 13, 3217–3224.
- Thiede, C., Fridman, V., Gerson-Gurwitz, A., Gheber, L., and Schmidt, C. F. (2012). Regulation of bi-directional movement of single kinesin-5 Cin8 molecules. *Bioarchitecture* 2, 70–74.
- Thiede, C., Lakämper, S., Wessel, A. D., Kramer, S., and Schmidt, C. F. (2013). A Chimeric Kinesin-1 Head / Kinesin-5 Tail Motor Switches between Diffusive and Processive Motility. *Biophys. J.* 104, 432–441.
- Tolic-Nørrelykke, I. M., Sacconi, L., Thon, G., and Pavone, F. S. (2004). Positioning and Elongation of the Fission Yeast Spindle by Microtubule-Based Pushing Iva. *Curr. Biol.* 14, 1181–1186.
- Tran, P. T., Walker, R. A., and Salmon, E. D. (1997). A metastable intermediate state of microtubule dynamic instability that differs significantly between plus and minus ends. *J. Cell Biol.* 138, 105–117.
- Varga, V., Helenius, J., Tanaka, K., Hyman, A. a, Tanaka, T. U., and Howard, J. (2006). Yeast kinesin-8 depolymerizes microtubules in a length-dependent manner. *Nat. Cell Biol.* 8, 957–962.
- Vernì, F., Somma, M. P., Gunsalus, K. C., Bonaccorsi, S., Belloni, G., Goldberg, M. L., and Gatti, M. (2004). Feo, the Drosophila Homolog of PRC1, Is Required for Central-Spindle Formation and Cytokinesis. *Curr. Biol.* 14, 1569–1575.
- Vleugel, M., Roth, S., Groenendijk, C. F., and Dogterom, M. (2016). Reconstitution of Basic Mitotic Spindles in Spherical Emulsion Droplets. *J. Vis. Exp.*, e54278–e54278.
- Wang, H., Brust-Mascher, I., Cheerambathur, D., and Scholey, J. M. (2010). Coupling between microtubule sliding, plus-end growth and spindle length revealed by kinesin-8 depletion. *Cytoskeleton* 67, 715–728.
- Wang, H., Brust-Mascher, I., and Scholey, J. M. (2015). The microtubule cross-linker Feo controls the midzone stability, motor composition, and elongation of the anaphase B spindle in Drosophila embryos. *Mol. Biol. Cell* 26, 1452–1462.

Ward, J. J., Roque, H., Antony, C., and Nédélec, F. (2014). Mechanical design principles of a mitotic spindle. *Elife* 3, e03398.

Wazawa, T., and Ueda, M. (2005). Total internal reflection fluorescence microscopy in single molecule nanobioscience. *Adv. Biochem. Eng. Biotechnol.* 95, 77–106.

van den Wildenberg, S. M. J. L., Tao, L., Kapitein, L. C., Schmidt, C. F., Scholey, J. M., and Peterman, E. J. G. (2008). The Homotetrameric Kinesin-5 KLP61F Preferentially Crosslinks Microtubules into Antiparallel Orientations. *Curr. Biol.* 18, 1860–1864.

Yamada, M., and Goshima, G. (2017). Mitotic Spindle Assembly in Land Plants: Molecules and Mechanisms. *Biology (Basel)*. 6, 6.

Zhu, C., and Jiang, W. (2004). Cell cycle-dependent translocation of PRC1 on the spindle by Kif4 is essential for midzone formation and cytokinesis. *Proc. Natl. Acad. Sci.* 102, 343–348.

Summary

Microtubules are long filamentous protein assemblies that form networks to facilitate important cellular processes like cell division, cell polarization and vesicular transport. Networks need to attain a high degree of spatial organization to perform their functions and an excellent example is the organization of the mitotic spindle. The spindle segregates chromosomes during mitosis but also plays a role in the coordination of the subsequent cytokinesis. In contrast to many other microtubule assemblies, the spindle is a bipolar structure with microtubules from two sides meeting each other at the centre of the network. Microtubules that point in two different directions form lateral contacts that have both a structural role in network assembly as well as signalling functions like in the coordination of membrane activities. The length of these so-called antiparallel overlaps is well-regulated. Maintaining overlaps within the region that is termed the spindle midzone is of crucial importance for the stability of spindles as is demonstrated by the loss of spindle bipolarity in the absence of proteins that bundle microtubules into overlaps.

Overlaps are not static structures but several activities concur to facilitate processes like spindle elongation and spindle length control. For spindle elongation, microtubules in overlaps grow by the addition of subunits and simultaneously slide apart by forces that are generated by molecular motor proteins along microtubules. To maintain overlaps at a certain length for a prolonged time it is thus essential that these dynamic processes are tightly coordinated. In this thesis I investigated how the microtubule dynamics, which includes apart from periods of growth episodes of rapid shrinkage, can be controlled within overlaps and how relative sliding between microtubules in overlaps can be coordinated with the length dynamics. For this I developed *in vitro* experiments in which microtubule activities are reconstituted from purified protein components. This allowed me to visualize and control processes in a higher detail than is possible in cells. In doing so I obtained mechanistic insights into regulatory mechanisms that are partially based on physical principles.

In **chapter 2** I describe the development of *in vitro* assays that allow for the combination of multiple microtubule-based activities. Most previous reconstitution assays have either looked at microtubule overlap formation by bundling proteins, inter-microtubule sliding by specific molecular motors, or the regulation of microtubule growth dynamics by yet other microtubule associated proteins (MAPs). However to investigate mechanisms that allow for coordination of these activities, multiple proteins had to be functional simultaneously. Using our methods allowed us to combine relative sliding activity with dynamic microtubules for the first time

In **chapter 3**, I investigated the conditions under which a regulator of microtubule growth dynamics can prolong the lifetime of microtubule overlaps. Microtubule overlaps will disassemble after one of the connected microtubule switches to a state of rapid shrinkage (termed a catastrophe). Microtubules have the unique ability to stochastically switch between states of elongation and shortening and the probabilities thereof are controlled by regulatory proteins. Overlaps in mitotic spindles of some cells were shown to contain the regulator CLASP which is thought to enable a switch from shrinkage back to growth (a rescue). I investigated the hypothesis that CLASP is recruited to overlaps through a binding-interaction with bundling proteins of the ase1/MAP65/PRC1 family, and that this stabilizes microtubules in the overlap. I show that CLASP from fission yeast (*cls1*) can be recruited by fission yeast *ase1* to overlaps but that differential rescue activity on single microtubules and microtubules in overlaps, i.e. context-specific regulation of growth dynamics, may require a precise tuning of protein levels that was not yet achieved in our assays.

In **chapter 4**, I investigate how the length of microtubule overlaps can be maintained by coordinating growth and sliding activities. Based on experiments in fission yeast cells I hypothesize that the rate of shortening of cellular overlaps through microtubule sliding may be adapted to match the rate at which overlaps elongate through microtubule growth. In other words, sliding in overlaps may be limited by the rate of microtubule growth. To test this I formed bundles of dynamic microtubules, used the motor *klp9* from fission yeast to induce sliding, and observed how *klp9* slides these microtubules apart from each other. By observing microtubules that simultaneously grow and slide I in essence reconstituted spindle elongation. *Klp9* alone moved overlapping microtubules apart in a primarily unidirectional manner. The direction of sliding however started to alternate in the presence of the microtubule bundling protein *ase1* and when microtubules moved apart. I thus propose that directional switching of motors may serve to prevent microtubules from sliding apart. Interestingly, the direction of sliding became coupled to the dynamic state of the bundled microtubules, i.e. growth or shrinkage, enabling overlaps between dynamic microtubules to be maintained for prolonged times. I propose that cells use feedback of growth on sliding to stabilize overlaps and potentially to regulate rates of spindle elongation and spindle flux, not by adapting motor action, but by changing rates of microtubule growth in overlaps.

In vivo, many microtubule associated proteins are active on the same microtubule. In this crowded environment, proteins could influence each other by competing for the same binding sites on the microtubules. Of special interest is the interplay between motor proteins and non-active microtubule associated proteins. Motors can directionally 'walk' along microtubules by alternatingly placing one of two binding heads forwards. The microtubule bundling protein ase1 on the other hand is able to bind to microtubules and diffuse along them in a non-directional stochastic manner. The outcome of simulations suggested that motor proteins can influence diffusing proteins by introducing a bias in their diffusion. I investigated the mutual interaction between ase1 and a motor protein on single microtubules (**Chapter 5**). I observed that ase1 can form accumulations at the microtubule end in presence of motor proteins. On the other hand, the binding of motors to microtubules was impeded by ase1, their rate of translocation was slowed down by ase1, but long processive runs were still possible. Motors and diffusely-bound proteins can therefore mutually affect each others localization and functioning.

Dankwoord

Lang, lang geleden begon ik bij de leerstoelgroep Celbiologie aan mijn PhD. Eerst probeerde ik met onzichtbare lasers en nano-gouddeeltjes microtubuli te temmen, helaas zonder succes. Later plakte ik de microtubuli vast, wat in ieder geval leidde tot een aantal gelukke experimenten en veel geploeter. Allereerst wil ik alle microtubuli bedanken, jullie stonden altijd voor me klaar in een epje met buffer op mijn labtafel. Maar daar stonden ze niet zomaar! Bedankt, iedereen die heeft geholpen met het opzuiveren en labelen van tubuline. Voor het vroege opstaan en het ophalen van de varkenshersenen in het slachthuis. Henk, bedankt voor de hulp met de voorbereidingen en planning, en voor het zorgen voor een goedlopend lab. Olja, mijn in vitro-maatje, bij wie ik altijd met vragen en voor droge humor terecht kon. Ik heb goede herinneringen aan ‘the resuspension song’, maar hoop dat lied nooit meer nodig te hebben ;) Joris, die nooit veel zei maar altijd het lab opvrolijkte met zijn oneindige glimlach en een mascotte was voor alle in vitro experimenten. 

Marcel, bedankt voor alle discussies, suggesties en ideeën, en voor de goede samenwerking tijdens de laatste maanden schrijven. Hannie voor het lezen van de hoofdstukken, mentale ondersteuning en af en toe een spelletje. Kris en Jeroen, voor alle plantenweetjes en ook voor de leuke vakanties, mijn bureautuin en lichtgevend badminton. En verder natuurlijk het hele lab voor alle gezelligheid, Juliane die jarenlang mijn buurvrouw was in de kantoortuin, Elysa die die plek overnam en Han, die we graag nuttige Nederlandse woorden leren zoals ‘rolgordijn’, en ook Gonda, Joanne, Christopher en alle andere BSc en MSc studenten van Celbiologie. Natuurlijk praatte we niet alleen over werk, maar ook over de pinguïns, vleermuizen en klompen die we in kiwi’s vonden tijdens de kiwipauze, met ook Rik en Sabine van de buurlabs, waarna we weer op volle kracht aan het werk konden. En natuurlijk de pubquiz, waarbij weer eens duidelijk werd dat we maar weinig weten (maar dat wisten we natuurlijk al, als wetenschappers) en alle chocola en appelwodka die we daar hebben gewonnen.

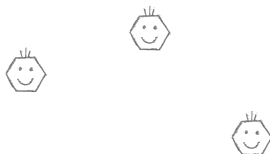
Ook mijn vrienden wil ik bedanken. Sabine en Pieter, voor jaren van saaje activiteiten, filmfestivals en het delen van PhD-frustraties, maar ook voor alle tips over het publiceren in Nature. We moeten binnenkort nodig een keer een ruimteschip repareren (in Berlijn?). Shirley, je had altijd tijd voor een kopje thee, een ijsje en nóg een potje Fluxx (voor de winnaar van de dag). Ook bedankt voor de kaarten (met of zonder kabouters) op precies de juiste momenten :) Mijn (oud-)huisgenoten voor de gezelligheid bij het avondeten en af en toe een spelletje. Vooral de laatste maanden

werd er goed voor me gezorgd! En speciaal Judith, die ook een PhD doet en dus aan een half woord genoeg heeft. Gelukkig liepen onze dipjes niet synchroon ;) We moeten snel weer eens koekenpannenbadmintonnen!

Schaatsen is een sport waarbij je ondertussen niet aan andere dingen, zoals microtubuli, kunt denken. Met heel veel plezier heb ik twee keer per week met STW getraind. Op maandag met N50, snel en met een fluitje. De late woensdagavond: N53, laat maar gezellig met twee armen op je rug. En sinds afgelopen jaar N51, technisch en met leuke afduwoefeningen. Bedankt voor alle gezelligheid, schaatsplezier en het niet te vaak vragen hoelang mijn PhD nog zou duren ;)

Soms is het nodig om er even tussenuit te gaan. Dat kon met mijn schaatsvrienden uit Breda. Elk jaar een weekje naar Collalbo en een weekend zomerschaatsen. Het ging daarbij niet alleen om het schaatsen, maar net zo goed om het eten, spelletjes, cryptogrammen en gezelligheid! Ook de STW-vierkampen met Ballangrudters, een leuke combinatie van mijn twee clubs, waren altijd erg leuk :) En jullie leerden me de belangrijke les: "Alles is moleculen, logistiek en/of core stability".

Tenslotte wil ik mijn familie bedanken. Opa en oma Jongerius voor de ijsjes op 'de camping'. Oma van Bommel voor af en toe gezellig pannenkoeken eten en de leuke kaartjes. John en Nina, waar ik altijd kan blijven slapen als ik toevallig in Utrecht ben. Ik vind alle komende parades en 'campings' nu al gezellig. Nina ook voor het ontwerpen van de omslag! Jella en Jolien voor onze urban chase avonturen en andere gezellige uitjes. En vooral mijn vader en moeder, die altijd voor me klaar stonden, van verhuizingen tot een mooie wandeling door het bos en eindeloze telefoongesprekken.

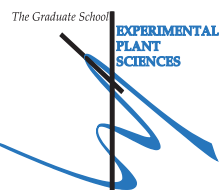


About the author

Aniek Jongerius was born on 4 January 1987 in Breda, the Netherlands. She obtained her gymnasium diploma from Stedelijk Gymnasium Breda in 2005 and then moved to Wageningen to start her studies of Molecular Sciences. She obtained her BSc in molecular science in September 2009. As part of her MSc, she carried out three research projects. At the Laboratory of Biophysics of Wageningen University she worked on non-photochemical quenching in cyanobacteria. At AMOLF, Amsterdam, she worked on in vitro experiments combining motor proteins to transport vesicles over microtubules. At the Biomaterials group of TU Berlin, she worked on PEG-based polymer patterning and cell adhesion. Enthusiastic about in vitro microtubule experiments, she started her PhD at the Laboratory of Cellbiology at Wageningen University. This thesis is the result.

Education Statement of the Graduate School

Experimental Plant Sciences



Issued to: Aniek W. Jongerius
Date: 5 July 2017
Group: Laboratory of Cell Biology
University: Wageningen University & Research

1) Start-up phase	date
▶ First presentation of your project	
Title: Non-centrosomal spindle organization	28 Apr 2012
▶ Writing or rewriting a project proposal	
▶ Writing a review or book chapter	
▶ MSc courses	
▶ Laboratory use of isotopes	

Subtotal Start-up Phase 1.5 credits*

2) Scientific Exposure	date
▶ EPS PhD student days	
EPS PhD student day, Amsterdam, NL	30 Nov 2012
EPS PhD student day, Leiden, NL	29 Nov 2013
EPS PhD student days 'Get2Gether', Soest, NL	29-30 Jan 2015
▶ EPS theme symposia	
EPS theme 1 'Developmental Biology of Plants', Leiden, NL	17 Jan 2013
EPS theme 1 'Developmental Biology of Plants', Wageningen, NL	24 Jan 2014
▶ Lunteren days and other National Platforms	
Dutch meeting on Molecular and Cellular Biophysics, Veldhoven, NL	03-04 Oct 2011
Annual meeting 'Experimental Plant Sciences', Lunteren, NL	02-03 Apr 2012
Dutch meeting on Molecular and Cellular Biophysics, Veldhoven, NL	01-02 Oct 2012
Dutch meeting on Molecular and Cellular Biophysics, Veldhoven, NL	30 Sep-01 Oct 2013
Dutch meeting on Molecular and Cellular Biophysics, Veldhoven, NL	29-30 Sep 2014
Dutch meeting on Molecular and Cellular Biophysics, Veldhoven, NL	28 Sep 2015
▶ Seminars (series), workshops and symposia	
KNAW Biophysics meeting (Heinrich)	13 Sep 2011
EPS Seminar Dr. Veronica Grieneisen	17 Nov 2011
KNAW Biophysics meeting (van Driel)	31 Jan 2012
CLB invited speaker Dr. Monique van Oers	23 Mar 2012
KNAW Biophysics meeting (Yan)	27 Mar 2012
CLB invited speaker Dr. Ir. Erwin Peterman	13 Apr 2012
FOM/f symposium	08 June 2012
Cell division symposium, Woods Hole	25 Jul 2012
Cytoskeletal and cell division seminars, Woods Hole	27 Jul 2012
CLB invited speaker Dr. Larry Griffin	16 Nov 2012
KNAW Biophysics meeting (Huck)	22 Jan 2013
EPS expectations day	01 Feb 2013
EPS Seminar Andrew Sugden	08 Feb 2013
KNAW Biophysics meeting (Petersen)	26 Mar 2013
CLB invited speaker Dr. Johannes Hohlbein	03 May 2013
WEES seminar Marten Scheffer	23 May 2013
SPAT meeting	30 May 2013
Symposium 'Life sciences with industry', Lorentz centre, Leiden, NL	07-11 Oct 2013
WGS 'The secret of a successful PhD'	06 Feb 2014
Colloquium Joshua Dijkstra	21 Mar 2014
EPS expectations day	28 Mar 2014
Biomolecular sciences seminar (Maizel)	08 Apr 2014
Inaugural lecture Jasper van der Gucht	10 Apr 2014
KNAW Biophysics meeting (Cohen)	13 May 2014
CLB invited speaker Dr. Erkan Tuzel	03 Jun 2014
CLB invited speaker Dr. Phong Tran	04 Sep 2014
Matlab academic tour 2014 image analysis	16 Oct 2014
PDB invited speaker Dr. Yara Sanchez-Corrales	13 Nov 2014
CLB invited speaker Dr. Jon Ward	06 Feb 2015
KNAW biophysics meeting (Gregor)	31 Mar 2015
CLB invited speaker Dr. Dimitrios Vavylonis	17 Apr 2015
Bela Mulder Science 'As sharp as your pencil'	02 Jun 2015
KNAW biophysics meeting (Bialek)	29 Mar 2016
▶ Seminar plus	

▶ International symposia and congresses	
European Cell Mechanics Meeting, Amsterdam	17-19 Oct 2011
Gordon conference Plant and Microbial Cytoskeleton	12-17 Aug 2012
the EMBO meeting	21-24 Sep 2013
EMBO Conference: Microtubules: Structure, regulation and functions	28-31 May 2014
▶ Presentations	
Poster: Winter School cellular biophysics	16 Jan 2012
Poster: Veldhoven 2012	01 Oct 2012
Poster: EMBO meeting 2013	22 Sep 2013
Poster: EMBO Microtubule conference 2014	30 May 2014
Talk: KNAW biophysics meeting	29 Mar 2016
▶ IAB interview	
Meeting with a member of the International Advisory Board of EPS	03 Dec 2014
▶ Excursions	
<i>Subtotal Scientific Exposure</i>	
<i>21.4 credits*</i>	

3) In-Depth Studies	<i>date</i>
▶ EPS courses or other PhD courses	
Winter school: "Cellular Biophysics: Molecules, Membranes and Mechanics", Ascona, Switzerland	15-20 Jan 2012
EMBO course: "Microscopy, modelling and biophysical methods"	08-20 Sep 2014
▶ Journal club	
Participant in the literature discussion group of CLB	2012-2014
▶ Individual research training	
Making masks for microfabricated chambers, AMOLF Amsterdam	07 Mar 2012
<i>Subtotal In-Depth Studies</i>	
<i>5.8 credits*</i>	

4) Personal development	<i>date</i>
▶ Skill training courses	
Competence Assessment	20 Mar 2012
Mobilising your - scientific - network	Mar 2015
Scientific writing	Sep 2015
▶ Organisation of PhD students day, course or conference	
▶ Membership of Board, Committee or PhD council	
<i>Subtotal Personal Development</i>	
<i>3.1 credits*</i>	

TOTAL NUMBER OF CREDIT POINTS*	31.8
---------------------------------------	-------------

Herewith the Graduate School declares that the PhD candidate has complied with the educational requirements set by the Educational Committee of EPS which comprises of a minimum total of 30 ECTS

* A credit represents a normative study load of 28 hours of study.

Colophon

The research described in this thesis was financially supported by HFSP grant RGP0026/2011 to Marcel E. Janson.

Financial support from Wageningen University for printing this thesis is gratefully acknowledged.

Cover design: Nina Rosens
Doodles: Aniek Jongerius